

# Constraining a general $U(1)'$ inverse seesaw model from vacuum stability, dark matter and collider

Arindam Das,<sup>1,\*</sup> Srubabati Goswami,<sup>2,†</sup> Vishnudath K. N.,<sup>2,3,‡</sup> and Takaaki Nomura<sup>4,§</sup>

<sup>1</sup>*Department of Physics, Osaka University, Toyonaka, Osaka 560-0043, Japan*

<sup>2</sup>*Theoretical Physics Division, Physical Research Laboratory, Ahmedabad - 380009, India*

<sup>3</sup>*Discipline of Physics, Indian Institute of Technology, Gandhinagar - 382355, India*

<sup>4</sup>*School of Physics, KIAS, Seoul 02455, Korea*

## Abstract

We consider a class of gauged  $U(1)$  extensions of the Standard Model (SM), where the light neutrino masses are generated by an inverse seesaw mechanism. In addition to the three right handed neutrinos, we add three singlet fermions and demand an extra  $Z_2$  symmetry under which, the third generations of both of the neutral fermions are odd, which in turn gives us a stable dark matter candidate. We express the  $U(1)$  charges of all the fermions in terms of the  $U(1)$  charges of the standard model Higgs and the new complex scalar. We study the bounds on the parameters of the model from vacuum stability, perturbative unitarity, dark matter relic density and direct detection constraints. We also obtain the collider constraints on the  $Z'$  mass and the  $U(1)'$  gauge coupling. Finally we compare all the bounds on the  $Z'$  mass versus the  $U(1)'$  gauge coupling plane.

---

\* Email Address: arindam.das@het.phys.sci.osaka-u.ac.jp

† Email Address: sruba@prl.res.in

‡ Email Address: vishnudath@prl.res.in

§ Email Address: nomura@kias.re.kr

## I. INTRODUCTION

The discovery of the Higgs boson with a mass of 125 GeV at the Large Hadron Collider (LHC) [1, 2] has placed the SM on a firm footing. However, the SM still does not have answers to some of the very fundamental questions like the origin of the neutrino masses and the existence of dark matter (DM). A straight forward way to include the generation of the sub-eV scale neutrino masses and the presence of the DM into the SM is by adding extra particles, which may or may not involve the extension of the SM gauge group.

Among the various beyond standard model (BSM) scenarios that have been proposed in the literature, the models in which the SM is extended by a  $U(1)$  gauge group has received some attention. The models with an extra  $U(1)$  gauge group naturally contain three right handed neutrinos as a result of the conditions for the gauge anomaly cancellation. Thus, the active light neutrino masses can be generated via the canonical type-I seesaw mechanism [3–6]. However, in canonical type-I seesaw model, which is considered in most of the  $U(1)$  extended models, one either has to go for extremely large Majorana masses ( $\sim 10^{14}$  GeV) or very small Yukawa couplings ( $\sim 10^{-6}$ ), making it difficult to probe the heavy neutrinos at the colliders. Motivated by testability in colliders, various TeV scale extensions of the type-I seesaw model have been considered in the literature (for recent reviews, see [7–10]). One of the most popular TeV scale seesaw models is the inverse seesaw model [11] where the smallness of the neutrino mass can then be attributed to a small lepton number violating term. A tiny value of this lepton number violating term is deemed natural, since when this parameter is zero, the global  $U(1)$  lepton number symmetry is reinstated and neutrinos are massless. Especially, an inverse seesaw mechanism in the context of a  $U(1)_{B-L}$  extension of the SM has been studied in reference [12]. In these models, the presence of extra singlet fermions (in addition to the right handed neutrinos) helps us to bring down the seesaw scale (which is the  $U(1)$  breaking scale) to  $\sim O(\text{TeV})$ , simultaneously allowing for large Yukawa couplings,  $Y_\nu \sim O(0.1)$ .

An important aspect of the  $U(1)$  extended models which has been scrutinized recently is the implications for the stability of the electroweak (EW) vacuum [13–22]. The measured values of the SM parameters, especially the top mass  $M_t$  and strong coupling constant  $\alpha_s$  implies that there exists an extra deeper minima near the Planck scale ( $M_{Planck}$ ), which threatens the stability of the

present EW vacuum [23, 24], since this may tunnel into that true vacuum. The calculation of the decay probability suggests that the present EW vacuum is metastable at  $3\sigma$  which means that the decay time is greater than the age of the universe. It is well known that the scalar couplings pull the vacuum towards stability whereas the Yukawa couplings push it towards instability. The EW vacuum stability in the context of a class of minimal  $U(1)$  extensions containing extra scalars and fermions have been studied by the authors of [16–18, 20] and they have shown that the behaviour of the EW vacuum depends also on the  $U(1)$  quantum numbers chosen, since the renormalization group equations (RGEs) depend on these quantum numbers. The conformal symmetric versions of such models have been considered in references [21, 22].

As already mentioned, the existence of the DM is another major motivation for going beyond the standard model. Measurements by Planck and WMAP demonstrate that nearly 85 percent of the Universe’s matter density is dark [25]. Hence, it is very important to study models that can simultaneously explain neutrino mass as well as DM and their theoretical as well as phenomenological implications. The models with an extra  $U(1)$  gauge group can accommodate a DM candidate even in the minimal version (with type-I seesaw), by adding an additional  $Z_2$  symmetry [26, 27], where the third generation of the right handed neutrinos act as the DM candidate. Other versions of the  $U(1)_{B-L}$  extension with scalar DM have been studied in [28–31]. Also, there are various realizations of the grand unified theories (GUTs) that predict the existence of extra  $Z'$  boson [32, 33]. The presence of the extra  $Z'$  boson that couples to the quarks and the leptons also gives rise to a rich collider phenomenology in the  $U(1)$  models [20, 22, 34–37]. Searches for such  $Z'$  boson through its decay dileptons have been conducted by the ATLAS and the CMS collaborations and lower limits on the  $Z'$  mass has been obtained [38–40].

In this paper, we consider a class of gauged  $U(1)$  extensions of the SM, where active light neutrino masses are generated by an inverse seesaw mechanism. In addition to the three right handed neutrinos, we add three singlet fermions and demand an extra  $Z_2$  symmetry under which, the third generations of both the neutral fermions are odd, which in turn gives us a stable DM candidate. This allows us to consider large neutrino Yukawa couplings and at the same time, keeping the  $U(1)'$  symmetry breaking scale to be of the order of  $\sim O(1)$  TeV. The main difference of this inverse seesaw model from that considered in [12] is that the extra neutral fermions that we are adding are singlets under the gauge group and hence we do not have to worry about anomaly

cancellation. Also, instead of considering one particular model, we express the  $U(1)$  charges of all the fermions in terms of the  $U(1)$  charges of the SM Higgs and the new complex scalar. We perform a comprehensive study of the bounds on the model parameters from low energy neutrino data, vacuum stability, perturbative unitarity and DM as well as collider constraints. The rest of the paper is organized as follows. In sections II and III, we introduce the class of the  $U(1)$  models under consideration and discuss the fermionic and the scalar sectors. We discuss the fitting of the neutral fermion mass matrix in section IV, by taking all the experimental constraints into account. In section V, we discuss the RGE evolution of the couplings and present the parameter space allowed by vacuum stability and perturbative unitarity in various planes. This is followed by a discussion on the DM scenario in these models, where we present the parameter space giving the correct relic density and satisfying the direct detection bounds at the same time. In section VII, we discuss the combined bounds from vacuum stability, unitarity, DM relic density and the collider constraints and finally, we summarize in section VIII.

## II. MODEL AND NEUTRINO MASS AT THE TREE LEVEL

The model considered is based on the gauge group  $SU(3)_c \times SU(2)_L \times U(1)_Y \times U(1)'$ . In addition to the SM particles, we have three right handed neutrinos  $\nu_{Ri}$ , a complex scalar  $\Phi$  required to break the  $U(1)'$  symmetry and three gauge singlet Majorana fermions  $S_i$ . An extra  $Z_2$  symmetry is imposed to have a stable fermionic dark matter. The matter and Higgs sector field content along with their transformation properties under  $SU(3)_c \times SU(2)_L \times U(1)_Y \times U(1)'$  are given below.

$$Q_L = \begin{bmatrix} u_L \\ d_L \end{bmatrix} \sim (3, 2, \frac{1}{6}, x_q) ; d_R \sim (3, 1, -\frac{1}{3}, x_d) ; u_R \sim (3, 1, \frac{2}{3}, x_u), \quad (2.1)$$

$$l_L = \begin{bmatrix} \nu_L \\ e_L \end{bmatrix} \sim (1, 2, -\frac{1}{2}, x_l) ; e_R \sim (1, 1, -1, x_e) ; \nu_R \sim (1, 1, 0, x_\nu), \quad (2.2)$$

$$H = \frac{1}{\sqrt{2}} \begin{pmatrix} G^+ \\ v + h + iG^0 \end{pmatrix} \sim (1, 2, \frac{1}{2}, \frac{x_H}{2}) ; \Phi = \frac{1}{\sqrt{2}}(\phi + u + i\chi) \sim (1, 1, 0, -x_\Phi), \quad (2.3)$$

$$S \sim (1, 1, 0, 0). \quad (2.4)$$

Note that the generation indices have been suppressed here. Under  $Z_2$ , the third generation of  $\nu_R$  and  $S$ , i.e.,  $\nu_{R3}$  and  $S_3$  are odd whereas all the other particles are even and we assume that this  $Z_2$  is not broken.

The  $U(1)'$  charges of the fermions are defined to satisfy the gauge and gravitational anomaly-free conditions:

$$\begin{aligned}
U(1)' \times [SU(3)_c]^2 & : 2x_q - x_u - x_d = 0, \\
U(1)' \times [SU(2)_L]^2 & : 3x_q + x_l = 0, \\
U(1)' \times [U(1)_Y]^2 & : x_q - 8x_u - 2x_d + 3x_l - 6x_e = 0, \\
[U(1)']^2 \times U(1)_Y & : x_q^2 - 2x_u^2 + x_d^2 - x_l^2 + x_e^2 = 0, \\
[U(1)']^3 & : 6x_q^3 - 3x_u^3 - 3x_d^3 + 2x_l^3 - x_\nu^3 - x_e^3 = 0, \\
U(1)' \times [\text{grav}]^2 & : 6x_q - 3x_u - 3x_d + 2x_l - x_\nu - x_e = 0.
\end{aligned} \tag{2.5}$$

The most general Yukawa Lagrangian (along with the Majorana mass for  $S$ ) invariant under  $SU(3)_c \times SU(2)_L \times U(1)_Y \times U(1)'$  that could be written using the fields given above is,

$$-L_{\text{Yukawa}} = Y_e \bar{l}_L H e_R + Y_\nu \bar{l}_L \tilde{H} \nu_R + Y_u \bar{Q}_L \tilde{H} u_R + Y_d \bar{Q}_L H d_R + y_{NS} \bar{\nu}_R \Phi S + \frac{1}{2} \overline{S^c} M_\mu S + \text{h.c.}, \tag{2.6}$$

where  $\tilde{H} = i\sigma_2 H^*$ . The invariance of this Yukawa Lagrangian under the  $U(1)'$  symmetry gives us the following conditions :

$$\frac{x_H}{2} = -x_q + x_u = x_q - x_d = -x_l + x_\nu = x_l - x_e \quad ; \quad -x_\Phi = x_\nu. \tag{2.7}$$

Using these conditions and the anomaly-free conditions, the  $U(1)'$  charges of all the fermions could be determined in terms of  $x_H$  and  $x_\Phi$  as,

$$\begin{aligned}
x_\nu = -x_\Phi \quad ; \quad x_l = -x_\Phi - \frac{x_H}{2} \quad ; \quad x_e = -x_\Phi - x_H, \\
x_q = \frac{1}{6}(2x_\Phi + x_H) \quad ; \quad x_u = \frac{1}{3}(2x_H + x_\Phi) \quad ; \quad x_d = \frac{1}{3}(x_\Phi - x_H),
\end{aligned} \tag{2.8}$$

Note that the choice  $x_\Phi = 1$  and  $x_H = 0$  correspond to the well known  $U(1)_{B-L}$  model. From Eq.(2.6), after symmetry breaking, the terms relevant for neutrino mass are,

$$-L_{\text{mass}} = \bar{\nu}_L M_D \nu_R + \overline{\nu}_R M_R S + \frac{1}{2} \overline{S^c} M_\mu S + \text{h.c.}, \tag{2.9}$$

where,  $M_D = Y_\nu \langle H \rangle$  and  $M_R = y_{NS} \langle \Phi \rangle$ . The neutral fermion mass matrix  $M_\nu$  can be defined as,

$$-L_{mass} = \frac{1}{2} (\overline{\nu}_L^c \quad \overline{\nu}_R \quad \overline{S}^c) \begin{pmatrix} 0 & M_D^* & 0 \\ M_D^\dagger & 0 & M_R \\ 0 & M_R^T & M_\mu \end{pmatrix} \begin{pmatrix} \nu_L \\ \nu_R^c \\ S \end{pmatrix} + \text{h.c.} \quad (2.10)$$

The mass scales of the three sub-matrices of  $M_\nu$  may naturally have a hierarchy  $M_R \gg M_D \gg M_\mu$ . Then, the effective light neutrino mass matrix in the seesaw approximation is given by,

$$M_{light} = M_D^* (M_R^T)^{-1} M_\mu M_R^{-1} M_D^\dagger. \quad (2.11)$$

Because of the extra  $Z_2$  symmetry, the Yukawa coupling matrices  $Y_\nu$  and  $y_{NS}$  and hence the mass matrices  $M_D$  and  $M_R$  will have the following textures,

$$M_R = y_{NS} \langle \Phi \rangle \sim \begin{pmatrix} \times & \times & 0 \\ \times & \times & 0 \\ 0 & 0 & \times \end{pmatrix} \quad \text{and} \quad M_D = Y_\nu \langle H \rangle \sim \begin{pmatrix} \times & \times & 0 \\ \times & \times & 0 \\ \times & \times & 0 \end{pmatrix}. \quad (2.12)$$

In addition, we will choose  $M_\mu$  to be diagonal without loss of generality. Since  $\nu_{R3}$  and  $S_3$  do not mix with other neutral fermions, they will not contribute to the seesaw mechanism and we will have a minimal inverse seesaw mechanism (3  $\nu_L$  + 2  $\nu_R$  + 2 S case) in which the lightest active neutrino will be massless. The two fermions  $\nu_{R3}$  and  $S_3$  mix among themselves and the lightest mass eigenstate could be a stable DM candidate. In the heavy sector, we will have two pairs of degenerate pseudo-Dirac neutrinos of masses of the order  $\sim M_R \pm M_\mu$  that mix with the active light neutrinos. Thus, we have an inverse seesaw mechanism in which the smallness of  $M_{light}$  is naturally attributed to the smallness of both  $M_\mu$  and  $\frac{M_D}{M_R}$ . For instance,  $M_{light} \sim \mathcal{O}(0.1)$  eV can easily be achieved by taking  $\frac{M_D}{M_R} \sim 10^{-2}$  and  $M_\mu \sim \mathcal{O}(1)$  keV. Thus, the seesaw scale can be lowered down considerably for typical values of the parameters –  $Y_\nu \sim \mathcal{O}(0.1)$ ,  $M_D \sim 10$  GeV and  $M_R \sim 1$  TeV.

### III. SCALAR POTENTIAL OF THE MODEL AND SYMMETRY BREAKING

The scalar potential of the model is given by,

$$V(\Phi, H) = m_1^2 H^\dagger H + \lambda_1 (H^\dagger H)^2 + \lambda_3 H^\dagger H \Phi^\dagger \Phi + m_2^2 \Phi^\dagger \Phi + \lambda_2 (\Phi^\dagger \Phi)^2. \quad (3.1)$$

The trivial conditions that give a stable potential are,

$$\lambda_1 > 0 \quad ; \quad \lambda_2 > 0 \quad \text{and} \quad \lambda_3 > 0, \quad (3.2)$$

and if  $\lambda_3 < 0$ , the stability of the potential can still be achieved by satisfying the following conditions :

$$\lambda_1 > 0, \quad \lambda_2 > 0, \quad 4\lambda_1\lambda_2 - \lambda_3^2 > 0. \quad (3.3)$$

The above conditions are obtained by demanding the Hessian matrix corresponding to the potential to be positive definite at large field values [16, 41, 42].

The two scalar fields acquire vacuum expectation values(*vevs*) given by,

$$\langle H \rangle = \frac{1}{\sqrt{2}} \begin{pmatrix} 0 \\ v \end{pmatrix} \quad ; \quad \langle \Phi \rangle = \frac{u}{\sqrt{2}}. \quad (3.4)$$

The values of  $v$  and  $u$  are determined by the minimization conditions and are given by,

$$v^2 = \frac{m_2^2\lambda_3/2 - m_1^2\lambda_2}{\lambda_1\lambda_2 - \lambda_3^2/4} \quad ; \quad u^2 = \frac{m_1^2\lambda_3/2 - m_2^2\lambda_1}{\lambda_1\lambda_2 - \lambda_3^2/4}. \quad (3.5)$$

After symmetry breaking, the mixing between the fields  $h$  and  $\phi$  could be rotated away by an orthogonal transformation to get the physical mass eigenstates as, The values of  $v$  and  $u$  are determined by the minimization conditions and are given by,

$$v^2 = \frac{m_2^2\lambda_3/2 - m_1^2\lambda_2}{\lambda_1\lambda_2 - \lambda_3^2/4} \quad ; \quad u^2 = \frac{m_1^2\lambda_3/2 - m_2^2\lambda_1}{\lambda_1\lambda_2 - \lambda_3^2/4}. \quad (3.6)$$

After symmetry breaking, the mixing between the fields  $h$  and  $\phi$  could be rotated away by an orthogonal transformation to get the physical mass eigenstates as, The values of  $v$  and  $u$  are determined by the minimization conditions and are given by,

$$v^2 = \frac{m_2^2\lambda_3/2 - m_1^2\lambda_2}{\lambda_1\lambda_2 - \lambda_3^2/4} \quad ; \quad u^2 = \frac{m_1^2\lambda_3/2 - m_2^2\lambda_1}{\lambda_1\lambda_2 - \lambda_3^2/4}. \quad (3.7)$$

After symmetry breaking, the mixing between the fields  $h$  and  $\phi$  could be rotated away by an orthogonal transformation to get the physical mass eigenstates as,

$$\begin{pmatrix} h_1 \\ h_2 \end{pmatrix} = \begin{pmatrix} \cos\theta & -\sin\theta \\ \sin\theta & \cos\theta \end{pmatrix} \begin{pmatrix} h \\ \phi \end{pmatrix}, \quad (3.8)$$

The masses of the scalar eigenstates are,

$$m_{h_{1,2}}^2 = \lambda_1 v^2 + \lambda_2 u^2 \mp \sqrt{(\lambda_1 v^2 - \lambda_2 u^2)^2 + (\lambda_3 uv)^2}. \quad (3.9)$$

From these, one can get the relations,

$$\begin{aligned} \lambda_1 &= \frac{m_{h_1}^2}{4v^2}(1 + \cos 2\theta) + \frac{m_{h_2}^2}{4v^2}(1 - \cos 2\theta), \\ \lambda_2 &= \frac{m_{h_1}^2}{4u^2}(1 - \cos 2\theta) + \frac{m_{h_2}^2}{4u^2}(1 + \cos 2\theta), \\ \lambda_3 &= \sin 2\theta \left( \frac{m_{h_2}^2 - m_{h_1}^2}{2uv} \right). \end{aligned} \quad (3.10)$$

We use these equations to set the initial conditions on the scalar couplings  $\lambda_1$ ,  $\lambda_2$  and  $\lambda_3$  while running the renormalization group equations. Also, from the above equations, one can get,

$$\tan 2\theta = \frac{\lambda_3 uv}{\lambda_1 v^2 - \lambda_2 u^2}. \quad (3.11)$$

### A. Perturbative Unitarity

In addition to the vacuum stability conditions, the constraints from the perturbative unitarity conditions also put bounds on the model parameters. By considering the  $hh \rightarrow hh$  and  $\phi\phi \rightarrow \phi\phi$  processes, one can derive combined constraints on the three couplings appearing in the scalar potential[43, 44] :

$$|\lambda_3| \leq 8\pi \quad ; \quad 3(\lambda_1 + \lambda_2) \pm \sqrt{\lambda_3^2 + 9(\lambda_1 - \lambda_2)^2} \leq 8\pi \quad (3.12)$$

Demanding the other running couplings to remain in the perturbative regime gives us,

$$g_i \leq \sqrt{4\pi}, \quad (3.13)$$

where  $g_i$  stands for SM gauge couplings. For the  $U(1)$  gauge coupling  $g'$ , we require,

$$(x_{q,d,u,l,e,\nu,\Phi})g', \quad (x_H/2)g' < \sqrt{4\pi}. \quad (3.14)$$



## IV. NUMERICAL ANALYSIS AND PARAMETER SCANNING IN THE NEUTRINO SECTOR

To study the parameter space allowed by vacuum stability as well as perturbativity bounds up to  $M_{Planck}$  using the RGEs, we have to first fix the initial values for all the couplings. While setting the initial values for the neutrino Yukawa couplings  $Y_\nu$  and  $y_{NS}$ , we have to make sure that they reproduce the correct oscillation parameters and satisfy all the experimental constraints. To do this, we find sample benchmark points for  $Y_\nu$ ,  $y_{NS}$  and  $M_\mu$  and the vev of the extra scalar  $\Phi(u)$  by fitting them with all the constraints using the downhill simplex method [45]. Note that here,  $Y_\nu$  is a complex  $3 \times 2$  matrix,  $y_{NS}$  is a complex  $2 \times 2$  matrix and  $M_\mu$  is a  $2 \times 2$  diagonal matrix with real entries. The various constraints we have taken are:

Parameter	$NH$
$\Delta m_{sol}^2/10^{-5}eV^2$	6.80 $\rightarrow$ 8.02
$\Delta m_{atm}^2/10^{-3}eV^2$	+2.399 $\rightarrow$ +2.593
$\sin^2 \theta_{12}$	0.272 $\rightarrow$ 0.346
$\sin^2 \theta_{23}$	0.418 $\rightarrow$ 0.613
$\sin^2 \theta_{13}$	0.01981 $\rightarrow$ 0.02436

TABLE I: The oscillation parameters in their  $3\sigma$  range, for NH as given by the global analysis of neutrino oscillation data with three light active neutrinos [46].

- Cosmological constraint on the sum of light neutrino masses as given by the Planck 2018 results [47]. This puts an upper limit on the sum of active light neutrino masses to be,

$$\Sigma = m_1 + m_2 + m_3 < 0.14 \text{ eV}. \quad (4.1)$$

Note that in our case, the lightest active neutrino is massless and also we are restricting our analysis only to the normal hierarchy (NH) of the active neutrino masses since the vacuum stability, dark matter and collider analyses are independent of the hierarchy of the light neutrino masses. In addition, it has been found that the best fit of the data is for the NH

and IH is disfavored with a  $\Delta\chi^2 = 4.7(9.3)$  without (with) Super-Kamiokande atmospheric neutrino data [48]. Thus we have,

$$m_1 = 0, \quad m_2 = \sqrt{\Delta m_{sol}^2}; \quad m_3 = \sqrt{\Delta m_{atm}^2} \quad (4.2)$$

- The constraints on the oscillation parameters in their  $3\sigma$  range, given by the global analysis [46, 49] of neutrino oscillation data with three light active neutrinos following NH are given in Table I. We use the standard parametrization of the PMNS matrix in which,

$$U_\nu = \begin{pmatrix} c_{12}c_{13} & s_{12}c_{13} & s_{13}e^{-i\delta} \\ -c_{23}s_{12} - s_{23}s_{13}c_{12}e^{i\delta} & c_{23}c_{12} - s_{23}s_{13}s_{12}e^{i\delta} & s_{23}c_{13} \\ s_{23}s_{12} - c_{23}s_{13}c_{12}e^{i\delta} & -s_{23}c_{12} - c_{23}s_{13}s_{12}e^{i\delta} & c_{23}c_{13} \end{pmatrix} P \quad (4.3)$$

where  $c_{ij} = \cos\theta_{ij}$ ,  $s_{ij} = \sin\theta_{ij}$  and the phase matrix  $P = \text{diag}(1, e^{i\alpha_2}, e^{i(\alpha_3+\delta)})$  contains the Majorana phases.

- The constraints on the non-unitarity of  $U_{PMNS} = U_L$  as given by the analysis of electroweak precision observables along with various other low energy precision observables [50]. At 90% confidence level, we have,

$$|U_L U_L^\dagger| = \begin{pmatrix} 0.9979 - 0.9998 & < 10^{-5} & < 0.0021 \\ < 10^{-5} & 0.9996 - 1.0 & < 0.0008 \\ < 0.0021 & < 0.0008 & 0.9947 - 1.0 \end{pmatrix}. \quad (4.4)$$

This also takes care of the constraints coming from various charged lepton flavor violating decays like  $l_i \rightarrow l_j \gamma$ . For example, the branching ratio for the decay  $\mu \rightarrow e \gamma$  is constrained as [51],

$$\text{Br}(\mu \rightarrow e \gamma) < 4.2 \times 10^{-13}. \quad (4.5)$$

In addition, it has been shown in reference [52] that the  $\mu \rightarrow e$  conversion in nuclei can give the strongest bound out of all the flavor violating observables in the case of type-I seesaw models. The bound on the branching ratio for the  $\mu \rightarrow e$  conversion in Gold ( $Au$ ) nucleus reads as [53],

$$\text{Br}(\mu \text{ Au} \rightarrow e \text{ Au}) < 7 \times 10^{-3}. \quad (4.6)$$

This has been converted into a bound on the parameter  $\hat{R}_{e\mu}$  in reference [52] as,

$$\hat{R}_{e\mu} < 9.7 \times 10^{-6}, \quad (4.7)$$

where,

$$\hat{R}_{e\mu} = 2 \sum_j (Y_\nu)_{ej}^* (Y_\nu)_{\mu j} \left( \frac{m_W^2}{M_j^2} \right) \text{Log} \left( \frac{M_j}{m_W} \right) \quad (4.8)$$

where  $j = 1, 2$ ,  $M_1, M_2$  are the heavy neutrino masses such that  $M_1 \neq M_2$  and the factor of 2 takes care of the degeneracy in mass spectrum. In our fitting, we have made sure that the parameter sets that we consider satisfy all these bounds.

In table (II), we give two benchmark points consistent with all the experimental data discussed above. As a consistency check, we also give the value of  $Br(\mu \rightarrow e \gamma)$  obtained at the two benchmark points.

## V. RGE EVOLUTION

The couplings in any quantum field theory get corrections from higher-order loop diagrams and as a result, the couplings run with the renormalization scale. We have the renormalization group equation (RGE) for a coupling  $C$  as,

$$\mu \frac{dC}{d\mu} = \sum_i \frac{\beta_C^{(i)}}{(16\pi^2)^i}, \quad (5.1)$$

where  $i$  stands for the  $i^{\text{th}}$  loop and  $\beta_C$  is the corresponding  $\beta$  function.

We have evaluated the SM coupling constants at the top quark mass scale and then run them using the RGEs from  $M_t$  to  $M_{Planck}$ . For this, we have taken into account the various threshold corrections at  $M_t$  [54–56]. Then the SM RGEs are used to run all the couplings up to the  $vev$  of the new scalar, after which, the new couplings enter. The modified RGEs for the  $SU(3)_c \times SU(2)_L \times U(1)_Y \times U(1)'$  have been used. These have been generated using SARAH [57]. We have used two-loop RGEs for all the SM parameters and  $g'$  and the new scalar couplings  $\lambda_2$  and  $\lambda_3$ , whereas for the neutrino Yukawa couplings, we have used the one-loop RGEs. The one- and the two-loop RGEs of the model are given in the appendix. Throughout this paper, we have

Parameter	$BM - I$	$BM - II$
$Tr[Y_\nu Y_\nu^\dagger]$	0.0898	0.4000
$[Y_\nu]_{3 \times 2}$	$\begin{pmatrix} 0.0694 - i 0.1182 & 0 - i 0.0499 \\ 0.0038 - i 0.0022 & 0.0778 + i 0.0442 \\ -0.0008 - i 0.2183 & -0.0071 - i 0.1128 \end{pmatrix}$	$\begin{pmatrix} -0.0210 + i 0.2269 & -0.0329 + i 0.0036 \\ 0.0495 - i 0.0352 & -0.2321 - i 0.3021 \\ -0.1081 - i 0.3771 & 0.1450 + i 0.1526 \end{pmatrix}$
$Tr[y_{NS} Y_R^\dagger]$	0.0101	0.1472
$[y_{NS}]_{2 \times 2}$	$\begin{pmatrix} 0.0031 - i 0.0082 & 0.0375 - i 0.0351 \\ 0.0821 + i 0.0093 & -0.0002 - i 0.0241 \end{pmatrix}$	$\begin{pmatrix} 0.2861 + i 0.0073 & -0.0025 + i 0.1521 \\ 0.0623 - i 0.0545 & -0.1596 - i 0.0990 \end{pmatrix}$
$[M_\mu]_{2 \times 2} \text{ GeV}$	$\begin{pmatrix} 1.0921 \times 10^{-6} & 0 \\ 0 & -2.2092 \times 10^{-8} \end{pmatrix}$	$\begin{pmatrix} 1.2655 \times 10^{-8} & 0 \\ 0 & -2.5248 \times 10^{-8} \end{pmatrix}$
$M_j \text{ GeV}$	1766.82, 1766.82, 3085.87, 3085.87	2227.88, 2227.88, 3659.58, 3659.58
$Br(\mu \rightarrow e \gamma)$	$4.0946 \times 10^{-13}$	$2.2954 \times 10^{-13}$
$u \text{ (TeV)}$	50	12

TABLE II: Two sample benchmark points for the neutrino sector. The above parameters give the correct mixing angles and satisfies the non-unitarity constraints on  $U_{PMNS}$ . The value of  $Br(\mu \rightarrow e \gamma)$  is given as a check.

fixed the standard model parameters as  $m_h = 125.7 \text{ GeV}$ ,  $M_t = 173.4 \text{ GeV}$  and  $\alpha_s = 0.1184$ . Also, we have kept the  $U(1)$  gauge mixing to be 0 at the scale  $u$  throughout this paper.

Fig. 1 displays the allowed region in the  $m_{h_2} - \theta$  plane for the model with  $x_H = x_\Phi = 1$ , keeping all the other parameters fixed. For the neutrino Yukawa couplings, we have used BM-I from the Table II and we have fixed  $g' = 0.1$  and  $y_{NS}^{33} = 0.5$ . From the figure, one can see that for higher values of  $\theta$ , only smaller values of  $m_{h_2}$  are allowed whereas for smaller values of  $\theta$ , larger values of  $m_{h_2}$  over a wider range are allowed. Also it can be seen that for this model with the considered set of parameters, the values of  $m_{h_2} > 33 \text{ TeV}$  and  $\theta > 0.013$  are disallowed.

In Fig. 2, we have plotted the running of  $\lambda_1$ ,  $\lambda_2$  and  $\lambda_3$  for the model with  $x_H = x_\Phi = 1$  for two different values of  $m_{h_2}$  and  $\theta$ . The figure in the left side is for  $m_{h_2} = 15 \text{ TeV}$  and  $\theta = 0.004$  whereas the one in the right side is for  $m_{h_2} = 20 \text{ TeV}$  and  $\theta = 0.003$ . For the neutrino Yukawa

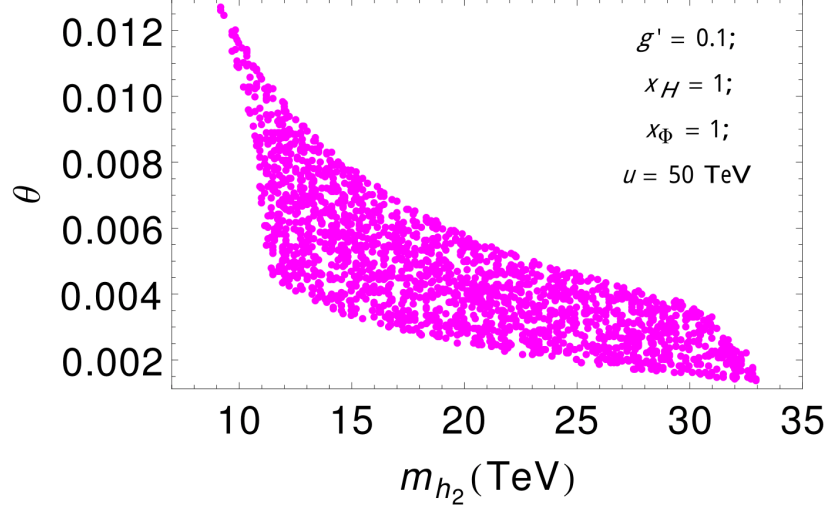


FIG. 1: Region in the  $m_{h_2} - \theta$  plane allowed by both vacuum stability and perturbativity bounds up to  $M_{Planck}$  for the model with  $x_H = x_\Phi = 1$ . For the neutrino Yukawa couplings, we have used BM-I from the Table II and we have fixed  $g' = 0.1$  and  $y_{NS}^{33} = 0.5$ .

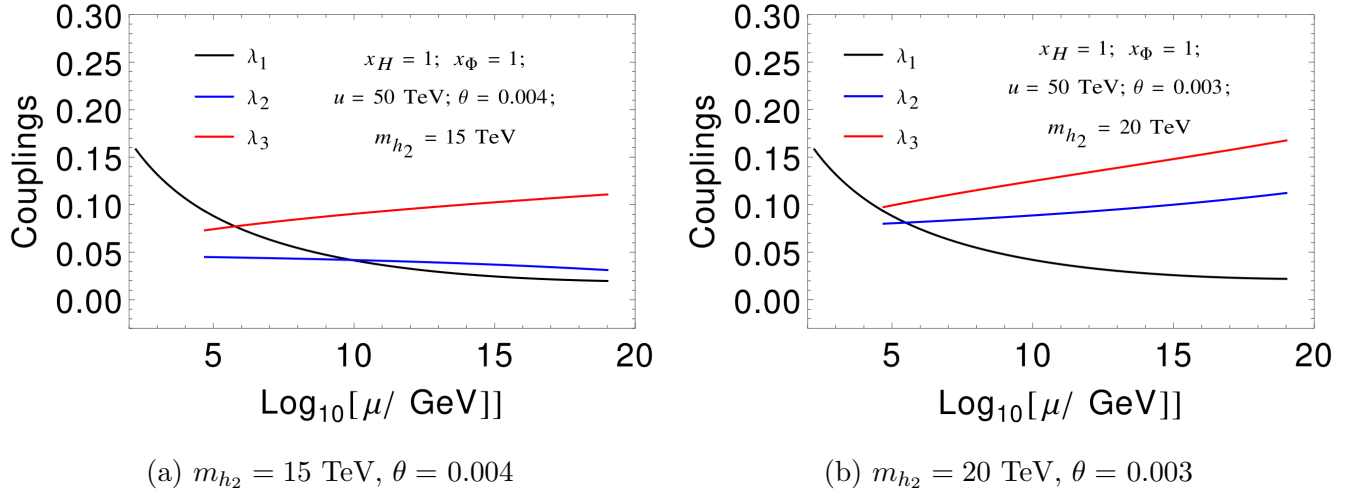


FIG. 2: Running of  $\lambda_1, \lambda_2, \lambda_3$  and  $4\lambda_1\lambda_2 - \lambda_3^2$  for the model with  $x_H = x_\Phi = 1$  for two different values of  $m_{h_2}$  and  $\theta$ . For the neutrino Yukawa couplings, we have used BM-I from the Table II and we have fixed  $g' = 0.1$  and  $y_{NS}^{33} = 0.5$ .

couplings, we have used BM-I from the Table II and we have fixed  $g' = 0.1$  and  $y_{NS}^{33} = 0.5$ . We can see that all the three quartic couplings remain positive up to  $M_{Planck}$  for both the cases implying

that the electroweak vacuum is absolutely stable. This can be seen from Fig. 1 as well where the above mentioned points fall in the stable region. Here, the presence of the extra scalar coupling helps in stabilizing the vacuum.

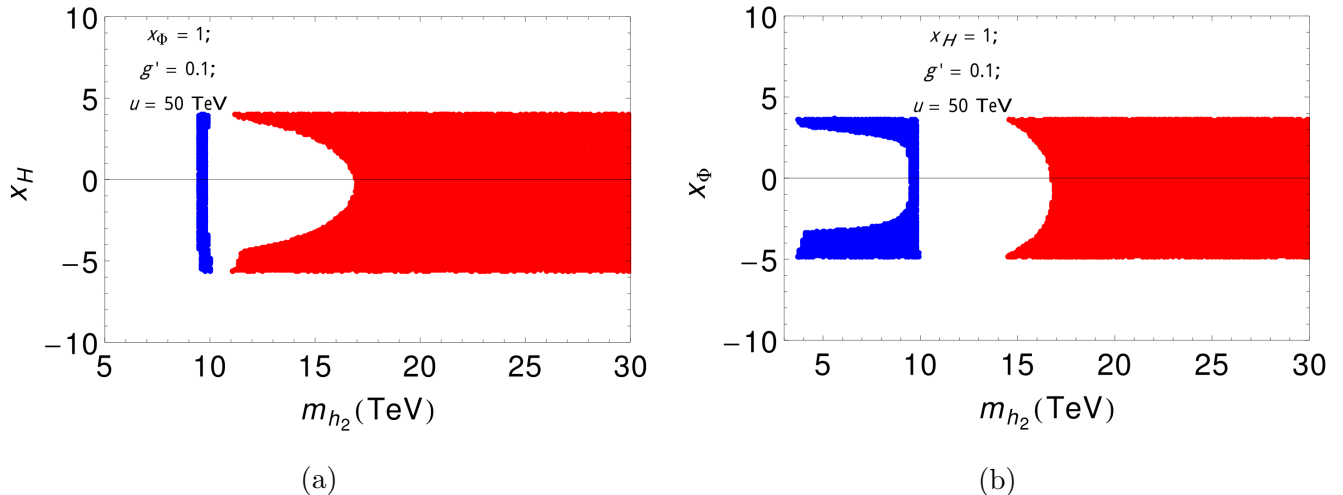


FIG. 3: Regions in the  $m_{h_2} - x_H$  and  $m_{h_2} - x_\Phi$  planes allowed by both vacuum stability and perturbativity bounds up to  $M_{Planck}$  for two different values of  $\theta$ . For the left panel, we have fixed  $x_\Phi = 1$  and for the right panel, we have fixed  $x_H = 1$ . For the neutrino Yukawa couplings, we have used BM-I from the Table II and we have fixed  $g' = 0.1$  and  $y_{NS}^{33} = 0.5$ . The red region is for  $\theta = 0.003$  and the blue region is for  $\theta = 0.01$ .

In Fig. 3, we have plotted the regions allowed by both vacuum stability and perturbativity bounds up to  $M_{Planck}$  in the  $m_{h_2} - x_H$  and  $m_{h_2} - x_\Phi$  planes, for two different values of  $\theta$ . The red regions are for  $\theta = 0.003$  and the blue regions are for  $\theta = 0.01$ . Fig. 3a shows the allowed regions in the  $m_{h_2} - x_H$  plane keeping all the other parameters fixed. For the neutrino Yukawa couplings, we have used BM-I from the Table II and we have fixed  $x_\Phi = 1$ ,  $g' = 0.1$  and  $y_{NS}^{33} = 0.5$ . It can be seen that for  $\theta = 0.01$ , a very narrow region of  $m_{h_2}$  in the range  $\approx 9 - 10$  TeV is allowed by the stability and perturbativity constraints and the corresponding allowed range of  $x_H$  is  $\approx -5.7 - 4.1$ . Here, the higher values of  $m_{h_2}$  are disfavored by the perturbativity constraints whereas the lower values of  $m_{h_2}$  are disfavored by the constraints from vacuum stability. At the same time, for  $\theta = 0.003$ ,  $m_{h_2} \approx 11 - 30$  TeV is allowed depending on the value of  $x_H$ .

Similarly, in Fig. 3b, we have shown the allowed region in the  $m_{h_2} - x_\Phi$  plane keeping  $x_H = 1$

and all the other parameters fixed for two different values of  $\theta$ . Here also, for  $\theta = 0.01$ , the values of  $m_{h_2}$  greater than 10 TeV are disfavored by unitarity constraints. The lower values of  $m_{h_2}$  are disfavored by the stability constraints depending on the value of  $x_\Phi$ . For  $-3 \leq x_\Phi \leq 3$ , values of  $m_{h_2}$  less than  $\sim 9$  TeV are disallowed, whereas for  $-5.5 \leq x_\Phi \leq -3$  and  $3 \leq x_\Phi \leq 4$ , values of  $m_{h_2}$  as low as  $\sim 3$  TeV are allowed. For  $\theta = 0.003$ , values of  $m_{h_2} < 14 - 15.5$  TeV are disallowed depending on the values of  $x_H$ , but values as high as 30 TeV are allowed for  $-5 \leq x_H \leq 4$ . These results are consistent with the observations from Fig. 1 where we have seen that for  $x_H = x_\Phi = 1$ , larger(smaller) values of  $m_{h_2}$  are disfavored for larger(smaller) values of  $\theta$ .

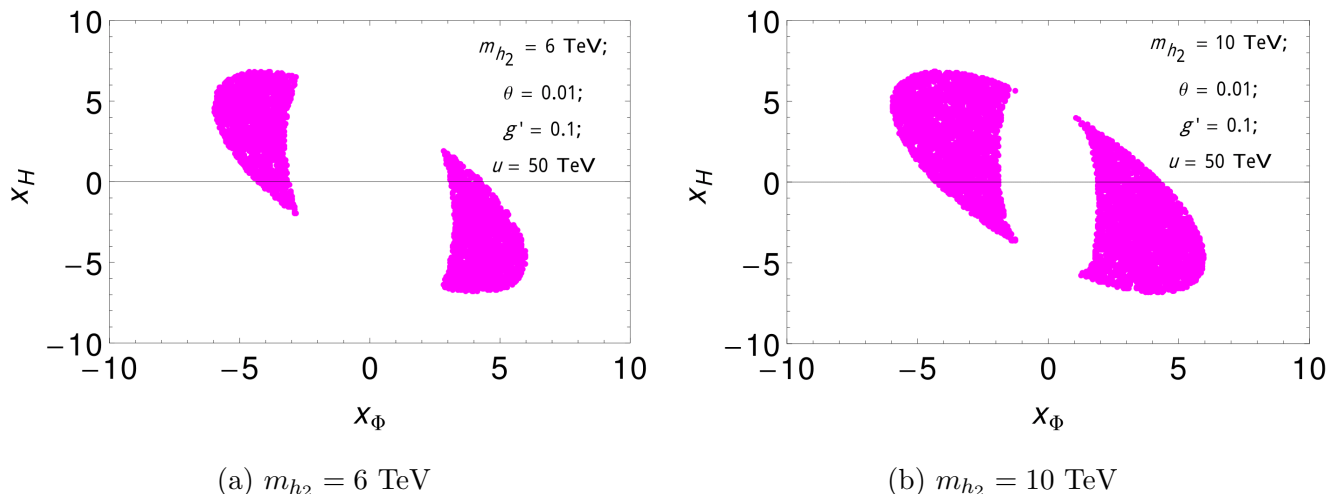


FIG. 4: Regions in the  $x_\Phi - x_H$  plane allowed by both vacuum stability and perturbativity up to  $M_{Planck}$ . We have taken the mass of the extra scalar to be 6 TeV (10 TeV) in the left (right) panel. For the neutrino Yukawa couplings, we have used BM-I from the Table II and we have fixed  $\theta = 0.01$ ,  $g' = 0.1$  and  $y_{NS}^{33} = 0.5$  for both the plots.

In Fig.4, we have presented the regions in the  $x_\Phi - x_H$  plane allowed by both vacuum stability (absolute stability) and perturbativity up to  $M_{Planck}$  for fixed values of  $m_{h_2}$ ,  $\theta$  and  $g'$ . For the neutrino Yukawa couplings, we have used the BM-I in Table II and we have taken and  $y_{NS}^{33} = 0.5$ . The mass of the extra scalar have been taken to be 6 TeV (10 TeV) in the left (right) panel and the values of  $\theta$  and  $g'$  are taken to be 0.01 and 0.1 respectively for both the plots. From these two figures, we can see that increasing the scalar mass will allow more values of  $x_\Phi$  for a given value of  $x_H$ . In fact, one can see that the allowed values for  $x_\Phi$  lie in the ranges  $\approx \pm 3$  to  $\pm 6$  and  $\approx \pm 1$  to

$\pm 6$  for the figures in the left and the right panels respectively. Also,  $x_H$  lies in the range  $\approx -7$  to 7 for both the cases with the considered values of the parameters. This can be understood from Eq.3.10 which shows that higher value of  $m_{h_2}$  implies higher value of the scalar couplings which in turn favors stability.

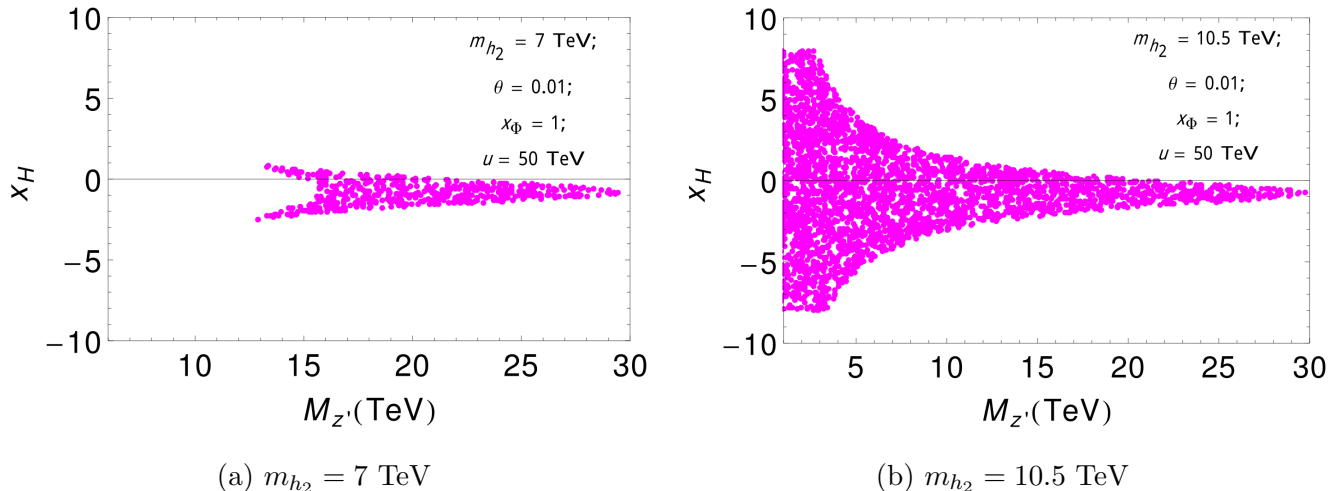


FIG. 5: Regions in the  $M_{Z'} - x_H$  plane allowed by both vacuum stability and perturbativity bounds up to  $M_{Planck}$ . We have taken the mass of the extra scalar to be 7 TeV (10.5 TeV) in the left (right) panel. For the neutrino Yukawa couplings, we have used BM-I from the Table II and we have fixed  $\theta = 0.01$ ,  $x_{\Phi} = 1$  and  $y_{NS}^{33} = 0.5$  for both the plots.

Fig.5, displays the regions allowed by both vacuum stability and perturbativity up to  $M_{Planck}$  in the  $M_{Z'} - x_H$  plane for fixed values of  $m_{h_2}$ ,  $\theta$  and  $x_{\Phi}$ . Here also, we have used the BM-I in Table II for the neutrino Yukawa couplings and we have taken  $y_{NS}^{33} = 0.5$ . The mass of the extra scalar have been taken to be 7 and 10.5 TeV in the left and the right panels respectively and the values of  $\theta$  and  $x_{\Phi}$  are taken to be 0.01 and 1 for both the plots. Also, we have varied  $g'$  from 0 to 1 keeping  $u$  fixed at 50 TeV and  $x_H$  in the range -8 to 8. The corresponding values of  $M_{Z'}$  have been calculated using,

$$M_{Z'} = \sqrt{(x_{\Phi}g'u)^2 + \left(\frac{x_H}{2}g'v_{SM}\right)^2}. \quad (5.2)$$

From these figures, we can see that lower values of  $M_{Z'}$  allow large values of  $x_H$  (or, equivalently lower values of  $g'$ ). From these figures, one can see that for a lower scalar mass, the lower values of  $M'_{Z'}$  (or equivalently, lower values of  $g'$ ) are disfavored. For  $m_{h_2} = 7$  TeV, values of  $M_{Z'}$  less



than 12 TeV are disallowed and a very small range of  $x_H$  is allowed whereas for  $m_{h_2} = 10.5$  TeV, values of  $M_{Z'}$  as low as 1 TeV are allowed and correspondingly,  $x_H$  is allowed from  $-8$  to  $8$ .

## VI. DARK MATTER SCENARIO

In this section we discuss dark matter physics in our model with respect to the constraints from relic density and direct detection experiments. As mentioned earlier, the third generations of  $N_R$  and  $S_L$  ( $N_R^3, S_L^3$ ) are odd under the  $Z_2$  parity in the general  $U(1)'$  inverse seesaw model that we consider. This ensures the stability of  $N_R^3$  and  $S_L^3$  which is required for these to be potential DM candidates. As a result the relevant interactions in the Lagrangian can be written as

$$-\mathcal{L}_{mass}^2 \supset y_{NS}^{33} \overline{N_R^3} S_L^3 \Phi + M_S^{33} \overline{S_L^3} S_L^3. \quad (6.1)$$

Note that  $N_R^3$  can not couple to the SM Higgs and lepton doublets due to the  $Z_2$  symmetry. After the symmetry breaking we have  $\langle \Phi \rangle = \frac{u}{\sqrt{2}}$  and the mass matrix can be written as,

$$M_{N^3 S^3} = \begin{pmatrix} 0 & M_{NS}^{33} \\ M_{NS}^{33} & M_S^{33} \end{pmatrix} \quad (6.2)$$

where  $M_{NS}^{33} = \frac{y_{NS}^{33} u}{\sqrt{2}}$ . Now rotating the basis we can write the physical eigenstates as

$$\begin{pmatrix} N_R^{3c} \\ S_L^3 \end{pmatrix} = \begin{pmatrix} \cos \bar{\theta} & \sin \bar{\theta} \\ -\sin \bar{\theta} & \cos \bar{\theta} \end{pmatrix} \begin{pmatrix} \psi_1 \\ \psi_2 \end{pmatrix} \quad (6.3)$$

where  $\tan 2\bar{\theta} = \left| \frac{2M_{NS}^{33}}{-M_S^{33}} \right| = \sqrt{2} \frac{y_{NS}^{33} u}{M_S^{33}}$ . Note that  $\psi_1$  and  $\psi_2$  are Majorana fermions. The mass eigenvalues are obtained as

$$m_{\psi_1, \psi_2} = \frac{1}{2} \sqrt{(M_S^{33})^2 + 4(M_{NS}^{33})^2} \mp \frac{1}{2} M_S^{33}, \quad (6.4)$$

where we take  $m_{\psi_1} < m_{\psi_2}$ . Thus  $\psi_1$  is the lightest  $Z_2$  odd particle and our DM candidate. Putting  $\psi_1$  and  $\psi_2$  back into Eq. 6.1 along with the physical mass eigenstates of  $h$  and  $\phi$  we write the interaction among  $Z_2$  odd fermion and scalars as,

$$-\mathcal{L} \supset y_{NS}^{33} \left( -\sin \theta \cos \bar{\theta} \cos \bar{\theta} h_1 + \cos \theta \sin \bar{\theta} \sin \bar{\theta} h_2 \right) \left( -\overline{\psi_1^c} \psi_1 + \overline{\psi_2^c} \psi_2 \right). \quad (6.5)$$

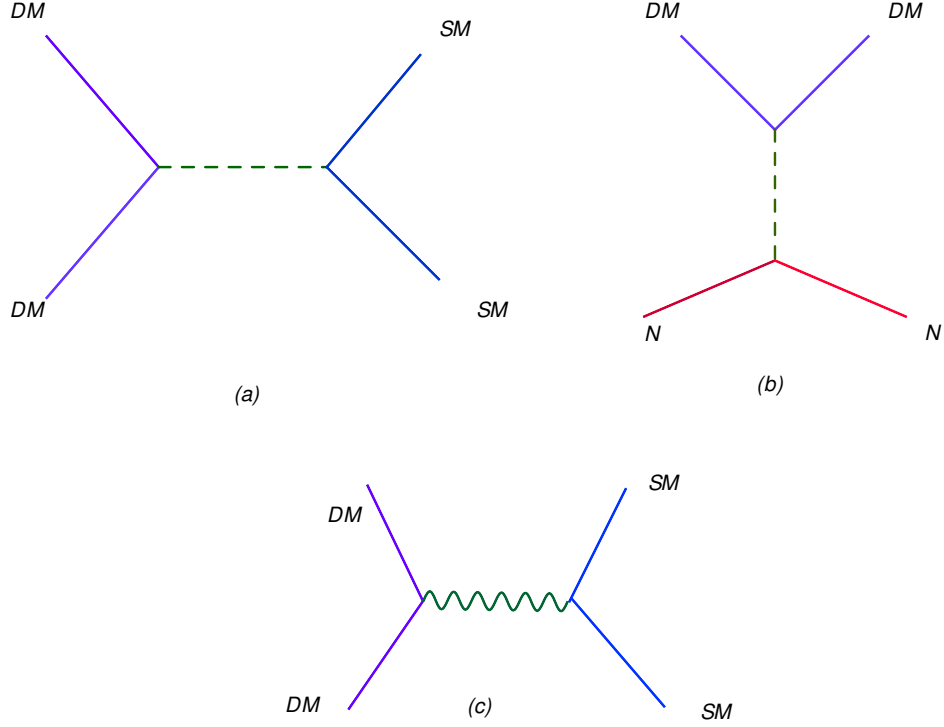


FIG. 6: (a) Scalar mediated DM annihilation (b) Direct detection and (c)  $Z'$  mediated DM annihilation.

Then the DM candidate can annihilate through the scalar portal (Fig. 6a), where interactions between  $h_2$  and SM particles are induced by scalar mixing (See Eq.3.8) and these couplings are equal to the SM Higgs couplings times  $\sin \theta$ . In addition, the DM can annihilate to the SM particles via  $Z'$  exchange (Fig. 6c) where the gauge interactions are given by,

$$\mathcal{L} \supset -\frac{x_\Phi g'}{2} Z'_\mu (\cos^2 \theta \bar{\psi}_1 \gamma^\mu \gamma_5 \psi_1 + \sin^2 \theta \bar{\psi}_2 \gamma^\mu \gamma_5 \psi_2 - 2 \cos \theta \sin \theta \bar{\psi}_1 \gamma^\mu \gamma_5 \psi_2). \quad (6.6)$$

Furthermore, DM can annihilate into  $Z'Z'$  mode via scalar portal where the relevant scalar- $Z'Z'$  interaction is given by

$$\mathcal{L} \supset \frac{M_{Z'}^2}{u} \cos \theta h_2 Z' Z' - \frac{M_{Z'}^2}{u} \sin \theta h_1 Z' Z'. \quad (6.7)$$

## A. Relic density

Here we analyze the relic density of our DM candidate. The DM candidate  $\psi_1$  annihilate into the SM particles via processes induced by  $Z'$  and scalar boson interactions as shown in Fig. 6. Then we estimate the relic density using *micrOMEGAs 4.3.5* [58] implementing the relevant interactions. Firstly we focus on the parameter space where the  $Z'$  mediated process dominates for DM annihilation. For illustration, in Fig. 7, we show the relic density as a function of DM mass ( $M_{DM} \equiv m_{\psi_1}$ ) for  $m_{Z'} = 4$  TeV, fixing the other parameters as indicated in the plot. The plot indicates that the required gauge coupling is  $g' \gtrsim 0.5$  but it is excluded by the LHC data as we will see later. Note that in this case, the value of  $g'$  that gives the correct relic density depends on the choice of  $x_H$  and  $x_\Phi$  since the interaction strength of  $Z'$  with the other particles is a product of  $g'$  and a linear combination of  $x_H$  and  $x_\Phi$ . If we increase  $x_H$  and  $x_\Phi$ , then the value of  $g'$  that can give the correct relic density can be lowered. However, for smaller values of  $g'$ , the LHC constraints imply much lower values of  $M'_Z$  where the  $Z'$  exchange is not a dominant process. We also find that the  $Z'$  mediated process cannot provide sufficient annihilation cross section to explain the observed relic density if DM is heavier than  $\sim 3$  TeV, complying with the requirement that the gauge coupling satisfy  $(x_{q,d,u,l,e,\nu,\Phi})g'$ ,  $(x_H/2)g' < \sqrt{4\pi}$  for perturbativity. This tendency comes from the fact that the annihilation cross section is P-wave suppressed since our DM is Majorana fermion.

We will now focus on the contribution of  $h_2$  exchange process to the relic density of DM. For illustrating the effect of this process, we show the relic density as a function of DM mass for different values of  $y_{NS}^{33}$  and  $m_{h_2}$  in Fig. 8. In the left panel, we have fixed  $y_{NS}^{33} = 2.5$  and plotted the relic density as a function of  $M_{DM}$  for three different values of  $m_{h_2}$ , keeping all the other parameters fixed. Similarly, we have taken  $m_{h_2} = 13$  TeV in the right plot and plotted the relic density for three different values of  $y_{NS}^{33}$ . We find that the observed relic density can be realized for  $y_{NS}^{33} \gtrsim 2$  when  $m_{h_2} = 13$  TeV. In addition,  $m_{h_2} \sim 2M_{DM}$  is preferred to enhance the annihilation cross section which implies that  $m_{h_2}$  mass is around  $\mathcal{O}(10)$  TeV in our model. Note that such a heavy mass scale for  $h_2$  is also preferred in stabilizing the scalar potential as we already discussed in the previous section.

We perform a parameter scan and search for the allowed regions which can explain the relic

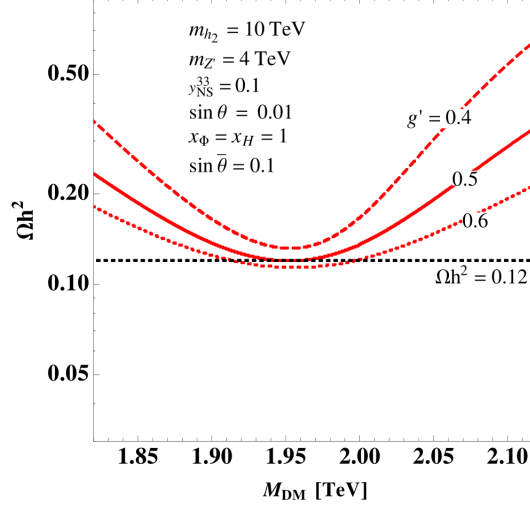


FIG. 7: Relic abundance as a function of DM mass for different values of  $g'$ . All the other parameters have been fixed as given in the plot.

density of DM. Firstly, we perform parameter scan in the following ranges focusing on the scalar exchange process,

$$\begin{aligned}
 M_{DM} \in [1.0, 10.0] \text{ TeV}, \quad m_{h_2} \in [1.8M_{DM}, 2.2M_{DM}], \quad y_{NS}^{33} \in [0.2, 3.0], \quad \sin \theta \in [0.001, 0.02], \\
 x_H \in [-5, 5], \quad x_\Phi \in [-5, 5], \quad \sin \bar{\theta} \in [0.2, 0.7], \quad m_{Z'} = 5 \text{ TeV}, \quad g' = 0.01.
 \end{aligned} \tag{6.8}$$

We fixed  $Z'$  mass and  $g'$  for simplicity. Note that we chose  $m_{h_2} \sim 2M_{DM}$  since we can obtain the observed relic density in this region via  $h_2$  exchange process as discussed above. In Fig. 9, we show the allowed parameter space in  $M_{DM} - y_{NS}^{33}$  and  $m_{h_2} - \sin \theta$  planes that give the correct relic density of DM,  $0.11 < \Omega h^2 < 0.13$ , adopting the approximate range around the best fit value [47]. From the left panel of Fig. 9, we can see that in general, for larger values of  $M_{DM}$ , the allowed values of  $y_{NS}^{33}$  are large. But, a few points with smaller values of  $y_{NS}^{33}$  are also obtained for  $M_{DM} > M_{Z'}$  since  $\psi_1 \psi_1 \rightarrow h_2 \rightarrow Z' Z'$  process is kinematically allowed there. In the right panel of Fig. 9, we have shown the allowed parameter space in the  $m_{h_2} - \sin \theta$  plane. From this plot, we can see that  $\sin \theta$  can be small for  $M_{DM} > M_{Z'}$  ( $m_{h_2} \sim 2M_{DM}$ ) since  $h_2 Z' Z'$  coupling is not suppressed by  $\sin \theta$  as we can see from Eq. (6.7). However, we have some lower limit of  $\sin \theta$  for  $M_{DM} < m_{Z'}$  since here,  $\psi_1 \psi_1 \rightarrow h_2 \rightarrow Z' Z'$  process is kinematically disallowed and the coupling

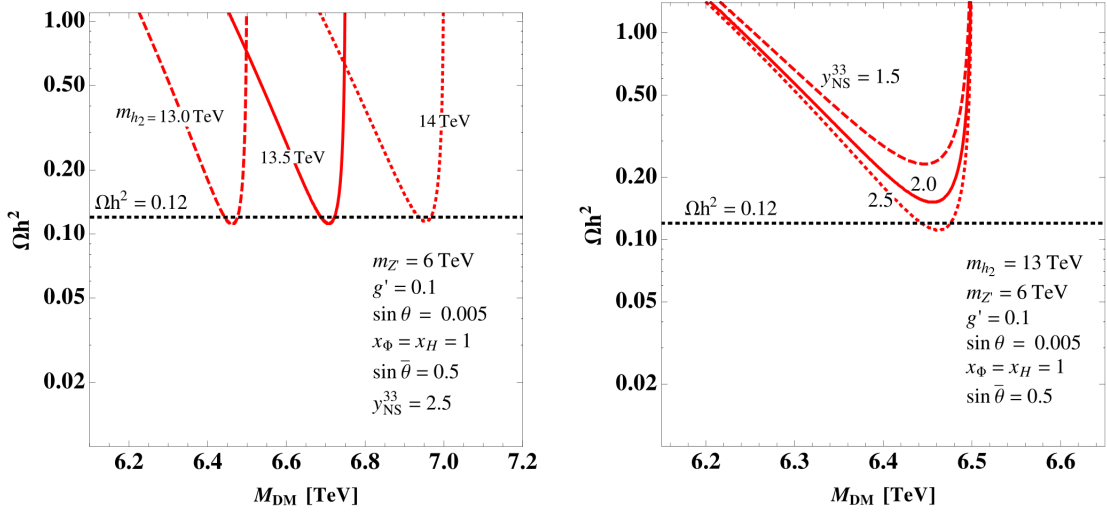


FIG. 8: Relic abundance as a function of DM mass : (a) For different values of  $y_{NS}^{33}$  and fixed  $m_{h_2} = 13$  TeV ; (b) For different values of  $m_{h_2}$  and fixed  $y_{NS}^{33} = 2.5$ .

of  $h_2$  to the SM particles is suppressed by  $\sin \theta$ .

## B. Direct detection

Here we briefly discuss the constraints from the direct detection experiments estimating the DM-nucleon ( $N$ ) scattering in our model. Firstly note that the  $Z'$  exchange process between DM and nucleon will not get stringent constraint since DM- $Z'$  interaction is via axial vector current due to the Majorana property of DM and provides spin-dependent operator for DM-nucleon interaction. We thus focus on the scalar mediated processes for DM-nucleon scattering where the corresponding Feynman diagram is given in Fig 6b. In our case, the DM interacts with the nucleon through the scalar boson exchange ( $h_1, h_2$ ). The relevant interaction Lagrangian with the mixing effect is given by,

$$\mathcal{L} \supset C_{\psi_1 \psi_1 h_1} h_1 \bar{\psi}_1^c \psi_1 + C_{\psi_1 \psi_1 h_2} h_2 \bar{\psi}_1^c \psi_1 + C_{NN h_1} h_1 \bar{N} N + C_{NN h_2} h_2 \bar{N} N, \quad (6.9)$$

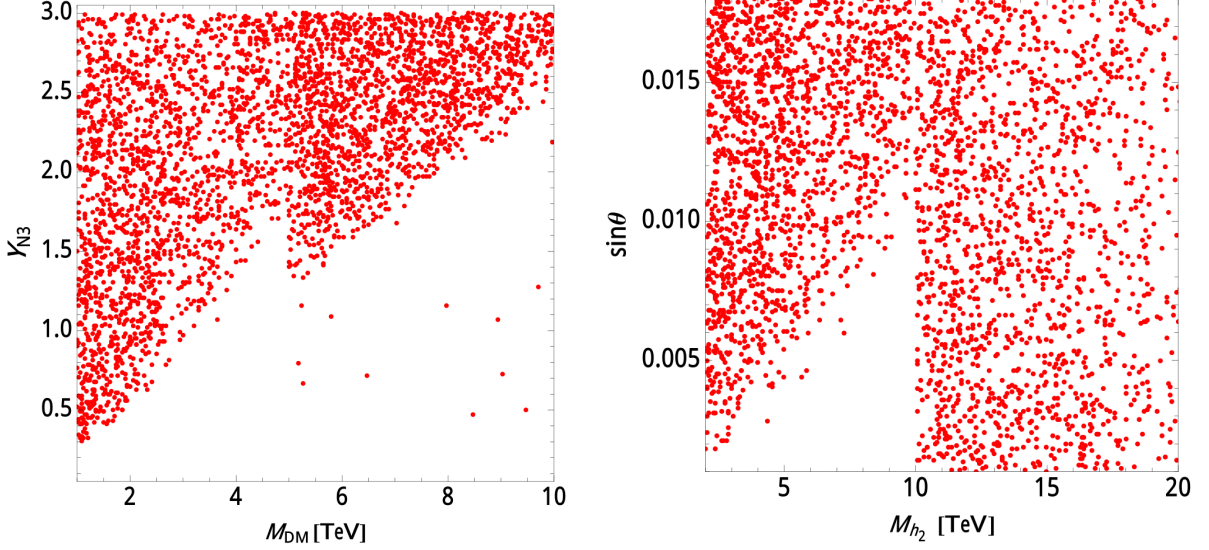


FIG. 9: Parameter regions that give the correct relic density of DM in  $M_{DM}$ - $y_{NS}^{33}$  and  $M_{h_2}$ - $\sin \theta$  planes for scanning done in the ranges of parameters as given by Eq. (6.8).

where the effective couplings are,

$$C_{\psi_1\psi_1h_1} = \sin \bar{\theta} \cos \bar{\theta} \cos \theta \frac{y_{NS}^{33}}{\sqrt{2}}, \quad C_{\psi_1\psi_1h_2} = -\sin \bar{\theta} \cos \bar{\theta} \sin \theta \frac{y_{NS}^{33}}{\sqrt{2}}, \quad (6.10)$$

$$C_{NNh_1} = \sin \theta g_{hNN}, \quad C_{NNh_2} = \cos \theta g_{hNN}. \quad (6.11)$$

Hence the effective Lagrangian can be written as,

$$\mathcal{L}_{eff} = G_h \bar{\psi}_1 \psi_1 \bar{N} N, \quad (6.12)$$

$$G_h = \left[ \frac{C_{\psi_1\psi_1h_1} C_{h_1NN}}{m_{h_1}^2} + \frac{C_{\psi_2\psi_2h_2} C_{h_2NN}}{m_{h_2}^2} \right] \quad (6.13)$$

where  $m_{h_1}$  and  $m_{h_2}$  are the SM and BSM Higgs masses. The corresponding cross section of Fig. 6b in the non-relativistic limit can be calculated as,

$$\sigma = g_{hNN}^2 \frac{M_{DM}^2 M_N^2}{16\pi (M_{DM}^2 + M_N^2)^2} (y_{NS}^{33} \sin 2\bar{\theta} \sin 2\theta)^2 \left( \frac{1}{m_{h_1}^2} - \frac{1}{m_{h_2}^2} \right)^2, \quad (6.14)$$

where,  $M_{DM}$  and  $M_N$  are the DM and nucleon masses respectively. The effective coupling can be written as  $g_{hNN} = \frac{f_N M_N}{v\sqrt{2}}$  where we apply  $f_N = 0.287$  for neutron [61]<sup>1</sup> and  $v = 246$  GeV. We

<sup>1</sup>  $f_N$  for proton has similar value and we here just use  $f_N$  in estimating the cross section.

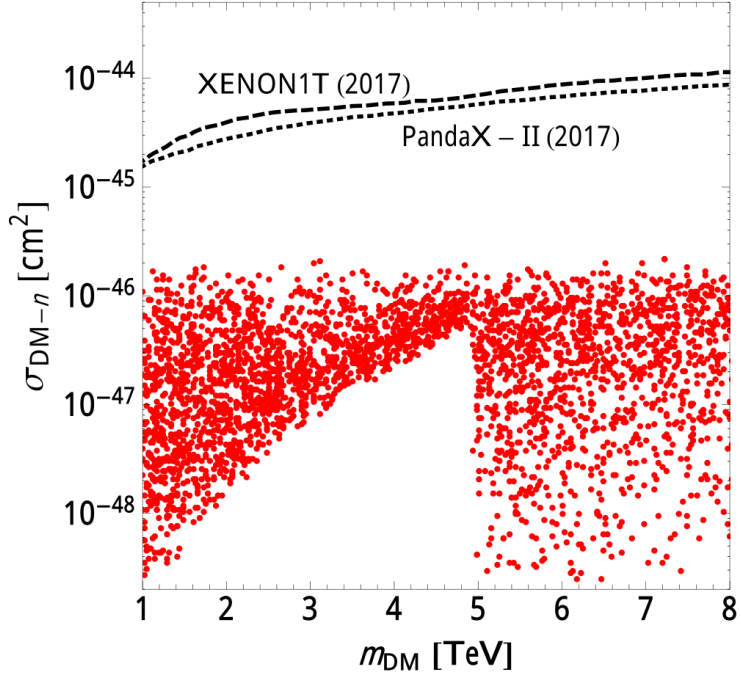


FIG. 10: Nucleon-DM scattering cross section as a function of DM mass for parameters that give the correct relic density. The current upper bounds from PANDAX-II [59] (black dotted line) and XENON-1t [60] (back dashed line) are also shown.

then estimate the cross sections applying allowed parameter sets obtained in previous subsection and the results are shown in Fig. 10. The black dotted and dashed lines show the current upper bounds from PANDAX-II [59] and XENON-1t [60] respectively. We find that our parameter region is allowed by the direct detection constraints since the cross section is suppressed by small  $\sin \theta$  which is also preferred by the constraints from vacuum stability. The cross section will be further explored by the future direct detection experiments like XENON 1t, PandaX, etc.

## VII. BOUNDS ON THE $M'_Z - g'$ PLANE

In this section, we consider the production of  $Z'$  from the proton proton collision at the LHC and its decay into different types of leptons. We first calculate the  $Z'$  production cross section at the LHC from protons followed by the decay into lepton,  $pp \rightarrow Z' \rightarrow \ell^+\ell^-$  with  $\ell = e, \mu$ .

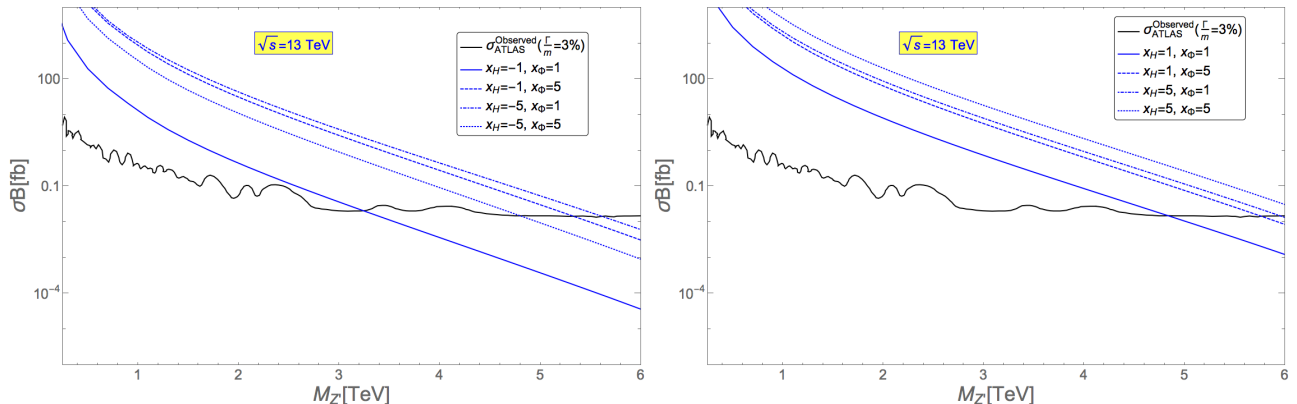


FIG. 11: Comparison between the ATLAS [40] (black solid line) result and model cross sections (blue lines) for the different values of  $x_H$  and  $x_\Phi$ . The model cross sections are produced with  $g_{\text{Model}} = 0.05$ . The left and right panels correspond to  $x_H < 0$  and  $x_H > 0$  respectively and we have considered  $x_\Phi > 0$  for both the cases.

In our analysis we calculate the cross section combining the electron and muon final states. We compare our cross section with the latest ATLAS search [40] for the heavy  $Z'$  resonance. Since we are considering  $U(1)'$  models with extra  $Z'$ , the ATLAS results can be compared directly with our results. Atlas analysis has considered different models like SSM and  $Z'_\psi$  [62] where the  $Z'$  decays into  $e$  and  $\mu$ . Conservatively considering these limits for our case we first produce the  $Z'$  ( $300 \text{ GeV} \leq M'_Z \leq 6 \text{ TeV}$ ) at the 13 TeV LHC followed by the decay into the dilepton mode and finally compare with the cross sections in our model. To calculate the bounds on the  $g'$ , we calculate the model cross section,  $\sigma_{\text{Model}}$ , for the process  $pp \rightarrow Z' \rightarrow 2e, 2\mu$ , with a  $U(1)'$  coupling constant  $g_{\text{Model}}$  at the LHC at the 13TeV center of mass energy. Then we compare this with the observed ATLAS bound ( $\sigma_{\text{ATLAS}}^{\text{Observed}}$ ) for  $\frac{\Gamma}{m} = 3\%$  which has been studied for the SSM. The corresponding cross sections are plotted in Fig. 11 for different choices of  $x_H$  and  $x_\Phi$ . Thus, the value of  $g'$  corresponding to a given  $M_{Z'}$  is given as,

$$g' = \sqrt{\frac{\sigma_{\text{ATLAS}}^{\text{Observed}}}{\left(\frac{\sigma_{\text{Model}}}{g_{\text{Model}}^2}\right)}}, \quad (7.1)$$

since the cross section varies with the square of the  $U(1)'$  coupling ( $g_{\text{Model}}^2$ ).



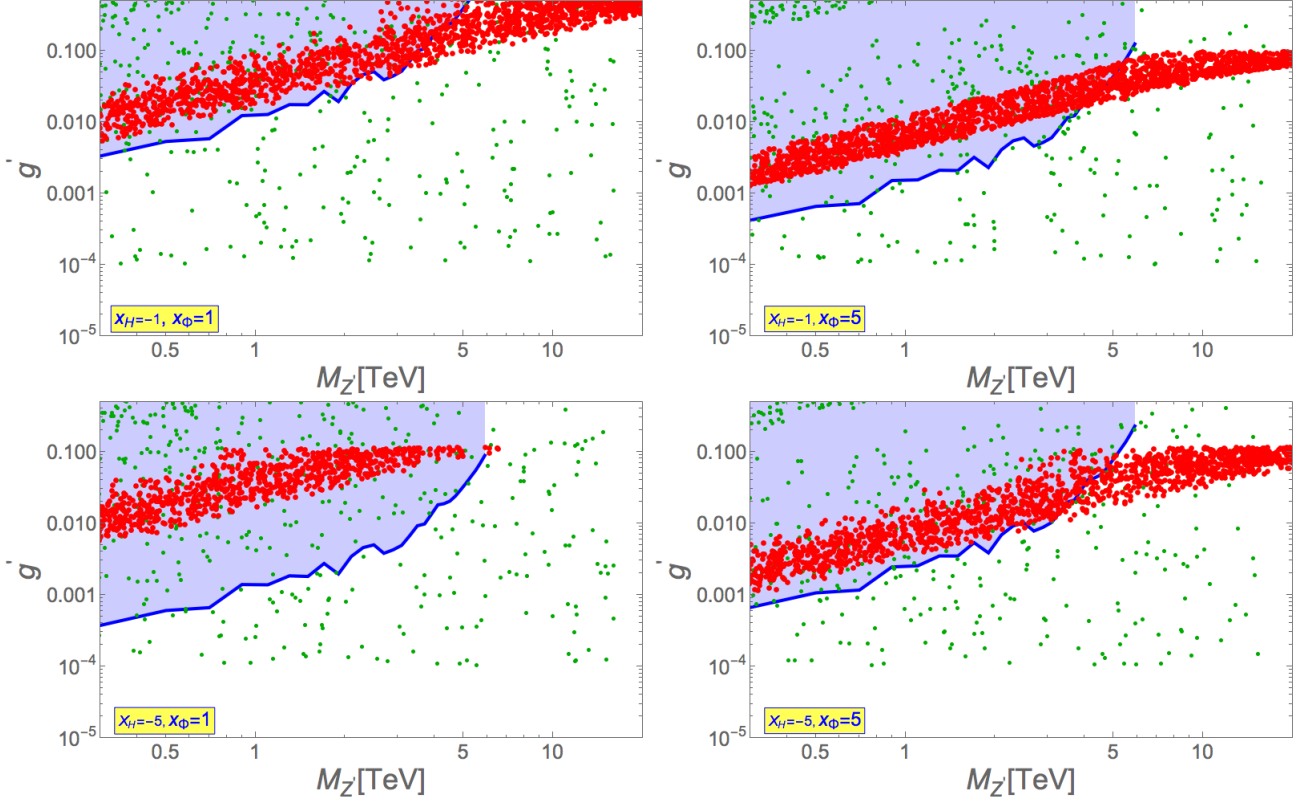


FIG. 12: Allowed parameter space combining the bounds obtained on  $g'$  as a function of  $M'_Z$  from vacuum stability and perturbativity (red dots), DM constraints (green dots) and collider (region below the blue solid line). The blue shaded regions are ruled out by the recent ATLAS search [40] at  $139 \text{ fb}^{-1}$  luminosity.

In this analysis we consider several choices of the  $x_H$  and  $x_\Phi$  to calculate the bounds in the  $M'_Z - g'$  plane. These correspond to two scenarios : (1)  $x_H$  is negative and  $x_\Phi$  is positive for which the results are shown in Fig. 12 and (2) both  $x_H$  and  $x_\Phi$  are positive and the corresponding constraints in the  $M'_Z - g'$  plane are shown in Fig. 13. The interaction of the  $Z'$  with the fermions via the covariant derivative will depend on the  $x_H$  and  $x_\Phi$  values and is given by the Lagrangian,

$$-L_{int} \supset \overline{f_L} \gamma^\mu g' Q_x Z'_\mu f_L + \overline{f_R} \gamma^\mu g' Q'_x Z'_\mu f_R. \quad (7.2)$$

Here,  $f_L$  and  $f_R$  are the left handed and right handed fermions and  $Q_x$  and  $Q'_x$  are the corresponding charges under the  $U(1)'$  gauge group. These charges are linear combinations of  $x_H$  and

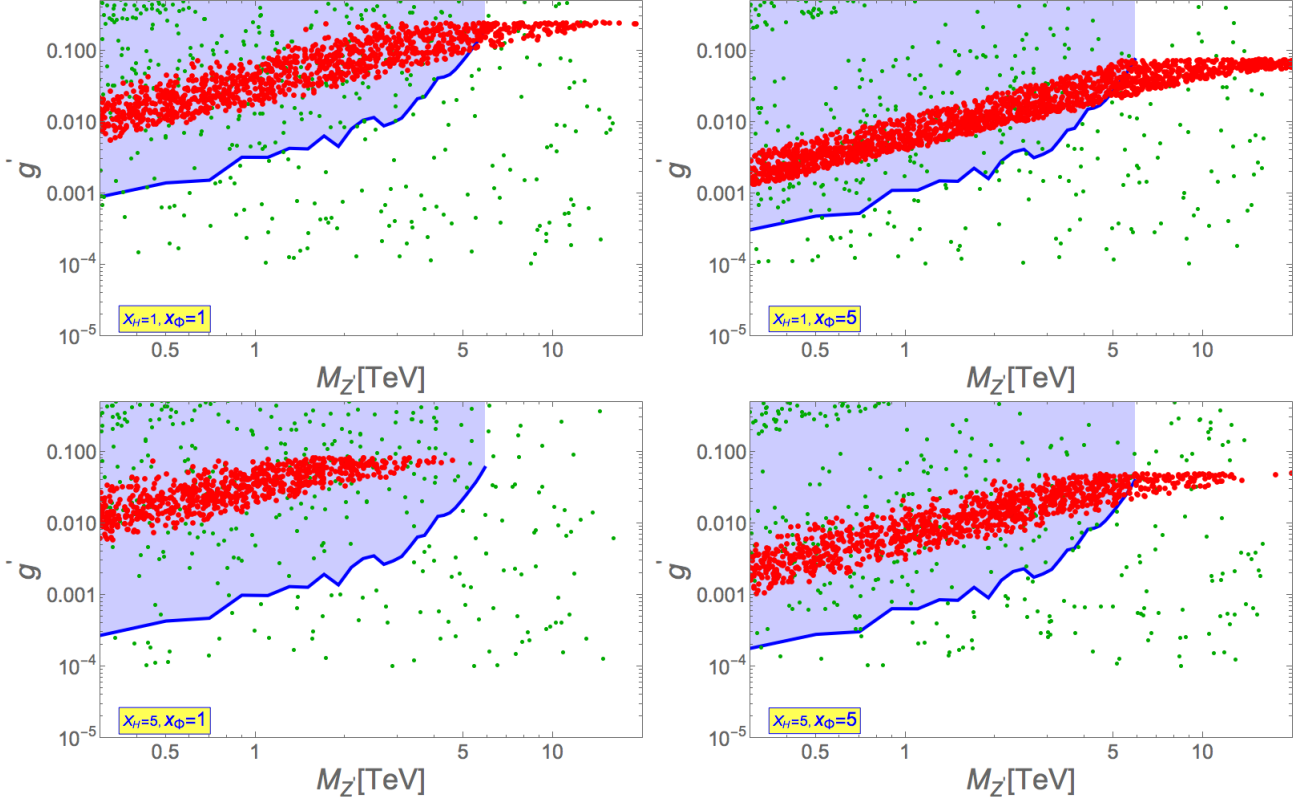


FIG. 13: Allowed parameter space combining the bounds obtained on  $g'$  as a function of  $M'_Z$  from vacuum stability and perturbativity (red dots), DM constraints (green dots) and collider (region below the blue solid line). The blue shaded regions are ruled out by the recent ATLAS search [40] at  $139 \text{ fb}^{-1}$  luminosity.

$x_\Phi$  and will appear in the  $C_V$  and  $C_A$  coefficients of the  $Z'$  interactions. The  $Z'$  interaction with the colored fermions will contain the color factor  $N_c = 3$  in the interaction whereas  $N_c = 1$  for the uncolored fermions. The bounds from the collider for various models are shown by the blue solid lines in Figs. 12 and 13. The blue shaded regions in these figures are ruled out by the current LHC data obtained from the ATLAS experiment [40] at  $139 \text{ fb}^{-1}$  luminosity.

In these figures, we have also given the bounds from vacuum stability, perturbativity and relic density for purposes of comparison. For finding the regions that are allowed by vacuum stability and perturbativity, we have done a scanning in the following ranges of parameters,

$$g' \in [0.0001, 1.0], \quad u \in [0.3, 100] \text{ TeV} \quad m_{h_2} \in [2.0, 16] \text{ TeV}, \quad y_{NS}^{33} \in [0.2, 2.5], \quad (7.3)$$

with  $\theta = 0.01$ . For  $Y_\nu$  and  $(y_{NS})_{2 \times 2}$ , we have used BM-I from the Table II and we have scaled  $y_{NS}$  according to the variation in  $u$ . The values of  $M_{Z'}$  have been calculated using Eq.5.2 and the allowed regions are shown by the red points in Figs. 12 and 13. It can be seen from these figures that the bulk of the parameter space allowed by vacuum stability lies in the region disfavoured by the ATLAS results. Regions beyond  $M_{Z'} > 5 \text{ TeV}$  that is not explored by ATLAS are seen to be allowed by vacuum stability and perturbativity constraints. Future ATLAS results will be able to explore this region.

Similarly, to find out the points that can give the correct DM relic density, we have performed a scanning of parameters in the ranges,

$$g' \in [0.0001, 1.0], \quad m_{Z'} \in [0.1, 16] \text{ TeV} \quad m_{h_2} \in [2.0, 16] \text{ TeV}, \\ y_{NS}^{33} \in [0.2, 2.5], M_{DM} \in [1.0, 10.0] \text{ TeV}. \quad (7.4)$$

Here also, we have fixed  $\theta = 0.01$ . The green dots in Figs. 12 and 13 correspond to the values that give the correct DM relic density. The constraints coming from this is seen to be less stringent than the combined constraints from vacuum stability, perturbativity and ATLAS analysis.

## VIII. CONCLUDING REMARKS

In this paper we have studied the inverse seesaw model in a class of general  $U(1)$  extensions of the SM. We have studied the parameter spaces in various planes that are allowed by vacuum stability and perturbativity as well as consistent with the low energy neutrino data. In addition, this model has a prospective DM candidate resulting from the stabilization of the third generations of the  $SU(2)_L$  singlet neutral fermions using the odd parity under the discrete  $Z_2$  symmetry. Comparing the  $Z'$  production and its decay into the dilepton mode at the LHC with the current ATLAS results, we find the bounds on the  $U(1)'$  coupling constant with respect to the  $Z'$  mass. Finally, combining all the constraints, we obtain the resultant allowed parameter space which can be probed in the future experiments.

## ACKNOWLEDGMENTS

This work of A. D. is supported by the Japan Society for the Promotion of Science (JSPS) Postdoctoral Fellowship for Research in Japan.

### A. ONE-LOOP RG EQUATIONS

$$\begin{aligned} \beta_{g_1} = \frac{1}{6} & \left( 41g_1^3 + g_1^2 g_{1p1} (78x_H + 64x_\Phi) + g_{11p} g_{1p1} (39g_{11p} x_H + 41g' x_H^2 + 32g_{11p} x_\Phi \right. \\ & + 64g' x_H x_\Phi + 66g' x_\Phi^2) + g_1 (41g_{11p}^2 + g_{11p} g' (39x_H + 32x_\Phi) \\ & \left. + g_{1p1}^2 (41x_H^2 + 64x_H x_\Phi + 66x_\Phi^2)) \right) \end{aligned} \quad (1.1)$$

$$\beta_{g_2} = \frac{(-19g_2^3)}{6} \quad (1.2)$$

$$\beta_{g_3} = (-7g_3^3) \quad (1.3)$$

$$\begin{aligned} \beta_{g'} = \frac{1}{6} & \left( 41g_{11p}^2 g' + g_{11p} (41g_1 g_{1p1} + (2g'^2 + g_{1p1}^2) (39x_H + 32x_\Phi)) \right. \\ & \left. + g' (g_1 g_{1p1} (39x_H + 32x_\Phi) + (g'^2 + g_{1p1}^2) (41x_H^2 + 64x_H x_\Phi + 66x_\Phi^2)) \right) \end{aligned} \quad (1.4)$$

$$\begin{aligned} \beta_{g_{1p1}} = \frac{1}{6} & \left( 41g_1^2 g_{1p1} + g_1 (41g_{11p} g' + (g'^2 + 2g_{1p1}^2) (39x_H + 32x_\Phi)) + \right. \\ & \left. g_{1p1} (g_{11p} g' (39x_H + 32x_\Phi) + (g'^2 + g_{1p1}^2) (41x_H^2 + 64x_H x_\Phi + 66x_\Phi^2)) \right) \end{aligned} \quad (1.5)$$

$$\begin{aligned} \beta_{g_{11p}} = \frac{1}{6} & \left( g_1^2 (41g_{11p} + 39g' x_H + 32g' x_\Phi) + g_1 g_{1p1} (39g_{11p} x_H + 41g' x_H^2 + 32g_{11p} x_\Phi \right. \\ & + 64g' x_H x_\Phi + 66g' x_\Phi^2) + g_{11p} (41g_{11p}^2 + g_{11p} g' (78x_H + 64x_\Phi) \\ & \left. + g'^2 (41x_H^2 + 64x_H x_\Phi + 66x_\Phi^2)) \right) \end{aligned} \quad (1.6)$$

$$\begin{aligned}
\beta_{\lambda_1} = \frac{1}{8} & \left( 3g_1^4 + 6g_1^2g_{11p}^2 + 3g_{11p}^4 + 6g_1^2g_2^2 + 6g_{11p}^2g_2^2 + 9g_2^4 - 24g_1^2\lambda_1 - 24g_{11p}^2\lambda_1 - 72g_2^2\lambda_1 \right. \\
& + 192\lambda_1^2 + 8\lambda_3^2 - 12g_1^2g_{11p}g'x_H - 12g_{11p}^3g'x_H - 12g_1^3g_{1p1}x_H - 12g_1g_{11p}^2g_{1p1}x_H \\
& - 12g_{11p}g'g_2^2x_H - 12g_1g_{1p1}g_2^2x_H + 48g_{11p}g'\lambda_1x_H + 48g_1g_{1p1}\lambda_1x_H + 6g_1^2g'^2x_H^2 \\
& + 18g_{11p}^2g'^2x_H^2 + 24g_1g_{11p}g'g_{1p1}x_H^2 + 18g_1^2g_{1p1}^2x_H^2 + 6g_{11p}^2g_{1p1}^2x_H^2 + 6g'^2g_2^2x_H^2 \\
& + 6g_{1p1}^2g_2^2x_H^2 - 24g'^2\lambda_1x_H^2 - 24g_{1p1}^2\lambda_1x_H^2 - 12g_{11p}g'^3x_H^3 - 12g_1g'^2g_{1p1}x_H^3 \\
& - 12g_{11p}g'g_{1p1}^2x_H^3 - 12g_1g_{1p1}^3x_H^3 + 3g'^4x_H^4 + 6g'^2g_{1p1}^2x_H^4 + 3g_{1p1}^4x_H^4 + 96\lambda_1y_t^2 \\
& \left. + 32\lambda_1\text{Tr}[Y_\nu Y_\nu^\dagger] - 48y_t^4 - 16\text{Tr}[Y_\nu Y_\nu^\dagger Y_\nu Y_\nu^\dagger] \right) \quad (1.7)
\end{aligned}$$

$$\beta_{\lambda_2} = \left( 10\lambda_2^2 + \lambda_3^2 - 6g'^2\lambda_2x_\Phi^2 - 6g_{1p1}^2\lambda_2x_\Phi^2 + 3g'^4x_\Phi^4 + 2\lambda_2\text{Tr}[y_{NS}y_{NS}^\dagger] - \text{Tr}[y_{NS}y_{NS}^\dagger y_{NS}y_{NS}^\dagger] \right) \quad (1.8)$$

$$\begin{aligned}
\beta_{\lambda_3} = \frac{1}{2} & \left( -3g_1^2\lambda_3 - 3g_{11p}^2\lambda_3 - 9g_2^2\lambda_3 + 24\lambda_1\lambda_3 + 16\lambda_2\lambda_3 + 8\lambda_3^2 + 6g_{11p}g'\lambda_3x_H + 6g_1g_{1p1}\lambda_3x_H \right. \\
& - 3g'^2\lambda_3x_H^2 - 3g_{1p1}^2\lambda_3x_H^2 + 6g_{11p}^2g'^2x_\Phi^2 - 12g'^2\lambda_3x_\Phi^2 - 12g_{1p1}^2\lambda_3x_\Phi^2 - 12g_{11p}g'^3x_Hx_\Phi^2 \\
& \left. + 6g'^4x_Hx_\Phi^2 + 12\lambda_3y_t^2 + 4\lambda_3\text{Tr}[Y_\nu Y_\nu^\dagger] + 4\lambda_3\text{Tr}[y_{NS}y_{NS}^\dagger] - 8\text{Tr}[y_{NS}y_{NS}^\dagger Y_\nu Y_\nu^\dagger] \right) \quad (1.9)
\end{aligned}$$

$$\begin{aligned}
\beta_{y_t^{(1)}} = \frac{1}{12} & \left( - \left( (17g_1^2 + 17g_{11p}^2 + 27g_2^2 + 96g_3^2 + 34g_{11p}g'x_H + 34g_1g_{1p1}x_H + 17g'^2x_H^2 \right. \right. \\
& + 17g_{1p1}^2x_H^2 + 20g_{11p}g'x_\Phi + 20g_1g_{1p1}x_\Phi + 20g'^2x_Hx_\Phi + 20g_{1p1}^2x_Hx_\Phi + 8g'^2x_\Phi^2 \\
& \left. \left. + 8g_{1p1}^2x_\Phi^2 - 36y_t^2 - 12\text{Tr}[Y_\nu Y_\nu^\dagger] \right) y_t \right) + 18(y_t^3) \quad (1.10)
\end{aligned}$$

$$\beta_{y_{NS}^{(1)}} = \left( \left( -3(g'^2 + g_{1p1}^2)x_\Phi^2 + \text{Tr}[y_{NS}y_{NS}^\dagger] \right) y_{NS} + y_{NS}y_{NS}^\dagger y_{NS} + Y_\nu^T Y_\nu^* y_{NS} \right) \quad (1.11)$$

$$\begin{aligned}
\beta_{Y_\nu^{(1)}} = \frac{1}{4} & \left( - \left( (3g_1^2 + 3g_{11p}^2 + 9g_2^2 + 6g_{11p}g'x_H + 6g_1g_{1p1}x_H + 3g'^2x_H^2 + 3g_{1p1}^2x_H^2 \right. \right. \\
& + 12g_{11p}g'x_\Phi + 12g_1g_{1p1}x_\Phi + 12g'^2x_Hx_\Phi + 12g_{1p1}^2x_Hx_\Phi + 24g'^2x_\Phi^2 \\
& \left. \left. + 24g_{1p1}^2x_\Phi^2 - 12y_t^2 - 4\text{Tr}[Y_\nu Y_\nu^\dagger] \right) Y_\nu \right) + 2(3Y_\nu Y_\nu^\dagger Y_\nu + Y_\nu y_{NS}^* y_{NS}^T) \quad (1.12)
\end{aligned}$$

## B. TWO-LOOP RG EQUATIONS

$$\begin{aligned}
\beta_{g_1}^{(2)} = & \frac{1}{18} \left( 199g_1^5 + 398g_1^3g_{11p}^2 + 199g_1g_{11p}^4 + 81g_1^3g_2^2 + 81g_1g_{11p}^2g_2^2 + 264g_1^3g_3^2 + 264g_1g_{11p}^2g_3^2 + 543g_1^3g_{11p}g'x_H \right. \\
& + 543g_1g_{11p}^3g'x_H + 724g_1^4g_{1p1}x_H + 905g_1^2g_{11p}^2g_{1p1}x_H + 181g_{11p}^4g_{1p1}x_H + 27g_1g_{11p}g'g_2^2x_H \\
& + 54g_1^2g_{1p1}g_2^2x_H + 27g_{11p}^2g_{1p1}g_2^2x_H + 264g_1g_{11p}g'g_3^2x_H + 528g_1^2g_{1p1}g_3^2x_H + 264g_{11p}^2g_{1p1}g_3^2x_H \\
& + 199g_1^3g'^2x_H^2 + 597g_1g_{11p}^2g'^2x_H^2 + 1393g_1^2g_{11p}g'g_{1p1}x_H^2 + 597g_{11p}^3g'g_{1p1}x_H^2 + 1194g_1^3g_{1p1}^2x_H^2 \\
& + 796g_1g_{11p}^2g_{1p1}^2x_H^2 + 81g_{11p}g'g_{1p1}g_2^2x_H^2 + 81g_1g_{1p1}^2g_2^2x_H^2 + 264g_{11p}g'g_{1p1}g_3^2x_H^2 + 264g_1g_{1p1}^2g_3^2x_H^2 \\
& + 181g_1g_{11p}g'^3x_H^3 + 362g_1^2g'^2g_{1p1}x_H^3 + 543g_{11p}^2g'^2g_{1p1}x_H^3 + 905g_1g_{11p}g'g_{1p1}^2x_H^3 + 724g_1^2g_{1p1}^3x_H^3 \\
& + 181g_{11p}^2g_{1p1}^3x_H^3 + 199g_{11p}g'^3g_{1p1}x_H^4 + 199g_1g'^2g_{1p1}^2x_H^4 + 199g_{11p}g'g_{1p1}^3x_H^4 + 199g_1g_{1p1}^4x_H^4 \\
& + 492g_1^3g_{11p}g'x_\Phi + 492g_1g_{11p}^3g'x_\Phi + 656g_1^4g_{1p1}x_\Phi + 820g_1^2g_{11p}^2g_{1p1}x_\Phi + 164g_{11p}^4g_{1p1}x_\Phi \\
& + 108g_1g_{11p}g'g_2^2x_\Phi + 216g_1^2g_{1p1}g_2^2x_\Phi + 108g_{11p}^2g_{1p1}g_2^2x_\Phi + 96g_1g_{11p}g'g_3^2x_\Phi + 192g_1^2g_{1p1}g_3^2x_\Phi \\
& + 96g_{11p}^2g_{1p1}g_3^2x_\Phi + 328g_1^3g'^2x_Hx_\Phi + 984g_1g_{11p}^2g'^2x_Hx_\Phi + 2296g_1^2g_{11p}g'g_{1p1}x_Hx_\Phi + 984g_{11p}^3g'g_{1p1}x_Hx_\Phi \\
& + 1968g_1^3g_{1p1}^2x_Hx_\Phi + 1312g_1g_{11p}^2g_{1p1}^2x_Hx_\Phi + 216g_{11p}g'g_{1p1}g_2^2x_Hx_\Phi + 216g_1g_{1p1}^2g_2^2x_Hx_\Phi \\
& + 192g_{11p}g'g_{1p1}g_3^2x_Hx_\Phi + 192g_1g_{1p1}^2g_3^2x_Hx_\Phi + 492g_1g_{11p}g'^3x_H^2x_\Phi + 984g_1^2g'^2g_{1p1}x_H^2x_\Phi \\
& + 1476g_{11p}^2g'^2g_{1p1}x_H^2x_\Phi + 2460g_1g_{11p}g'g_{1p1}^2x_H^2x_\Phi + 1968g_1^2g_{1p1}^3x_H^2x_\Phi + 492g_{11p}^2g_{1p1}^3x_H^2x_\Phi \\
& + 656g_{11p}g'^3g_{1p1}x_H^3x_\Phi + 656g_1g'^2g_{1p1}^2x_H^3x_\Phi + 656g_{11p}g'g_{1p1}^3x_H^3x_\Phi + 656g_1g_{1p1}^4x_H^3x_\Phi + 184g_1^3g'^2x_\Phi^2 \\
& + 552g_1g_{11p}^2g'^2x_\Phi^2 + 1288g_1^2g_{11p}g'g_{1p1}x_\Phi^2 + 552g_{11p}^3g'g_{1p1}x_\Phi^2 + 1104g_1^3g_{1p1}^2x_\Phi^2 + 736g_1g_{11p}^2g_{1p1}^2x_\Phi^2 \\
& + 216g_{11p}g'g_{1p1}g_2^2x_\Phi^2 + 216g_1g_{1p1}^2g_2^2x_\Phi^2 + 192g_{11p}g'g_{1p1}g_3^2x_\Phi^2 + 192g_1g_{1p1}^2g_3^2x_\Phi^2 + 552g_1g_{11p}g'^3x_Hx_\Phi^2 \\
& + 1104g_1^2g'^2g_{1p1}x_Hx_\Phi^2 + 1656g_{11p}^2g'^2g_{1p1}x_Hx_\Phi^2 + 2760g_1g_{11p}g'g_{1p1}^2x_Hx_\Phi^2 + 2208g_1^2g_{1p1}^3x_Hx_\Phi^2 \\
& + 552g_{11p}^2g_{1p1}^3x_Hx_\Phi^2 + 1104g_{11p}g'^3g_{1p1}x_H^2x_\Phi^2 + 1104g_1g'^2g_{1p1}^2x_H^2x_\Phi^2 + 1104g_{11p}g'g_{1p1}^3x_H^2x_\Phi^2 \\
& + 1104g_1g_{1p1}^4x_H^2x_\Phi^2 + 224g_1g_{11p}g'^3x_\Phi^3 + 448g_1^2g'^2g_{1p1}x_\Phi^3 + 672g_{11p}^2g'^2g_{1p1}x_\Phi^3 + 1120g_1g_{11p}g'g_{1p1}^2x_\Phi^3 \\
& + 896g_1^2g_{1p1}^3x_\Phi^3 + 224g_{11p}^2g_{1p1}^3x_\Phi^3 + 896g_{11p}g'^3g_{1p1}x_Hx_\Phi^3 + 896g_1g'^2g_{1p1}^2x_Hx_\Phi^3 + 896g_{11p}g'g_{1p1}^3x_Hx_\Phi^3 \\
& + 896g_1g_{1p1}^4x_Hx_\Phi^3 + 520g_{11p}g'^3g_{1p1}x_\Phi^4 + 520g_1g'^2g_{1p1}^2x_\Phi^4 + 520g_{11p}g'g_{1p1}^3x_\Phi^4 + 520g_1g_{1p1}^4x_\Phi^4 - 51g_1^3y_t^2 \\
& - 51g_1g_{11p}^2y_t^2 - 51g_1g_{11p}g'x_Hy_t^2 - 102g_1^2g_{1p1}x_Hy_t^2 - 51g_{11p}^2g_{1p1}x_Hy_t^2 - 51g_{11p}g'g_{1p1}x_H^2y_t^2 \\
& - 51g_1g_{1p1}^2x_H^2y_t^2 - 30g_1g_{11p}g'x_\Phi y_t^2 - 60g_1^2g_{1p1}x_\Phi y_t^2 - 30g_{11p}^2g_{1p1}x_\Phi y_t^2 - 60g_{11p}g'g_{1p1}x_Hx_\Phi y_t^2
\end{aligned}$$

$$\begin{aligned}
& -60g_1g_{1p1}^2x_Hx_\Phi y_t^2 - 24g_{11p}g'g_{1p1}x_\Phi^2y_t^2 - 24g_1g_{1p1}^2x_\Phi^2y_t^2 + \text{Tr}[Y_\nu Y_\nu^\dagger] \left( -9g_1^3 - 9g_1g_{11p}^2 - 9g_1g_{11p}g'x_H \right. \\
& - 18g_1^2g_{1p1}x_H - 9g_{11p}^2g_{1p1}x_H - 9g_{11p}g'g_{1p1}x_H^2 - 9g_1g_{1p1}^2x_H^2 - 18g_1g_{11p}g'x_\Phi - 36g_1^2g_{1p1}x_\Phi \\
& \left. - 18g_{11p}^2g_{1p1}x_\Phi - 36g_{11p}g'g_{1p1}x_Hx_\Phi - 36g_1g_{1p1}^2x_Hx_\Phi - 72g_{11p}g'g_{1p1}x_\Phi^2 - 72g_1g_{1p1}^2x_\Phi^2 \right) \\
& - 18g_{11p}g'g_{1p1}x_\Phi^2 \text{Tr}[y_{NS}y_{NS}^\dagger] - 18g_1g_{1p1}^2x_\Phi^2 \text{Tr}[y_{NS}y_{NS}^\dagger] \Big)
\end{aligned} \tag{2.1}$$

$$\begin{aligned}
\beta_{g_2}^{(2)} = & \frac{g_2^3}{6} \left( 9g_1^2 + 9g_{11p}^2 + 35g_2^2 + 72g_3^2 + 6g_{11p}g'x_H + 6g_1g_{1p1}x_H + 9g'^2x_H^2 + 9g_{1p1}^2x_H^2 + 24g_{11p}g'x_\Phi \right. \\
& \left. + 24g_1g_{1p1}x_\Phi + 24g'^2x_Hx_\Phi + 24g_{1p1}^2x_Hx_\Phi + 24g'^2x_\Phi^2 + 24g_{1p1}^2x_\Phi^2 - 9y_t^2 - 3\text{Tr}[Y_\nu Y_\nu^\dagger] \right)
\end{aligned} \tag{2.2}$$

$$\begin{aligned}
\beta_{g_3}^{(2)} = & \frac{g_3^3}{6} \left( 11g_1^2 + 11g_{11p}^2 + 27g_2^2 - 156g_3^2 + 22g_{11p}g'x_H + 22g_1g_{1p1}x_H + 11g'^2x_H^2 + 11g_{1p1}^2x_H^2 \right. \\
& \left. + 8g_{11p}g'x_\Phi + 8g_1g_{1p1}x_\Phi + 8g'^2x_Hx_\Phi + 8g_{1p1}^2x_Hx_\Phi + 8g'^2x_\Phi^2 + 8g_{1p1}^2x_\Phi^2 - 12y_t^2 \right)
\end{aligned} \tag{2.3}$$

$$\begin{aligned}
\beta_{g'}^{(2)} = & \frac{1}{18} \left( 199g_1^2g_{11p}^2g' + 199g_{11p}^4g' + 199g_1^3g_{11p}g_{1p1} + 199g_1g_{11p}^3g_{1p1} + 81g_{11p}^2g'g_2^2 + 81g_1g_{11p}g_{1p1}g_2^2 \right. \\
& + 264g_{11p}^2g'g_3^2 + 264g_1g_{11p}g_{1p1}g_3^2 + 362g_1^2g_{11p}g'^2x_H + 724g_{11p}^3g'^2x_H + 181g_1^3g'g_{1p1}x_H \\
& + 905g_1g_{11p}^2g'g_{1p1}x_H + 543g_1^2g_{11p}g_{1p1}^2x_H + 181g_{11p}^3g_{1p1}^2x_H + 54g_{11p}g'^2g_2^2x_H + 27g_1g'g_{1p1}g_2^2x_H \\
& + 27g_{11p}g_{1p1}^2g_2^2x_H + 528g_{11p}g'^2g_3^2x_H + 264g_1g'g_{1p1}g_3^2x_H + 264g_{11p}g_{1p1}^2g_3^2x_H + 199g_1^2g'^3x_H^2 \\
& + 1194g_{11p}^2g'^3x_H^2 + 1393g_1g_{11p}g'^2g_{1p1}x_H^2 + 597g_1^2g'g_{1p1}^2x_H^2 + 796g_{11p}^2g'g_{1p1}^2x_H^2 + 597g_1g_{11p}g_{1p1}^3x_H^2 \\
& + 81g'^3g_2^2x_H^2 + 81g'g_{1p1}^2g_2^2x_H^2 + 264g'^3g_3^2x_H^2 + 264g'g_{1p1}^2g_3^2x_H^2 + 724g_{11p}g'^4x_H^3 \\
& + 543g_1g'^3g_{1p1}x_H^3 + 905g_{11p}g'^2g_{1p1}^3x_H^3 + 543g_1g'g_{1p1}^3x_H^3 + 181g_{11p}g_{1p1}^4x_H^3 + 199g'^5x_H^4 \\
& + 398g'^3g_{1p1}^2x_H^4 + 199g'g_{1p1}^4x_H^4 + 328g_1^2g_{11p}g'^2x_\Phi + 656g_{11p}^3g'^2x_\Phi + 164g_1^3g'g_{1p1}x_\Phi \\
& + 820g_1g_{11p}^2g'g_{1p1}x_\Phi + 492g_1^2g_{11p}g_{1p1}^2x_\Phi + 164g_{11p}^3g_{1p1}^2x_\Phi + 216g_{11p}g'^2g_2^2x_\Phi + 108g_1g'g_{1p1}g_2^2x_\Phi \\
& + 108g_{11p}g_{1p1}^2g_2^2x_\Phi + 192g_{11p}g'^2g_3^2x_\Phi + 96g_1g'g_{1p1}g_3^2x_\Phi + 96g_{11p}g_{1p1}^2g_3^2x_\Phi + 328g_1^2g'^3x_Hx_\Phi \\
& + 1968g_{11p}^2g'^3x_Hx_\Phi + 2296g_1g_{11p}g'^2g_{1p1}x_Hx_\Phi + 984g_1^2g'g_{1p1}^2x_Hx_\Phi + 1312g_{11p}^2g'g_{1p1}^2x_Hx_\Phi \\
& + 984g_1g_{11p}g_{1p1}^3x_Hx_\Phi + 216g'^3g_2^2x_Hx_\Phi + 216g'g_{1p1}^2g_2^2x_Hx_\Phi + 192g'^3g_3^2x_Hx_\Phi + 192g'g_{1p1}^2g_3^2x_Hx_\Phi \Big)
\end{aligned}$$

$$\begin{aligned}
& + 1968g_{11p}g'^4x_H^2x_\Phi + 1476g_1g'^3g_{1p1}x_H^2x_\Phi + 2460g_{11p}g'^2g_{1p1}^2x_H^2x_\Phi + 1476g_1g'g_{1p1}^3x_H^2x_\Phi \\
& + 492g_{11p}g_{1p1}^4x_H^2x_\Phi + 656g'^5x_H^3x_\Phi + 1312g'^3g_{1p1}^2x_H^3x_\Phi + 656g'g_{1p1}^4x_H^3x_\Phi + 184g_1^2g'^3x_\Phi^2 \\
& + 1104g_{11p}^2g'^3x_\Phi^2 + 1288g_1g_{11p}g'^2g_{1p1}x_\Phi^2 + 552g_1^2g'g_{1p1}^2x_\Phi^2 + 736g_{11p}^2g'g_{1p1}^2x_\Phi^2 + 552g_1g_{11p}g_{1p1}^3x_\Phi^2 \\
& + 216g'^3g_2^2x_\Phi^2 + 216g'g_{1p1}^2g_2^2x_\Phi^2 + 192g'^3g_3^2x_\Phi^2 + 192g'g_{1p1}^2g_3^2x_\Phi^2 + 2208g_{11p}g'^4x_Hx_\Phi^2 + 1104g'^5x_H^2x_\Phi^2 \\
& + 1656g_1g'^3g_{1p1}x_Hx_\Phi^2 + 2760g_{11p}g'^2g_{1p1}^2x_Hx_\Phi^2 + 1656g_1g'g_{1p1}^3x_Hx_\Phi^2 + 552g_{11p}g_{1p1}^4x_Hx_\Phi^2 \\
& + 2208g'^3g_{1p1}^2x_H^2x_\Phi^2 + 1104g'g_{1p1}^4x_H^2x_\Phi^2 + 896g_{11p}g'^4x_\Phi^3 + 672g_1g'^3g_{1p1}x_\Phi^3 + 1120g_{11p}g'^2g_{1p1}^2x_\Phi^3 \\
& + 672g_1g'g_{1p1}^3x_\Phi^3 + 224g_{11p}g_{1p1}^4x_\Phi^3 + 896g'^5x_Hx_\Phi^3 + 1792g'^3g_{1p1}^2x_Hx_\Phi^3 + 896g'g_{1p1}^4x_Hx_\Phi^3 \\
& + 520g'^5x_\Phi^4 + 1040g'^3g_{1p1}^2x_\Phi^4 + 520g'g_{1p1}^4x_\Phi^4 - 51g_{11p}^2g'y_t^2 - 51g_1g_{11p}g_{1p1}y_t^2 \\
& - 102g_{11p}g'^2x_Hy_t^2 - 51g_1g'g_{1p1}x_Hy_t^2 - 51g_{11p}g_{1p1}^2x_Hy_t^2 - 51g'^3x_H^2y_t^2 - 51g'g_{1p1}^2x_Hy_t^2 \\
& - 60g_{11p}g'^2x_\Phi y_t^2 - 30g_1g'g_{1p1}x_\Phi y_t^2 - 30g_{11p}g_{1p1}^2x_\Phi y_t^2 - 60g'^3x_Hx_\Phi y_t^2 - 60g'g_{1p1}^2x_Hx_\Phi y_t^2 \\
& - 24g'^3x_\Phi^2y_t^2 - 24g'g_{1p1}^2x_\Phi^2y_t^2 - 9g_{11p}^2g'\text{Tr}[Y_\nu Y_\nu^\dagger] - 9g_1g_{11p}g_{1p1}\text{Tr}[Y_\nu Y_\nu^\dagger] \\
& - 18g_{11p}g'^2x_H\text{Tr}[Y_\nu Y_\nu^\dagger] - 9g_1g'g_{1p1}x_H\text{Tr}[Y_\nu Y_\nu^\dagger] - 9g_{11p}g_{1p1}^2x_H\text{Tr}[Y_\nu Y_\nu^\dagger] - 9g'^3x_H^2\text{Tr}[Y_\nu Y_\nu^\dagger] \\
& - 9g'g_{1p1}^2x_H^2\text{Tr}[Y_\nu Y_\nu^\dagger] - 36g_{11p}g'^2x_\Phi\text{Tr}[Y_\nu Y_\nu^\dagger] - 18g_1g'g_{1p1}x_\Phi\text{Tr}[Y_\nu Y_\nu^\dagger] - 18g_{11p}g_{1p1}^2x_\Phi\text{Tr}[Y_\nu Y_\nu^\dagger] \\
& - 36g'^3x_Hx_\Phi\text{Tr}[Y_\nu Y_\nu^\dagger] - 36g'g_{1p1}^2x_Hx_\Phi\text{Tr}[Y_\nu Y_\nu^\dagger] - 72g'^3x_\Phi^2\text{Tr}[Y_\nu Y_\nu^\dagger] - 72g'g_{1p1}^2x_\Phi^2\text{Tr}[Y_\nu Y_\nu^\dagger] \\
& - 18g'^3x_\Phi^2\text{Tr}[y_{NS}y_{NS}^\dagger] - 18g'g_{1p1}^2x_\Phi^2\text{Tr}[y_{NS}y_{NS}^\dagger]
\end{aligned} \tag{2.4}$$

$$\begin{aligned}
\beta_{g_{1p1}}^{(2)} = & \frac{1}{18} \left( 199g_1^3g_{11p}g' + 199g_1g_{11p}^3g' + 199g_1^4g_{1p1} + 199g_1^2g_{11p}^2g_{1p1} + 81g_1g_{11p}g'g_2^2 \right. \\
& + 81g_1^2g_{1p1}g_2^2 + 264g_1g_{11p}g'g_3^2 + 264g_1^2g_{1p1}g_3^2 + 181g_1^3g'^2x_H + 543g_1g_{11p}g'^2x_H \\
& + 905g_1^2g_{11p}g'g_{1p1}x_H + 181g_{11p}^3g'g_{1p1}x_H + 724g_1^3g_{1p1}^2x_H + 362g_1g_{11p}^2g_{1p1}^2x_H + 27g_1g'^2g_2^2x_H \\
& + 27g_{11p}g'g_{1p1}g_2^2x_H + 54g_1g_{1p1}^2g_2^2x_H + 264g_1g'^2g_3^2x_H + 264g_{11p}g'g_{1p1}g_3^2x_H + 528g_1g_{1p1}^2g_3^2x_H \\
& + 597g_1g_{11p}g'^3x_H^2 + 796g_1^2g'^2g_{1p1}x_H^2 + 597g_{11p}^2g'^2g_{1p1}x_H^2 + 1393g_1g_{11p}g'g_{1p1}^2x_H^2 + 1194g_1^2g_{1p1}^3x_H^2 \\
& + 199g_{11p}^2g_{1p1}^3x_H^2 + 81g'^2g_{1p1}g_2^2x_H^2 + 81g_{1p1}^3g_2^2x_H^2 + 264g'^2g_{1p1}g_3^2x_H^2 + 264g_{1p1}^3g_3^2x_H^2 + 181g_1g'^4x_H^3 \\
& + 543g_{11p}g'^3g_{1p1}x_H^3 + 905g_1g'^2g_{1p1}^2x_H^3 + 543g_{11p}g'g_{1p1}^3x_H^3 + 724g_1g_{1p1}^4x_H^3 + 199g'^4g_{1p1}x_H^4 \\
& + 398g'^2g_{1p1}^3x_H^4 + 199g_{1p1}^5x_H^4 + 164g_1^3g'^2x_\Phi + 492g_1g_{11p}g'^2x_\Phi + 820g_1^2g_{11p}g'g_{1p1}x_\Phi
\end{aligned}$$



$$\begin{aligned}
& + 164g_{11p}^3g'g_{1p1}x_\Phi + 656g_1^3g_{1p1}^2x_\Phi + 328g_1g_{11p}^2g_{1p1}^2x_\Phi + 108g_1g'^2g_2^2x_\Phi + 108g_{11p}g'g_{1p1}g_2^2x_\Phi \\
& + 216g_1g_{1p1}^2g_2^2x_\Phi + 96g_1g'^2g_3^2x_\Phi + 96g_{11p}g'g_{1p1}g_3^2x_\Phi + 192g_1g_{1p1}^2g_3^2x_\Phi + 984g_1g_{11p}g'^3x_Hx_\Phi \\
& + 1312g_1^2g'^2g_{1p1}x_Hx_\Phi + 984g_{11p}^2g'^2g_{1p1}x_Hx_\Phi + 2296g_1g_{11p}g'g_{1p1}^2x_Hx_\Phi + 1968g_1^2g_{1p1}^3x_Hx_\Phi \\
& + 328g_{11p}^2g_{1p1}^3x_Hx_\Phi + 216g'^2g_{1p1}g_2^2x_Hx_\Phi + 216g_{1p1}^3g_2^2x_Hx_\Phi + 192g'^2g_{1p1}g_3^2x_Hx_\Phi \\
& + 192g_{1p1}^3g_3^2x_Hx_\Phi + 492g_1g^4x_H^2x_\Phi + 1476g_{11p}g'^3g_{1p1}x_H^2x_\Phi + 2460g_1g'^2g_{1p1}^2x_H^2x_\Phi \\
& + 1476g_{11p}g'g_{1p1}^3x_H^2x_\Phi + 1968g_1g_{1p1}^4x_H^2x_\Phi + 656g^4g_{1p1}x_H^3x_\Phi + 1312g'^2g_{1p1}^3x_H^3x_\Phi \\
& + 656g_{1p1}^5x_H^3x_\Phi + 552g_1g_{11p}g'^3x_\Phi^2 + 736g_1^2g'^2g_{1p1}x_\Phi^2 + 552g_{11p}^2g'^2g_{1p1}x_\Phi^2 \\
& + 1288g_1g_{11p}g'g_{1p1}^2x_\Phi^2 + 1104g_1^2g_{1p1}^3x_\Phi^2 + 184g_{11p}^2g_{1p1}^3x_\Phi^2 + 216g'^2g_{1p1}g_2^2x_\Phi^2 + 216g_{1p1}^3g_2^2x_\Phi^2 \\
& + 192g'^2g_{1p1}g_3^2x_\Phi^2 + 192g_{1p1}^3g_3^2x_\Phi^2 + 552g_1g^4x_Hx_\Phi^2 + 1656g_{11p}g'^3g_{1p1}x_Hx_\Phi^2 + 2760g_1g'^2g_{1p1}^2x_Hx_\Phi^2 \\
& + 1656g_{11p}g'g_{1p1}^3x_Hx_\Phi^2 + 2208g_1g_{1p1}^4x_Hx_\Phi^2 + 1104g^4g_{1p1}x_H^2x_\Phi^2 + 2208g'^2g_{1p1}^3x_H^2x_\Phi^2 + 1104g_{1p1}^5x_H^2x_\Phi^2 \\
& + 224g_1g^4x_\Phi^3 + 672g_{11p}g'^3g_{1p1}x_\Phi^3 + 1120g_1g'^2g_{1p1}^2x_\Phi^3 + 672g_{11p}g'g_{1p1}^3x_\Phi^3 + 896g_1g_{1p1}^4x_\Phi^3 \\
& + 896g^4g_{1p1}x_Hx_\Phi^3 + 1792g'^2g_{1p1}^3x_Hx_\Phi^3 + 896g_{1p1}^5x_Hx_\Phi^3 + 520g^4g_{1p1}x_\Phi^4 + 1040g'^2g_{1p1}^3x_\Phi^4 \\
& + 520g_{1p1}^5x_\Phi^4 - 51g_1g_{11p}g'y_t^2 - 51g_1^2g_{1p1}y_t^2 - 51g_1g'^2x_Hy_t^2 - 51g_{11p}g'g_{1p1}x_Hy_t^2 \\
& - 102g_1g_{1p1}^2x_Hy_t^2 - 51g'^2g_{1p1}x_H^2y_t^2 - 51g_{1p1}^3x_H^2y_t^2 - 30g_1g'^2x_\Phi y_t^2 - 30g_{11p}g'g_{1p1}x_\Phi y_t^2 \\
& - 60g_1g_{1p1}^2x_\Phi y_t^2 - 60g'^2g_{1p1}x_Hx_\Phi y_t^2 - 60g_{1p1}^3x_Hx_\Phi y_t^2 - 24g'^2g_{1p1}x_\Phi^2y_t^2 - 24g_{1p1}^3x_\Phi^2y_t^2 \\
& - 9g_1g_{11p}g'\text{Tr}[Y_\nu Y_\nu^\dagger] - 9g_1^2g_{1p1}\text{Tr}[Y_\nu Y_\nu^\dagger] - 9g_1g'^2x_H\text{Tr}[Y_\nu Y_\nu^\dagger] - 9g_{11p}g'g_{1p1}x_H\text{Tr}[Y_\nu Y_\nu^\dagger] \\
& - 18g_1g_{1p1}^2x_H\text{Tr}[Y_\nu Y_\nu^\dagger] - 9g'^2g_{1p1}x_H^2\text{Tr}[Y_\nu Y_\nu^\dagger] - 9g_{1p1}^3x_H^2\text{Tr}[Y_\nu Y_\nu^\dagger] - 18g_1g'^2x_\Phi\text{Tr}[Y_\nu Y_\nu^\dagger] \\
& - 18g_{11p}g'g_{1p1}x_\Phi\text{Tr}[Y_\nu Y_\nu^\dagger] - 36g_1g_{1p1}^2x_\Phi\text{Tr}[Y_\nu Y_\nu^\dagger] - 36g'^2g_{1p1}x_Hx_\Phi\text{Tr}[Y_\nu Y_\nu^\dagger] - 36g_{1p1}^3x_Hx_\Phi\text{Tr}[Y_\nu Y_\nu^\dagger] \\
& - 72g'^2g_{1p1}x_\Phi^2\text{Tr}[Y_\nu Y_\nu^\dagger] - 72g_{1p1}^3x_\Phi^2\text{Tr}[Y_\nu Y_\nu^\dagger] - 18g'^2g_{1p1}x_\Phi^2\text{Tr}[y_{NS}y_{NS}^\dagger] - 18g_{1p1}^3x_\Phi^2\text{Tr}[y_{NS}y_{NS}^\dagger]
\end{aligned} \tag{2.5}$$

$$\begin{aligned}
\beta_{g_{11p}}^{(2)} = & \frac{1}{18} \left( 199g_1^4g_{11p} + 398g_1^2g_{11p}^3 + 199g_{11p}^5 + 81g_1^2g_{11p}g_2^2 + 81g_{11p}^3g_2^2 \right. \\
& + 264g_1^2g_{11p}g_3^2 + 264g_{11p}^3g_3^2 + 181g_1^4g'x_H + 905g_1^2g_{11p}g'x_H + 724g_{11p}^4g'x_H \\
& + 543g_1^3g_{11p}g_{1p1}x_H + 543g_1g_{11p}^3g_{1p1}x_H + 27g_1^2g'g_2^2x_H + 54g_{11p}^2g'g_2^2x_H + 27g_1g_{11p}g_{1p1}g_2^2x_H \\
& \left. + 264g_1^2g'g_3^2x_H + 528g_{11p}^2g'g_3^2x_H + 264g_1g_{11p}g_{1p1}g_3^2x_H + 796g_1^2g_{11p}g'^2x_H^2 + 1194g_{11p}^3g'^2x_H^2 \right)
\end{aligned}$$

$$\begin{aligned}
& + 597g_1^3g'g_{1p1}x_H^2 + 1393g_1g_{11p}^2g'g_{1p1}x_H^2 + 597g_1^2g_{11p}g_{1p1}^2x_H^2 + 199g_{11p}^3g_{1p1}^2x_H^2 + 81g_{11p}g'^2g_2^2x_H^2 \\
& + 81g_1g'g_{1p1}g_2^2x_H^2 + 264g_{11p}g'^2g_3^2x_H^2 + 264g_1g'g_{1p1}g_3^2x_H^2 + 181g_1^2g'^3x_H^3 + 724g_{11p}^2g'^3x_H^3 \\
& + 905g_1g_{11p}g'^2g_{1p1}x_H^3 + 543g_1^2g'g_{1p1}^2x_H^3 + 362g_{11p}^2g'g_{1p1}^2x_H^3 + 181g_1g_{11p}g_{1p1}^3x_H^3 + 199g_{11p}g'^4x_H^4 \\
& + 199g_1g'^3g_{1p1}x_H^4 + 199g_{11p}g'^2g_{1p1}^2x_H^4 + 199g_1g'g_{1p1}^3x_H^4 + 164g_1^4g'x_\Phi + 820g_1^2g_{11p}^2g'x_\Phi \\
& + 656g_{11p}^4g'x_\Phi + 492g_1^3g_{11p}g_{1p1}x_\Phi + 492g_1g_{11p}^3g_{1p1}x_\Phi + 108g_1^2g'g_2^2x_\Phi + 216g_{11p}^2g'g_2^2x_\Phi \\
& + 108g_1g_{11p}g_{1p1}g_2^2x_\Phi + 96g_1^2g'g_3^2x_\Phi + 192g_{11p}^2g'g_3^2x_\Phi + 96g_1g_{11p}g_{1p1}g_3^2x_\Phi + 1312g_1^2g_{11p}g'^2x_Hx_\Phi \\
& + 1968g_{11p}^3g'^2x_Hx_\Phi + 984g_1^3g'g_{1p1}x_Hx_\Phi + 2296g_1g_{11p}^2g'g_{1p1}x_Hx_\Phi + 984g_1^2g_{11p}g_{1p1}^2x_Hx_\Phi \\
& + 328g_{11p}^3g_{1p1}^2x_Hx_\Phi + 216g_{11p}g'^2g_2^2x_Hx_\Phi + 216g_1g'g_{1p1}g_2^2x_Hx_\Phi + 192g_{11p}g'^2g_3^2x_Hx_\Phi \\
& + 192g_1g'g_{1p1}g_3^2x_Hx_\Phi + 492g_1^2g'^3x_H^2x_\Phi + 1968g_{11p}^2g'^3x_H^2x_\Phi + 2460g_1g_{11p}g'^2g_{1p1}x_H^2x_\Phi \\
& + 1476g_1^2g'g_{1p1}^2x_H^2x_\Phi + 984g_{11p}^2g'g_{1p1}^2x_H^2x_\Phi + 492g_1g_{11p}g_{1p1}^3x_H^2x_\Phi + 656g_{11p}g'^4x_H^3x_\Phi \\
& + 656g_1g'^3g_{1p1}x_H^3x_\Phi + 656g_{11p}g'^2g_{1p1}^2x_H^3x_\Phi + 656g_1g'g_{1p1}^3x_H^3x_\Phi + 736g_1^2g_{11p}g'^2x_\Phi^2 \\
& + 1104g_{11p}^3g'^2x_\Phi^2 + 552g_1^3g'g_{1p1}x_\Phi^2 + 1288g_1g_{11p}^2g'g_{1p1}x_\Phi^2 + 552g_1^2g_{11p}g_{1p1}^2x_\Phi^2 + 184g_{11p}^3g_{1p1}^2x_\Phi^2 \\
& + 216g_{11p}g'^2g_2^2x_\Phi^2 + 216g_1g'g_{1p1}g_2^2x_\Phi^2 + 192g_{11p}g'^2g_3^2x_\Phi^2 + 192g_1g'g_{1p1}g_3^2x_\Phi^2 + 552g_1^2g'^3x_Hx_\Phi^2 \\
& + 2208g_{11p}^2g'^3x_Hx_\Phi^2 + 2760g_1g_{11p}g'^2g_{1p1}x_Hx_\Phi^2 + 1656g_1^2g'g_{1p1}^2x_Hx_\Phi^2 + 1104g_{11p}^2g'g_{1p1}^2x_Hx_\Phi^2 \\
& + 552g_1g_{11p}g_{1p1}^3x_Hx_\Phi^2 + 1104g_{11p}g'^4x_H^2x_\Phi^2 + 1104g_1g'^3g_{1p1}x_H^2x_\Phi^2 + 1104g_{11p}g'^2g_{1p1}^2x_H^2x_\Phi^2 \\
& + 1104g_1g'g_{1p1}^3x_H^2x_\Phi^2 + 224g_1^2g'^3x_\Phi^3 + 896g_{11p}^2g'^3x_\Phi^3 + 1120g_1g_{11p}g'^2g_{1p1}x_\Phi^3 + 672g_1^2g'g_{1p1}^2x_\Phi^3 \\
& + 448g_{11p}^2g'g_{1p1}^2x_\Phi^3 + 224g_1g_{11p}g_{1p1}^3x_\Phi^3 + 896g_{11p}g'^4x_Hx_\Phi^3 + 896g_1g'^3g_{1p1}x_Hx_\Phi^3 + 896g_{11p}g'^2g_{1p1}^2x_Hx_\Phi^3 \\
& + 896g_1g'g_{1p1}^3x_Hx_\Phi^3 + 520g_{11p}g'^4x_\Phi^4 + 520g_1g'^3g_{1p1}x_\Phi^4 + 520g_{11p}g'^2g_{1p1}^2x_\Phi^4 + 520g_1g'g_{1p1}^3x_\Phi^4 \\
& - 51g_1^2g_{11p}y_t^2 - 51g_{11p}^3y_t^2 - 51g_1^2g'x_Hy_t^2 - 102g_{11p}^2g'x_Hy_t^2 - 51g_1g_{11p}g_{1p1}x_Hy_t^2 \\
& - 51g_{11p}g'^2x_Hy_t^2 - 51g_1g'g_{1p1}x_Hy_t^2 - 30g_1^2g'x_\Phi y_t^2 - 60g_{11p}^2g'x_\Phi y_t^2 - 30g_1g_{11p}g_{1p1}x_\Phi y_t^2 \\
& - 60g_{11p}g'^2x_Hx_\Phi y_t^2 - 60g_1g'g_{1p1}x_Hx_\Phi y_t^2 - 24g_{11p}g'^2x_\Phi^2 y_t^2 - 24g_1g'g_{1p1}x_\Phi^2 y_t^2 - 9g_1^2g_{11p}\text{Tr}[Y_\nu Y_\nu^\dagger] \\
& - 9g_{11p}^3\text{Tr}[Y_\nu Y_\nu^\dagger] - 9g_1^2g'x_H\text{Tr}[Y_\nu Y_\nu^\dagger] - 18g_{11p}^2g'x_H\text{Tr}[Y_\nu Y_\nu^\dagger] - 9g_1g_{11p}g_{1p1}x_H\text{Tr}[Y_\nu Y_\nu^\dagger] \\
& - 9g_{11p}g'^2x_H^2\text{Tr}[Y_\nu Y_\nu^\dagger] - 9g_1g'g_{1p1}x_H^2\text{Tr}[Y_\nu Y_\nu^\dagger] - 18g_1^2g'x_\Phi\text{Tr}[Y_\nu Y_\nu^\dagger] - 36g_{11p}^2g'x_\Phi\text{Tr}[Y_\nu Y_\nu^\dagger] \\
& - 18g_1g_{11p}g_{1p1}x_\Phi\text{Tr}[Y_\nu Y_\nu^\dagger] - 36g_{11p}g'^2x_Hx_\Phi\text{Tr}[Y_\nu Y_\nu^\dagger] - 36g_1g'g_{1p1}x_Hx_\Phi\text{Tr}[Y_\nu Y_\nu^\dagger] - 72g_{11p}g'^2x_\Phi^2\text{Tr}[Y_\nu Y_\nu^\dagger] \\
& - 72g_1g'g_{1p1}x_\Phi^2\text{Tr}[Y_\nu Y_\nu^\dagger] - 18g_{11p}g'^2x_\Phi^2\text{Tr}[y_{NS}y_{NS}^\dagger] - 18g_1g'g_{1p1}x_\Phi^2\text{Tr}[y_{NS}y_{NS}^\dagger]
\end{aligned}$$

(2.6)

$$\begin{aligned}
\beta_{\lambda_1}^{(2)} = & \frac{1}{48} \left( -379g_1^6 - 469g_1^4g_{11p}^2 - 469g_1^2g_{11p}^4 - 379g_{11p}^6 - 559g_1^4g_2^2 - 450g_1^2g_{11p}^2g_2^2 - 559g_{11p}^4g_2^2 \right. \\
& - 289g_1^2g_2^4 - 289g_{11p}^2g_2^4 + 915g_2^6 + 1258g_1^4\lambda_1 + 828g_1^2g_{11p}^2\lambda_1 + 1258g_{11p}^4\lambda_1 + 468g_1^2g_2^2\lambda_1 + 468g_{11p}^2g_2^2\lambda_1 - \\
& + 1728g_1^2\lambda_1^2 + 1728g_{11p}^2\lambda_1^2 + 5184g_2^2\lambda_1^2 - 14976\lambda_1^3 - 480\lambda_1\lambda_3^2 - 192\lambda_3^3 \\
& + 938g_1^4g_{11p}g'x_H + 596g_1^2g_{11p}^3g'x_H + 994g_{11p}^5g'x_H + 994g_1^5g_{1p1}x_H + 596g_1^3g_{11p}^2g_{1p1}x_H \\
& + 938g_1g_{11p}^4g_{1p1}x_H + 900g_1^2g_{11p}g'g_2^2x_H + 956g_{11p}^3g'g_2^2x_H + 956g_1^3g_{1p1}g_2^2x_H + 900g_1g_{11p}^2g_{1p1}g_2^2x_H \\
& + 578g_{11p}g'g_2^4x_H + 578g_1g_{1p1}g_2^4x_H - 1656g_1^2g_{11p}g'\lambda_1x_H - 1832g_{11p}^3g'\lambda_1x_H - 1832g_1^3g_{1p1}\lambda_1x_H \\
& - 1656g_1g_{11p}^2g_{1p1}\lambda_1x_H - 936g_{11p}g'g_2^2\lambda_1x_H - 936g_1g_{1p1}g_2^2\lambda_1x_H - 3456g_{11p}g'\lambda_1^2x_H - 3456g_1g_{1p1}\lambda_1^2x_H \\
& - 469g_1^4g'^2x_H^2 - 254g_1^2g_{11p}^2g'^2x_H^2 - 565g_{11p}^4g'^2x_H^2 - 1192g_1^3g_{11p}g'g_{1p1}x_H^2 - 1192g_1g_{11p}^3g'g_{1p1}x_H^2 \\
& - 565g_1^4g_{1p1}^2x_H^2 - 254g_1^2g_{11p}^2g_{1p1}^2x_H^2 - 469g_{11p}^4g_{1p1}^2x_H^2 - 450g_1^2g'^2g_2^2x_H^2 - 794g_{11p}^2g'^2g_2^2x_H^2 \\
& - 1800g_1g_{11p}g'g_{1p1}g_2^2x_H^2 - 794g_1^2g_{1p1}^2g_2^2x_H^2 - 450g_{11p}^2g_{1p1}^2g_2^2x_H^2 - 289g'^2g_2^4x_H^2 - 289g_{1p1}^2g_2^4x_H^2 \\
& + 828g_1^2g'^2\lambda_1x_H^2 + 1148g_{11p}^2g'^2\lambda_1x_H^2 + 3312g_1g_{11p}g'g_{1p1}\lambda_1x_H^2 + 1148g_1^2g_{1p1}^2\lambda_1x_H^2 + 828g_{11p}^2g_{1p1}^2\lambda_1x_H^2 \\
& + 468g'^2g_2^2\lambda_1x_H^2 + 468g_{1p1}^2g_2^2\lambda_1x_H^2 + 1728g'^2\lambda_1^2x_H^2 + 1728g_{1p1}^2\lambda_1^2x_H^2 + 596g_1^2g_{11p}g'^3x_H^3 \\
& - 100g_{11p}^3g'^3x_H^3 + 596g_1^3g'^2g_{1p1}x_H^3 + 508g_1g_{11p}^2g'^2g_{1p1}x_H^3 + 508g_1^2g_{11p}g'g_{1p1}^2x_H^3 + 596g_{11p}^3g'g_{1p1}^2x_H^3 \\
& - 100g_1^3g_{1p1}^3x_H^3 + 596g_1g_{11p}^2g_{1p1}^3x_H^3 + 956g_{11p}g'^3g_2^2x_H^3 + 900g_1g'^2g_{1p1}g_2^2x_H^3 + 900g_{11p}g'g_{1p1}^2g_2^2x_H^3 \\
& + 956g_1g_{1p1}^3g_2^2x_H^3 - 1832g_{11p}g'^3\lambda_1x_H^3 - 1656g_1g'^2g_{1p1}\lambda_1x_H^3 - 1656g_{11p}g'g_{1p1}^2\lambda_1x_H^3 \\
& - 1832g_1g_{1p1}^3\lambda_1x_H^3 - 469g_1^2g'^4x_H^4 - 565g_{11p}^2g'^4x_H^4 - 1192g_1g_{11p}g'^3g_{1p1}x_H^4 - 254g_1^2g'^2g_{1p1}^2x_H^4 \\
& - 254g_{11p}^2g'^2g_{1p1}^2x_H^4 - 1192g_1g_{11p}g'g_{1p1}^3x_H^4 - 565g_1^2g_{1p1}^4x_H^4 - 469g_{11p}^2g_{1p1}^4x_H^4 - 559g'^4g_2^2x_H^4 \\
& - 450g'^2g_{1p1}^2g_2^2x_H^4 - 559g_{1p1}^4g_2^2x_H^4 + 1258g'^4\lambda_1x_H^4 + 828g'^2g_{1p1}^2\lambda_1x_H^4 + 1258g_{1p1}^4\lambda_1x_H^4 \\
& + 994g_{11p}g'^5x_H^5 + 938g_1g'^4g_{1p1}x_H^5 + 596g_{11p}g'^3g_{1p1}^2x_H^5 + 596g_1g'^2g_{1p1}^3x_H^5 + 938g_{11p}g'g_{1p1}^4x_H^5 \\
& + 994g_1g_{1p1}^5x_H^5 - 379g'^6x_H^6 - 469g'^4g_{1p1}^2x_H^6 - 469g'^2g_{1p1}^4x_H^6 - 379g_{1p1}^6x_H^6 \\
& - 512g_1^2g_{11p}^3g'x_\Phi - 512g_{11p}^5g'x_\Phi - 512g_1^5g_{1p1}x_\Phi - 512g_1^3g_{11p}^2g_{1p1}x_\Phi - 512g_{11p}^3g'g_2^2x_\Phi \\
& - 512g_1^3g_{1p1}g_2^2x_\Phi + 1280g_{11p}^3g'\lambda_1x_\Phi + 1280g_1^3g_{1p1}\lambda_1x_\Phi + 512g_1^2g_{11p}^2g'^2x_Hx_\Phi + 1536g_{11p}^4g'^2x_Hx_\Phi \\
& + 1024g_1^3g_{11p}g'g_{1p1}x_Hx_\Phi + 1024g_1g_{11p}^3g'g_{1p1}x_Hx_\Phi + 1536g_1^4g_{1p1}^2x_Hx_\Phi + 512g_1^2g_{11p}^2g_{1p1}^2x_Hx_\Phi \\
& + 512g_{11p}^2g'^2g_2^2x_Hx_\Phi + 512g_1^2g_{1p1}^2g_2^2x_Hx_\Phi - 1280g_{11p}^2g'^2\lambda_1x_Hx_\Phi - 1280g_1^2g_{1p1}^2\lambda_1x_Hx_\Phi \\
& + 512g_1^2g_{11p}g'^3x_H^2x_\Phi - 1024g_{11p}^3g'^3x_H^2x_\Phi - 512g_1^3g'^2g_{1p1}x_H^2x_\Phi - 1024g_1g_{11p}^2g'^2g_{1p1}x_H^2x_\Phi
\end{aligned}$$

$$\begin{aligned}
& - 1024g_1^2g_{11p}g'g_{1p1}^2x_H^2x_\Phi - 512g_{11p}^3g'g_{1p1}^2x_H^2x_\Phi - 1024g_1^3g_{1p1}^3x_H^2x_\Phi + 512g_1g_{11p}^2g_{1p1}^3x_H^2x_\Phi \\
& + 512g_{11p}g'^3g_2^2x_H^2x_\Phi + 512g_1g_{1p1}^3g_2^2x_H^2x_\Phi - 1280g_{11p}g'^3\lambda_1x_H^2x_\Phi - 1280g_1g_{1p1}^3\lambda_1x_H^2x_\Phi - 512g_1^2g'^4x_H^3x_\Phi \\
& - 1024g_{11p}^2g'^4x_H^3x_\Phi - 1024g_1g_{11p}g'^3g_{1p1}x_H^3x_\Phi + 512g_1^2g'^2g_{1p1}^2x_H^3x_\Phi + 512g_{11p}^2g'^2g_{1p1}^2x_H^3x_\Phi \\
& - 1024g_1g_{11p}g'g_{1p1}^3x_H^3x_\Phi - 1024g_1^2g_{1p1}^4x_H^3x_\Phi - 512g_{11p}^2g_{1p1}^4x_H^3x_\Phi - 512g'^4g_2^2x_H^3x_\Phi - 512g_{1p1}^4g_2^2x_H^3x_\Phi \\
& + 1280g'^4\lambda_1x_H^3x_\Phi + 1280g_{1p1}^4\lambda_1x_H^3x_\Phi + 1536g_{11p}g'^5x_H^4x_\Phi + 1024g_1g'^4g_{1p1}x_H^4x_\Phi + 512g_{11p}g'^3g_{1p1}^2x_H^4x_\Phi \\
& + 512g_1g'^2g_{1p1}^3x_H^4x_\Phi + 1024g_{11p}g'g_{1p1}^4x_H^4x_\Phi + 1536g_1g_{1p1}^5x_H^4x_\Phi - 512g'^6x_H^5x_\Phi - 512g'^4g_{1p1}^2x_H^5x_\Phi \\
& - 512g'^2g_{1p1}^4x_H^5x_\Phi - 512g_{1p1}^6x_H^5x_\Phi - 540g_1^2g_{11p}g'^2x_\Phi^2 - 540g_{11p}^4g'^2x_\Phi^2 - 540g_1^4g_{1p1}^2x_\Phi^2 \\
& - 540g_1^2g_{11p}g_{1p1}^2x_\Phi^2 - 540g_{11p}^2g'^2g_2^2x_\Phi^2 - 540g_1^2g_{1p1}^2g_2^2x_\Phi^2 + 1368g_{11p}^2g'^2\lambda_1x_\Phi^2 \\
& + 1368g_1^2g_{1p1}^2\lambda_1x_\Phi^2 + 240g_{11p}^2g'^2\lambda_3x_\Phi^2 + 384g'^2\lambda_3^2x_\Phi^2 + 384g_{1p1}^2\lambda_3^2x_\Phi^2 \\
& + 1080g_1^2g_{11p}g'^3x_Hx_\Phi^2 + 2160g_{11p}^3g'^3x_Hx_\Phi^2 + 1080g_1g_{11p}^2g'^2g_{1p1}x_Hx_\Phi^2 + 1080g_1^2g_{11p}g'g_{1p1}^2x_Hx_\Phi^2 \\
& + 2160g_1^3g_{1p1}^3x_Hx_\Phi^2 + 1080g_1g_{11p}^2g_{1p1}^3x_Hx_\Phi^2 + 1080g_{11p}g'^3g_2^2x_Hx_\Phi^2 + 1080g_1g_{1p1}^3g_2^2x_Hx_\Phi^2 \\
& - 2736g_{11p}g'^3\lambda_1x_Hx_\Phi^2 - 2736g_1g_{1p1}^3\lambda_1x_Hx_\Phi^2 - 480g_{11p}g'^3\lambda_3x_Hx_\Phi^2 - 540g_1^2g'^4x_Hx_\Phi^2 \\
& - 3240g_{11p}^2g'^4x_Hx_\Phi^2 - 2160g_1g_{11p}g'^3g_{1p1}x_Hx_\Phi^2 - 540g_1^2g'^2g_{1p1}^2x_Hx_\Phi^2 - 540g_{11p}^2g'^2g_{1p1}^2x_Hx_\Phi^2 \\
& - 2160g_1g_{11p}g'g_{1p1}^3x_Hx_\Phi^2 - 3240g_1^2g_{1p1}^4x_Hx_\Phi^2 - 540g_{11p}^2g_{1p1}^4x_Hx_\Phi^2 - 540g'^4g_2^2x_Hx_\Phi^2 \\
& - 540g_{1p1}^4g_2^2x_Hx_\Phi^2 + 1368g'^4\lambda_1x_Hx_\Phi^2 + 1368g_{1p1}^4\lambda_1x_Hx_\Phi^2 + 240g'^4\lambda_3x_Hx_\Phi^2 + 2160g_{11p}g'^5x_Hx_\Phi^2 \\
& + 1080g_1g'^4g_{1p1}x_Hx_\Phi^2 + 1080g_{11p}g'^3g_{1p1}^3x_Hx_\Phi^2 + 1080g_1g'^2g_{1p1}^3x_Hx_\Phi^2 + 1080g_{11p}g'g_{1p1}^4x_Hx_\Phi^2 \\
& + 2160g_1g_{1p1}^5x_Hx_\Phi^2 - 540g'^6x_Hx_\Phi^2 - 540g'^4g_{1p1}^2x_Hx_\Phi^2 - 540g'^2g_{1p1}^4x_Hx_\Phi^2 - 540g_{1p1}^6x_Hx_\Phi^2 \\
& + y_t^2 \left( - 228g_1^4 - 456g_1^2g_{11p}^2 - 228g_{11p}^4 + 504g_1^2g_2^2 + 504g_{11p}^2g_2^2 - 108g_2^4 + 680g_1^2\lambda_1 + 680g_{11p}^2\lambda_1 \right. \\
& + 1080g_2^2\lambda_1 + 3840g_3^2\lambda_1 - 6912\lambda_1^2 + 1360g_{11p}g'\lambda_1x_H + 1360g_1g_{1p1}\lambda_1x_H + 456g_1^2g'^2x_H^2 + 456g_{11p}^2g'^2x_H^2 \\
& + 456g_1^2g_{1p1}^2x_H^2 + 456g_{11p}^2g_{1p1}^2x_H^2 - 504g'^2g_2^2x_H^2 - 504g_{1p1}^2g_2^2x_H^2 + 680g'^2\lambda_1x_H^2 + 680g_{1p1}^2\lambda_1x_H^2 \\
& - 228g'^4x_H^4 - 456g'^2g_{1p1}^2x_H^4 - 228g_{1p1}^4x_H^4 - 480g_1^2g_{11p}g'x_\Phi - 480g_{11p}^3g'x_\Phi - 480g_1^3g_{1p1}x_\Phi \\
& - 480g_1g_{11p}^2g_{1p1}x_\Phi + 288g_{11p}g'g_2^2x_\Phi + 288g_1g_{1p1}g_2^2x_\Phi + 800g_{11p}g'\lambda_1x_\Phi + 800g_1g_{1p1}\lambda_1x_\Phi + 480g_1^2g'^2x_Hx_\Phi \\
& + 480g_{11p}^2g'^2x_Hx_\Phi + 480g_1^2g_{1p1}^2x_Hx_\Phi + 480g_{11p}^2g_{1p1}^2x_Hx_\Phi - 288g'^2g_2^2x_Hx_\Phi - 288g_{1p1}^2g_2^2x_Hx_\Phi \\
& + 800g'^2\lambda_1x_Hx_\Phi + 800g_{1p1}^2\lambda_1x_Hx_\Phi + 480g_{11p}g'^3x_Hx_\Phi + 480g_1g'^2g_{1p1}x_Hx_\Phi \\
& + 480g_{11p}g'g_{1p1}^2x_Hx_\Phi + 480g_1g_{1p1}^3x_Hx_\Phi - 480g'^4x_Hx_\Phi - 960g'^2g_{1p1}^2x_Hx_\Phi - 480g_{1p1}^4x_Hx_\Phi \\
& \left. - 192g_{11p}^2g'^2x_\Phi^2 - 384g_1g_{11p}g'g_{1p1}x_\Phi^2 - 192g_1^2g_{1p1}^2x_\Phi^2 + 320g'^2\lambda_1x_\Phi^2 + 320g_{1p1}^2\lambda_1x_\Phi^2 \right)
\end{aligned}$$

$$\begin{aligned}
& + 384g_{11p}g'^3x_Hx_\Phi^2 + 384g_1g'^2g_{1p1}x_Hx_\Phi^2 + 384g_{11p}g'g_{1p1}^2x_Hx_\Phi^2 + 384g_1g_{1p1}^3x_Hx_\Phi^2 \\
& - 192g'^4x_H^2x_\Phi^2 - 384g'^2g_{1p1}^2x_H^2x_\Phi^2 - 192g_{1p1}^4x_H^2x_\Phi^2 \Big) \\
& + \text{Tr}[Y_\nu Y_\nu^\dagger] \Big( - 12g_1^4 - 24g_1^2g_{11p}^2 - 12g_{11p}^4 - 24g_1^2g_2^2 - 24g_{11p}^2g_2^2 - 36g_2^4 + 120g_1^2\lambda_1 + 120g_{11p}^2\lambda_1 \\
& + 360g_2^2\lambda_1 - 2304\lambda_1^2 + 240g_{11p}g'\lambda_1x_H + 240g_1g_{1p1}\lambda_1x_H + 24g_1^2g'^2x_H^2 + 24g_{11p}^2g'^2x_H^2 + 24g_1^2g_{1p1}^2x_H^2 \\
& + 24g_{11p}^2g_{1p1}^2x_H^2 + 24g'^2g_2^2x_H^2 + 24g_{1p1}^2g_2^2x_H^2 + 120g'^2\lambda_1x_H^2 + 120g_{1p1}^2\lambda_1x_H^2 - 12g'^4x_H^4 - 24g'^2g_{1p1}^2x_H^4 \\
& - 12g_{1p1}^4x_H^4 - 288g_1^2g_{11p}g'x_\Phi - 288g_{11p}^3g'x_\Phi - 288g_1^3g_{1p1}x_\Phi - 288g_1g_{11p}^2g_{1p1}x_\Phi \\
& - 288g_{11p}g'g_2^2x_\Phi - 288g_1g_{1p1}g_2^2x_\Phi + 480g_{11p}g'\lambda_1x_\Phi + 480g_1g_{1p1}\lambda_1x_\Phi + 288g_1^2g'^2x_Hx_\Phi \\
& + 288g_{11p}^2g'^2x_Hx_\Phi + 288g_1^2g_{1p1}^2x_Hx_\Phi + 288g_{11p}^2g_{1p1}^2x_Hx_\Phi + 288g'^2g_2^2x_Hx_\Phi \\
& + 288g_{1p1}^2g_2^2x_Hx_\Phi + 480g'^2\lambda_1x_Hx_\Phi + 480g_{1p1}^2\lambda_1x_Hx_\Phi + 288g_{11p}g'^3x_H^2x_\Phi \\
& + 288g_1g'^2g_{1p1}x_H^2x_\Phi + 288g_{11p}g'g_{1p1}^2x_H^2x_\Phi + 288g_1g_{1p1}^3x_H^2x_\Phi - 288g'^4x_H^3x_\Phi - 576g'^2g_{1p1}^2x_H^3x_\Phi \\
& - 288g_{1p1}^4x_H^3x_\Phi - 576g_{11p}^2g'^2x_\Phi^2 - 1152g_1g_{11p}g'g_{1p1}x_\Phi^2 - 576g_1^2g_{1p1}^2x_\Phi^2 + 960g'^2\lambda_1x_\Phi^2 \\
& + 960g_{1p1}^2\lambda_1x_\Phi^2 + 1152g_{11p}g'^3x_Hx_\Phi^2 + 1152g_1g'^2g_{1p1}x_Hx_\Phi^2 + 1152g_{11p}g'g_{1p1}^2x_Hx_\Phi^2 + 1152g_1g_{1p1}^3x_Hx_\Phi^2 \\
& - 576g'^4x_H^2x_\Phi^2 - 1152g'^2g_{1p1}^2x_H^2x_\Phi^2 - 576g_{1p1}^4x_H^2x_\Phi^2 \Big) \\
& - 96\lambda_3^2\text{Tr}[y_{NS}y_{NS}^\dagger] - 128g_1^2y_t^4 - 128g_{11p}^2y_t^4 - 1536g_3^2y_t^4 - 144\lambda_1y_t^4 - 832g_{11p}g'x_Hy_t^4 \\
& - 832g_1g_{1p1}x_Hy_t^4 - 128g'^2x_H^2y_t^4 - 128g_{1p1}^2x_H^2y_t^4 - 320g_{11p}g'x_\Phi y_t^4 - 320g_1g_{1p1}x_\Phi y_t^4 \\
& - 320g'^2x_Hx_\Phi y_t^4 - 320g_{1p1}^2x_Hx_\Phi y_t^4 - 128g'^2x_\Phi^2y_t^4 - 128g_{1p1}^2x_\Phi^2y_t^4 - 48\lambda_1\text{Tr}[Y_\nu Y_\nu^\dagger Y_\nu Y_\nu^\dagger] \\
& - 192g_{11p}g'x_H\text{Tr}[Y_\nu Y_\nu^\dagger Y_\nu Y_\nu^\dagger] - 192g_1g_{1p1}x_H\text{Tr}[Y_\nu Y_\nu^\dagger Y_\nu Y_\nu^\dagger] - 192g_{11p}g'x_\Phi\text{Tr}[Y_\nu Y_\nu^\dagger Y_\nu Y_\nu^\dagger] \\
& - 192g_1g_{1p1}x_\Phi\text{Tr}[Y_\nu Y_\nu^\dagger Y_\nu Y_\nu^\dagger] - 192g'^2x_Hx_\Phi\text{Tr}[Y_\nu Y_\nu^\dagger Y_\nu Y_\nu^\dagger] - 192g_{1p1}^2x_Hx_\Phi\text{Tr}[Y_\nu Y_\nu^\dagger Y_\nu Y_\nu^\dagger] \\
& - 384g'^2x_\Phi^2\text{Tr}[Y_\nu Y_\nu^\dagger Y_\nu Y_\nu^\dagger] - 384g_{1p1}^2x_\Phi^2\text{Tr}[Y_\nu Y_\nu^\dagger Y_\nu Y_\nu^\dagger] - 144\lambda_1\text{Tr}[y_{NS}y_{NS}^\dagger Y_\nu^T Y_\nu^*] + 1440y_t^6 \\
& + 480\text{Tr}[Y_\nu Y_\nu^\dagger Y_\nu Y_\nu^\dagger Y_\nu Y_\nu^\dagger] + 96\text{Tr}[y_{NS}y_{NS}^\dagger Y_\nu^T Y_\nu^* Y_\nu^T Y_\nu^*] \Big)
\end{aligned} \tag{2.7}$$

$$\begin{aligned}
\beta_{\lambda_2}^{(2)} = & \frac{1}{3} \left( -720\lambda_2^3 + 12g_1^2\lambda_3^2 + 12g_{11p}^2\lambda_3^2 + 36g_2^2\lambda_3^2 - 60\lambda_2\lambda_3^2 \right. \\
& - 24\lambda_3^3 - 24g_{11p}g'\lambda_3^2x_H - 24g_1g_{1p1}\lambda_3^2x_H + 12g'^2\lambda_3^2x_H^2 + 12g_{1p1}^2\lambda_3^2x_H^2 \\
& + 211g_{11p}^2g'^2\lambda_2x_\Phi^2 + 211g_1^2g_{1p1}^2\lambda_2x_\Phi^2 + 336g'^2\lambda_2^2x_\Phi^2 + 336g_{1p1}^2\lambda_2^2x_\Phi^2 + 30g_{11p}^2g'^2\lambda_3x_\Phi^2 \\
& + 378g_{11p}g'^3\lambda_2x_Hx_\Phi^2 + 378g_1g_{1p1}^3\lambda_2x_Hx_\Phi^2 - 60g_{11p}g'^3\lambda_3x_Hx_\Phi^2 + 211g'^4\lambda_2x_H^2x_\Phi^2 + 211g_{1p1}^4\lambda_2x_H^2x_\Phi^2 \\
& + 30g'^4\lambda_3x_H^2x_\Phi^2 + 320g_{11p}g'^3\lambda_2x_\Phi^3 + 320g_1g_{1p1}^3\lambda_2x_\Phi^3 + 320g'^4\lambda_2x_Hx_\Phi^3 + 320g_{1p1}^4\lambda_2x_Hx_\Phi^3 \\
& - 334g_{11p}^2g'^4x_\Phi^4 + 636g'^4\lambda_2x_\Phi^4 + 36g'^2g_{1p1}^2\lambda_2x_\Phi^4 + 360g_{1p1}^4\lambda_2x_\Phi^4 - 612g_{11p}g'^5x_Hx_\Phi^4 \\
& - 334g'^6x_H^2x_\Phi^4 - 512g_{11p}g'^5x_\Phi^5 - 512g'^6x_Hx_\Phi^5 - 720g'^6x_\Phi^6 - 180g'^4g_{1p1}^2x_\Phi^6 - 36\lambda_3^2y_t^2 \\
& - 12\lambda_3^2\text{Tr}[Y_\nu Y_\nu^\dagger] - 120\lambda_2^2\text{Tr}[y_{NS}y_{NS}^\dagger] + 30g'^2\lambda_2x_\Phi^2\text{Tr}[y_{NS}y_{NS}^\dagger] + 30g_{1p1}^2\lambda_2x_\Phi^2\text{Tr}[y_{NS}y_{NS}^\dagger] \\
& - 12g'^4x_\Phi^4\text{Tr}[y_{NS}y_{NS}^\dagger] + 6\lambda_2\text{Tr}[y_{NS}y_{NS}^\dagger y_{NS}y_{NS}^\dagger] - 18\lambda_2\text{Tr}[y_{NS}y_{NS}^\dagger Y_\nu^T Y_\nu^*] + 24\text{Tr}[y_{NS}y_{NS}^\dagger y_{NS}y_{NS}^\dagger y_{NS}y_{NS}^\dagger] \\
& \left. + 12\text{Tr}[y_{NS}y_{NS}^\dagger Y_\nu^T Y_\nu^* y_{NS}y_{NS}^\dagger] \right)
\end{aligned} \tag{2.8}$$

$$\begin{aligned}
\beta_{\lambda_3}^{(2)} = & (557g_1^4\lambda_3)/48 + (45g_1^2g_{11p}^2\lambda_3)/8 + (557g_{11p}^4\lambda_3)/48 + (15g_1^2g_2^2\lambda_3)/8 + (15g_{11p}^2g_2^2\lambda_3)/8 - (145g_2^4\lambda_3)/16 \\
& + 24g_1^2\lambda_1\lambda_3 + 24g_{11p}^2\lambda_1\lambda_3 + 72g_2^2\lambda_1\lambda_3 - 60\lambda_1^2\lambda_3 - 40\lambda_2^2\lambda_3 + g_1^2\lambda_3^2 + g_{11p}^2\lambda_3^2 + 3g_2^2\lambda_3^2 \\
& - 72\lambda_1\lambda_3^2 - 48\lambda_2\lambda_3^2 - 11\lambda_3^3 - (45g_1^2g_{11p}g'\lambda_3x_H)/4 - (157g_{11p}^3g'\lambda_3x_H)/12 - (157g_1^3g_{1p1}\lambda_3x_H)/12 \\
& - (45g_1g_{11p}^2g_{1p1}\lambda_3x_H)/4 - (15g_{11p}g'g_2^2\lambda_3x_H)/4 - (15g_1g_{1p1}g_2^2\lambda_3x_H)/4 - 48g_{11p}g'\lambda_1\lambda_3x_H \\
& - 48g_1g_{1p1}\lambda_1\lambda_3x_H - 2g_{11p}g'\lambda_3^2x_H \\
& - 2g_1g_{1p1}\lambda_3^2x_H + (45g_1^2g'^2\lambda_3x_H^2)/8 + (71g_{11p}^2g'^2\lambda_3x_H^2)/24 + (45g_1g_{11p}g'g_{1p1}\lambda_3x_H^2)/2 \\
& + (71g_1^2g_{1p1}^2\lambda_3x_H^2)/24 + (45g_{11p}^2g_{1p1}^2\lambda_3x_H^2)/8 + (15g'^2g_2^2\lambda_3x_H^2)/8 + (15g_{1p1}^2g_2^2\lambda_3x_H^2)/8 \\
& + 24g'^2\lambda_1\lambda_3x_H^2 + 24g_{1p1}^2\lambda_1\lambda_3x_H^2 + g'^2\lambda_3^2x_H^2 + g_{1p1}^2\lambda_3^2x_H^2 \\
& - (157g_{11p}g'^3\lambda_3x_H^3)/12 - (45g_1g'^2g_{1p1}\lambda_3x_H^3)/4 - (45g_{11p}g'g_{1p1}^2\lambda_3x_H^3)/4 - (157g_1g_{1p1}^3\lambda_3x_H^3)/12 \\
& + (557g'^4\lambda_3x_H^4)/48 + (45g'^2g_{1p1}^2\lambda_3x_H^4)/8 + (557g_{1p1}^4\lambda_3x_H^4)/48 + (40g_{11p}^3g'\lambda_3x_\Phi)/3 \\
& + (40g_1^3g_{1p1}\lambda_3x_\Phi)/3 - (40g_{11p}^2g'^2\lambda_3x_Hx_\Phi)/3 - (40g_1^2g_{1p1}^2\lambda_3x_Hx_\Phi)/3 - (40g_{11p}g'^3\lambda_3x_H^2x_\Phi)/3 \\
& - (40g_1g_{1p1}^3\lambda_3x_H^2x_\Phi)/3 + (40g'^4\lambda_3x_H^3x_\Phi)/3 + (40g_{1p1}^4\lambda_3x_H^3x_\Phi)/3 - (15g_1^2g_{11p}g'^2x_\Phi^2)/4 \\
& - (713g_{11p}^4g'^2x_\Phi^2)/12 - (45g_{11p}^2g'^2g_2^2x_\Phi^2)/4 + 30g_{11p}^2g'^2\lambda_1x_\Phi^2 + 20g_{11p}^2g'^2\lambda_2x_\Phi^2
\end{aligned}$$

$$\begin{aligned}
& + (617g_{11p}^2g'^2\lambda_3x_\Phi^2)/12 + (593g_1^2g_{1p1}^2\lambda_3x_\Phi^2)/12 + 64g'^2\lambda_2\lambda_3x_\Phi^2 + 64g_{1p1}^2\lambda_2\lambda_3x_\Phi^2 \\
& + 4g'^2\lambda_3^2x_\Phi^2 + 4g_{1p1}^2\lambda_3^2x_\Phi^2 + (15g_1^2g_{11p}g'^3x_Hx_\Phi^2)/2 + (73g_{11p}^3g'^3x_Hx_\Phi^2)/3 \\
& + (15g_1g_{11p}^2g'^2g_{1p1}x_Hx_\Phi^2)/2 + (45g_{11p}g'^3g_2^2x_Hx_\Phi^2)/2 - 60g_{11p}g'^3\lambda_1x_Hx_\Phi^2 - 40g_{11p}g'^3\lambda_2x_Hx_\Phi^2 \\
& + (61g_{11p}g'^3\lambda_3x_Hx_\Phi^2)/2 + (69g_1g_{1p1}^3\lambda_3x_Hx_\Phi^2)/2 - (15g_1^2g'^4x_H^2x_\Phi^2)/4 + (421g_{11p}^2g'^4x_H^2x_\Phi^2)/6 \\
& - 15g_1g_{11p}g'^3g_{1p1}x_H^2x_\Phi^2 - (15g_{11p}^2g'^2g_{1p1}^2x_H^2x_\Phi^2)/4 - (45g'^4g_2^2x_H^2x_\Phi^2)/4 \\
& + 30g'^4\lambda_1x_H^2x_\Phi^2 + 20g'^4\lambda_2x_H^2x_\Phi^2 + (617g'^4\lambda_3x_H^2x_\Phi^2)/12 + (593g_{1p1}^4\lambda_3x_H^2x_\Phi^2)/12 \\
& + (73g_{11p}g'^5x_H^3x_\Phi^2)/3 + (15g_1g'^4g_{1p1}x_H^3x_\Phi^2)/2 + (15g_{11p}g'^3g_{1p1}^2x_H^3x_\Phi^2)/2 - (713g'^6x_H^4x_\Phi^2)/12 \\
& - (15g'^4g_{1p1}^2x_H^4x_\Phi^2)/4 - (256g_{11p}^3g'^3x_\Phi^3)/3 + (160g_{11p}g'^3\lambda_3x_\Phi^3)/3 + (160g_1g_{1p1}^3\lambda_3x_\Phi^3)/3 + \\
& (256g_{11p}^2g'^4x_Hx_\Phi^3)/3 + (160g'^4\lambda_3x_Hx_\Phi^3)/3 + (160g_{1p1}^4\lambda_3x_Hx_\Phi^3)/3 + (256g_{11p}g'^5x_H^2x_\Phi^3)/3 \\
& - (256g'^6x_H^3x_\Phi^3)/3 - 105g_{11p}^2g'^4x_\Phi^4 - 15g_{11p}^2g'^2g_{1p1}^2x_\Phi^4 + 82g'^4\lambda_3x_\Phi^4 \\
& + 6g'^2g_{1p1}^2\lambda_3x_\Phi^4 + 60g_{1p1}^4\lambda_3x_\Phi^4 + 210g_{11p}g'^5x_Hx_\Phi^4 + 30g_{11p}g'^3g_{1p1}^2x_Hx_\Phi^4 \\
& - 105g'^6x_H^2x_\Phi^4 - 15g'^4g_{1p1}^2x_H^2x_\Phi^4 + (85g_1^2\lambda_3y_t^2)/12 + (85g_{11p}^2\lambda_3y_t^2)/12 \\
& + (45g_2^2\lambda_3y_t^2)/4 + 40g_3^2\lambda_3y_t^2 - 72\lambda_1\lambda_3y_t^2 - 12\lambda_3^2y_t^2 + (85g_{11p}g'\lambda_3x_Hy_t^2)/6 \\
& + (85g_1g_{1p1}\lambda_3x_Hy_t^2)/6 + (85g'^2\lambda_3x_H^2y_t^2)/12 + (85g_{1p1}^2\lambda_3x_H^2y_t^2)/12 + (25g_{11p}g'\lambda_3x_\Phi y_t^2)/3 \\
& + (25g_1g_{1p1}\lambda_3x_\Phi y_t^2)/3 + (25g'^2\lambda_3x_Hx_\Phi y_t^2)/3 + (25g_{1p1}^2\lambda_3x_Hx_\Phi y_t^2)/3 - 19g_{11p}^2g'^2x_\Phi^2y_t^2 \\
& + (10g'^2\lambda_3x_\Phi^2y_t^2)/3 + (10g_{1p1}^2\lambda_3x_\Phi^2y_t^2)/3 - 38g_{11p}g'^3x_Hx_\Phi^2y_t^2 - 19g'^4x_H^2x_\Phi^2y_t^2 \\
& - 40g_{11p}g'^3x_\Phi^3y_t^2 - 40g'^4x_Hx_\Phi^3y_t^2 - 16g'^4x_\Phi^4y_t^2 + (5g_1^2\lambda_3\text{Tr}[Y_\nu Y_\nu^\dagger])/4 \\
& + (5g_{11p}^2\lambda_3\text{Tr}[Y_\nu Y_\nu^\dagger])/4 + (15g_2^2\lambda_3\text{Tr}[Y_\nu Y_\nu^\dagger])/4 - 24\lambda_1\lambda_3\text{Tr}[Y_\nu Y_\nu^\dagger] \\
& - 4\lambda_3^2\text{Tr}[Y_\nu Y_\nu^\dagger] + (5g_{11p}g'\lambda_3x_H\text{Tr}[Y_\nu Y_\nu^\dagger])/2 \\
& + (5g_1g_{1p1}\lambda_3x_H\text{Tr}[Y_\nu Y_\nu^\dagger])/2 + (5g'^2\lambda_3x_H^2\text{Tr}[Y_\nu Y_\nu^\dagger])/4 + (5g_{1p1}^2\lambda_3x_H^2\text{Tr}[Y_\nu Y_\nu^\dagger])/4 + 5g_{11p}g'\lambda_3x_\Phi\text{Tr}[Y_\nu Y_\nu^\dagger] \\
& + 5g_1g_{1p1}\lambda_3x_\Phi\text{Tr}[Y_\nu Y_\nu^\dagger] + 5g'^2\lambda_3x_Hx_\Phi\text{Tr}[Y_\nu Y_\nu^\dagger] + 5g_{1p1}^2\lambda_3x_Hx_\Phi\text{Tr}[Y_\nu Y_\nu^\dagger] \\
& - g_{11p}^2g'^2x_\Phi^2\text{Tr}[Y_\nu Y_\nu^\dagger] + 10g'^2\lambda_3x_\Phi^2\text{Tr}[Y_\nu Y_\nu^\dagger] + 10g_{1p1}^2\lambda_3x_\Phi^2\text{Tr}[Y_\nu Y_\nu^\dagger] \\
& - 2g_{11p}g'^3x_Hx_\Phi^2\text{Tr}[Y_\nu Y_\nu^\dagger] - g'^4x_H^2x_\Phi^2\text{Tr}[Y_\nu Y_\nu^\dagger] - 24g_{11p}g'^3x_\Phi^3\text{Tr}[Y_\nu Y_\nu^\dagger] \\
& - 24g'^4x_Hx_\Phi^3\text{Tr}[Y_\nu Y_\nu^\dagger] - 48g'^4x_\Phi^4\text{Tr}[Y_\nu Y_\nu^\dagger] - 16\lambda_2\lambda_3\text{Tr}[y_{NS}y_{NS}^\dagger] - 4\lambda_3^2\text{Tr}[y_{NS}y_{NS}^\dagger] \\
& - g_{11p}^2g'^2x_\Phi^2\text{Tr}[y_{NS}y_{NS}^\dagger] + 5g'^2\lambda_3x_\Phi^2\text{Tr}[y_{NS}y_{NS}^\dagger] + 5g_{1p1}^2\lambda_3x_\Phi^2\text{Tr}[y_{NS}y_{NS}^\dagger] + 2g_{11p}g'^3x_Hx_\Phi^2\text{Tr}[y_{NS}y_{NS}^\dagger] \\
& - g'^4x_H^2x_\Phi^2\text{Tr}[y_{NS}y_{NS}^\dagger] - (27\lambda_3y_t^4)/2 - (9\lambda_3\text{Tr}[Y_\nu Y_\nu^\dagger Y_\nu Y_\nu^\dagger])/2 - 3\lambda_3\text{Tr}[y_{NS}y_{NS}^\dagger y_{NS}y_{NS}^\dagger]
\end{aligned}$$

$$\begin{aligned}
& + (7\lambda_3 \text{Tr}[y_{NS} y_{NS}^\dagger Y_\nu^T Y_\nu^*]) / 2 \\
& - 4g_{11p} g' x_H \text{Tr}[y_{NS} y_{NS}^\dagger Y_\nu^T Y_\nu^*] - 4g_1 g_{1p1} x_H \text{Tr}[y_{NS} y_{NS}^\dagger Y_\nu^T Y_\nu^*] - 4g_{11p} g' x_\Phi \text{Tr}[y_{NS} y_{NS}^\dagger Y_\nu^T Y_\nu^*] \\
& - 4g_1 g_{1p1} x_\Phi \text{Tr}[y_{NS} y_{NS}^\dagger Y_\nu^T Y_\nu^*] - 4g'^2 x_H x_\Phi \text{Tr}[y_{NS} y_{NS}^\dagger Y_\nu^T Y_\nu^*] - 4g_{1p1}^2 x_H x_\Phi \text{Tr}[y_{NS} y_{NS}^\dagger Y_\nu^T Y_\nu^*] \\
& - 8g'^2 x_\Phi^2 \text{Tr}[y_{NS} y_{NS}^\dagger Y_\nu^T Y_\nu^*] - 8g_{1p1}^2 x_\Phi^2 \text{Tr}[y_{NS} y_{NS}^\dagger Y_\nu^T Y_\nu^*] + 6\text{Tr}[y_{NS} y_{NS}^\dagger y_{NS} y_{NS}^\dagger Y_\nu^T Y_\nu^*] \\
& + 4\text{Tr}[y_{NS} y_{NS}^\dagger Y_\nu^T Y_\nu^* y_{NS} y_{NS}^\dagger] + 14\text{Tr}[y_{NS} y_{NS}^\dagger Y_\nu^T Y_\nu^* Y_\nu^T Y_\nu^*]
\end{aligned} \tag{2.9}$$

$$\begin{aligned}
\beta_{y_{NS}^{(2)}} = & \frac{1}{24} \left( 4 \left( 24\lambda_2^2 + 6\lambda_3^2 + 44g_{11p}^2 g'^2 x_\Phi^2 + 88g_1 g_{11p} g' g_{1p1} x_\Phi^2 + 44g_1^2 g_{1p1}^2 x_\Phi^2 + 72g_{11p} g'^3 x_H x_\Phi^2 \right. \right. \\
& + 72g_1 g'^2 g_{1p1} x_H x_\Phi^2 + 72g_{11p} g' g_{1p1}^2 x_H x_\Phi^2 + 72g_1 g_{1p1}^3 x_H x_\Phi^2 + 44g'^4 x_H^2 x_\Phi^2 + 88g'^2 g_{1p1}^2 x_H^2 x_\Phi^2 \\
& + 44g_{1p1}^4 x_H^2 x_\Phi^2 + 64g_{11p} g'^3 x_\Phi^3 + 64g_1 g'^2 g_{1p1} x_\Phi^3 + 64g_{11p} g' g_{1p1}^2 x_\Phi^3 + 64g_1 g_{1p1}^3 x_\Phi^3 \\
& + 64g'^4 x_H x_\Phi^3 + 128g'^2 g_{1p1}^2 x_H x_\Phi^3 + 64g_{1p1}^4 x_H x_\Phi^3 + 36g'^4 x_\Phi^4 + 72g'^2 g_{1p1}^2 x_\Phi^4 \\
& \left. + 36g_{1p1}^4 x_\Phi^4 + 15(g'^2 + g_{1p1}^2) x_\Phi^2 \text{Tr}[y_{NS} y_{NS}^\dagger] - 9\text{Tr}[y_{NS} y_{NS}^\dagger y_{NS} y_{NS}^\dagger] - 9\text{Tr}[y_{NS} y_{NS}^\dagger Y_\nu^T Y_\nu^*] \right) y_{NS} \\
& + 3 \left( -4(16\lambda_2 - 26(g'^2 + g_{1p1}^2) x_\Phi^2 + 3\text{Tr}[y_{NS} y_{NS}^\dagger]) (y_{NS} y_{NS}^\dagger y_{NS}) \right. \\
& + (17g_1^2 + 17g_{11p}^2 + 51g_2^2 - 32\lambda_3 - 38g_{11p} g' x_H - 38g_1 g_{1p1} x_H + 17g'^2 x_H^2 + 17g_{1p1}^2 x_H^2 \\
& - 4g_{11p} g' x_\Phi - 4g_1 g_{1p1} x_\Phi - 4g'^2 x_H x_\Phi - 4g_{1p1}^2 x_H x_\Phi - 32g'^2 x_\Phi^2 - 32g_{1p1}^2 x_\Phi^2 - 36y_t^2 \\
& \left. - 12\text{Tr}[Y_\nu Y_\nu^\dagger] (Y_\nu^T Y_\nu^* y_{NS}) + 14(y_{NS} y_{NS}^\dagger y_{NS} y_{NS}^\dagger y_{NS}) - 2(y_{NS} y_{NS}^\dagger Y_\nu^T Y_\nu^* y_{NS}) - 2(Y_\nu^T Y_\nu^* Y_\nu^T Y_\nu^* y_{NS}) \right)
\end{aligned} \tag{2.10}$$



$$\begin{aligned}
\beta_{Y_v^{(2)}} = & \frac{1}{48} \left( 2 \left( 35g_1^4 + 70g_1^2g_{11p}^2 + 35g_{11p}^4 - 54g_1^2g_2^2 - 54g_{11p}^2g_2^2 - 138g_2^4 + 144\lambda_1^2 + 12\lambda_3^2 \right. \right. \\
& + 460g_1^2g_{11p}g'x_H + 460g_{11p}^3g'x_H + 460g_1^3g_{1p1}x_H + 460g_1g_{11p}^2g_{1p1}x_H + 162g_{11p}g'g_2^2x_H \\
& + 162g_1g_{1p1}g_2^2x_H + 288g_1^2g'^2x_H^2 + 574g_{11p}^2g'^2x_H^2 + 572g_1g_{11p}g'g_{1p1}x_H^2 + 574g_1^2g_{1p1}^2x_H^2 \\
& + 288g_{11p}^2g_{1p1}^2x_H^2 - 54g'^2g_2^2x_H^2 - 54g_{1p1}^2g_2^2x_H^2 + 460g_{11p}g'^3x_H^3 + 460g_1g'^2g_{1p1}x_H^3 \\
& + 460g_{11p}g'g_{1p1}^2x_H^3 + 460g_1g_{1p1}^3x_H^3 + 35g'^4x_H^4 + 70g'^2g_{1p1}^2x_H^4 + 35g_{1p1}^4x_H^4 + 504g_1^2g_{11p}g'x_\Phi \\
& + 504g_{11p}^3g'x_\Phi + 504g_1^3g_{1p1}x_\Phi + 504g_1g_{11p}^2g_{1p1}x_\Phi + 54g_{11p}g'g_2^2x_\Phi + 54g_1g_{1p1}g_2^2x_\Phi \\
& + 652g_1^2g'^2x_Hx_\Phi + 1664g_{11p}^2g'^2x_Hx_\Phi + 2024g_1g_{11p}g'g_{1p1}x_Hx_\Phi + 1664g_1^2g_{1p1}^2x_Hx_\Phi \\
& + 652g_{11p}^2g_{1p1}^2x_Hx_\Phi + 54g'^2g_2^2x_Hx_\Phi + 54g_{1p1}^2g_2^2x_Hx_\Phi + 1664g_{11p}g'^3x_H^2x_\Phi \\
& \left. \left. + 1664g_1g'^2g_{1p1}x_H^2x_\Phi + 1664g_{11p}g'g_{1p1}^2x_H^2x_\Phi + 1664g_1g_{1p1}^3x_H^2x_\Phi + 504g'^4x_H^3x_\Phi \right) \right)
\end{aligned}$$

$$\begin{aligned}
& + 1008g'^2g_{1p1}^2x_H^3x_\Phi + 504g_{1p1}^4x_H^3x_\Phi + 374g_1^2g'^2x_\Phi^2 + 1574g_{11p}^2g'^2x_\Phi^2 + 2400g_1g_{11p}g'g_{1p1}x_\Phi^2 \\
& + 1574g_1^2g_{1p1}^2x_\Phi^2 + 374g_{11p}^2g_{1p1}^2x_\Phi^2 + 162g'^2g_2^2x_\Phi^2 + 162g_{1p1}^2g_2^2x_\Phi^2 + 3080g_{11p}g'^3x_Hx_\Phi^2 \\
& + 3080g_1g'^2g_{1p1}x_Hx_\Phi^2 + 3080g_{11p}g'g_{1p1}^2x_Hx_\Phi^2 + 3080g_1g_{1p1}^3x_Hx_\Phi^2 + 1574g'^4x_H^2x_\Phi^2 \\
& + 3148g'^2g_{1p1}^2x_H^2x_\Phi^2 + 1574g_{1p1}^4x_H^2x_\Phi^2 + 1892g_{11p}g'^3x_\Phi^3 + 1892g_1g'^2g_{1p1}x_\Phi^3 + 1892g_{11p}g'g_{1p1}^2x_\Phi^3 \\
& + 1892g_1g_{1p1}^3x_\Phi^3 + 1892g'^4x_Hx_\Phi^3 + 3784g'^2g_{1p1}^2x_Hx_\Phi^3 + 1892g_{1p1}^4x_Hx_\Phi^3 + 1296g'^4x_\Phi^4 \\
& + 2592g'^2g_{1p1}^2x_\Phi^4 + 1296g_{1p1}^4x_\Phi^4 + 85g_1^2y_t^2 + 85g_{11p}^2y_t^2 + 135g_2^2y_t^2 + 480g_3^2y_t^2 + 170g_{11p}g'x_Hy_t^2 \\
& + 170g_1g_{1p1}x_Hy_t^2 + 85g'^2x_H^2y_t^2 + 85g_{1p1}^2x_H^2y_t^2 + 100g_{11p}g'x_\Phi y_t^2 + 100g_1g_{1p1}x_\Phi y_t^2 \\
& + 100g'^2x_Hx_\Phi y_t^2 + 100g_{1p1}^2x_Hx_\Phi y_t^2 + 40g'^2x_\Phi^2y_t^2 + 40g_{1p1}^2x_\Phi^2y_t^2 + 15g_1^2\text{Tr}[Y_\nu Y_\nu^\dagger] + 15g_{11p}^2\text{Tr}[Y_\nu Y_\nu^\dagger] \\
& + 45g_2^2\text{Tr}[Y_\nu Y_\nu^\dagger] + 30g_{11p}g'x_H\text{Tr}[Y_\nu Y_\nu^\dagger] + 30g_1g_{1p1}x_H\text{Tr}[Y_\nu Y_\nu^\dagger] + 15g'^2x_H^2\text{Tr}[Y_\nu Y_\nu^\dagger] \\
& + 15g_{1p1}^2x_H^2\text{Tr}[Y_\nu Y_\nu^\dagger] + 60g_{11p}g'x_\Phi\text{Tr}[Y_\nu Y_\nu^\dagger] + 60g_1g_{1p1}x_\Phi\text{Tr}[Y_\nu Y_\nu^\dagger] + 60g'^2x_Hx_\Phi\text{Tr}[Y_\nu Y_\nu^\dagger] \\
& + 60g_{1p1}^2x_Hx_\Phi\text{Tr}[Y_\nu Y_\nu^\dagger] + 120g'^2x_\Phi^2\text{Tr}[Y_\nu Y_\nu^\dagger] + 120g_{1p1}^2x_\Phi^2\text{Tr}[Y_\nu Y_\nu^\dagger] - 162y_t^4 - 54\text{Tr}[Y_\nu Y_\nu^\dagger Y_\nu Y_\nu^\dagger] \\
& - 18\text{Tr}[y_{NS}y_{NS}^\dagger Y_\nu^T Y_\nu^*])Y_\nu + 3\left(3(31g_1^2 + 31g_{11p}^2 + 45g_2^2 - 64\lambda_1 - 10g_{11p}g'x_H - 10g_1g_{1p1}x_H \right. \\
& + 31g'^2x_H^2 + 31g_{1p1}^2x_H^2 + 52g_{11p}g'x_\Phi + 52g_1g_{1p1}x_\Phi + 52g'^2x_Hx_\Phi + 52g_{1p1}^2x_Hx_\Phi + 64g'^2x_\Phi^2 \\
& \left. - 36y_t^2 - 12\text{Tr}[Y_\nu Y_\nu^\dagger])(Y_\nu Y_\nu^\dagger Y_\nu) - 4(8\lambda_3 - 11(g'^2 + g_{1p1}^2)x_\Phi^2 + 3\text{Tr}[y_{NS}y_{NS}^\dagger])(Y_\nu y_{NS}^* y_{NS}^T) \right. \\
& \left. + 24(Y_\nu Y_\nu^\dagger Y_\nu Y_\nu^\dagger) - 2(Y_\nu y_{NS}^* y_{NS}^T Y_\nu^\dagger Y_\nu) - 2(Y_\nu y_{NS}^* y_{NS}^T y_{NS}^* y_{NS}^T)\right)
\end{aligned} \tag{2.11}$$

$$\begin{aligned}
\beta_{y_t^{(2)}} = & \frac{1}{432} \left( 2 \left( 1187g_1^4 + 2374g_1^2g_{11p}^2 + 1187g_{11p}^4 - 162g_1^2g_2^2 - 162g_{11p}^2g_2^2 - 1242g_2^4 + 456g_1^2g_3^2 \right. \right. \\
& + 456g_{11p}^2g_3^2 + 1944g_2^2g_3^2 - 23328g_3^4 + 1296\lambda_1^2 + 108\lambda_3^2 + 7164g_1^2g_{11p}g'x_H + 7164g_{11p}^3g'x_H \\
& + 7164g_1^3g_{1p1}x_H + 7164g_1g_{11p}g_{1p1}x_H + 2106g_{11p}g'g_2^2x_H + 2106g_1g_{1p1}g_2^2x_H - 2544g_{11p}g'g_3^2x_H \\
& - 2544g_1g_{1p1}g_3^2x_H + 4160g_1^2g'^2x_H^2 + 9470g_{11p}^2g'^2x_H^2 + 10620g_1g_{11p}g'g_{1p1}x_H^2 + 9470g_1^2g_{1p1}^2x_H^2 \\
& + 4160g_{11p}^2g_{1p1}^2x_H^2 - 162g'^2g_2^2x_H^2 - 162g_{1p1}^2g_2^2x_H^2 + 456g'^2g_3^2x_H^2 + 456g_{1p1}^2g_3^2x_H^2 + 7164g_{11p}g'^3x_H^3 \\
& + 7164g_1g'^2g_{1p1}x_H^3 + 7164g_{11p}g'g_{1p1}^2x_H^3 + 7164g_1g_{1p1}^3x_H^3 + 1187g'^4x_H^4 + 2374g'^2g_{1p1}^2x_H^4 \\
& + 1187g_{1p1}^4x_H^4 + 4016g_1^2g_{11p}g'x_\Phi + 4016g_{11p}^3g'x_\Phi + 4016g_1^3g_{1p1}x_\Phi + 4016g_1g_{11p}^2g_{1p1}x_\Phi \\
& \left. + 486g_{11p}g'g_2^2x_\Phi + 486g_1g_{1p1}g_2^2x_\Phi - 480g_{11p}g'g_3^2x_\Phi - 480g_1g_{1p1}g_3^2x_\Phi + 5524g_1^2g'^2x_Hx_\Phi \right)
\end{aligned}$$

$$\begin{aligned}
& + 14344g_{11p}^2g'^2x_Hx_\Phi + 17640g_1g_{11p}g'g_{1p1}x_Hx_\Phi + 14344g_1^2g_{1p1}^2x_Hx_\Phi + 5524g_{11p}^2g_{1p1}^2x_Hx_\Phi \\
& + 486g'^2g_2^2x_Hx_\Phi + 486g_{1p1}^2g_2^2x_Hx_\Phi - 480g'^2g_3^2x_Hx_\Phi - 480g_{1p1}^2g_3^2x_Hx_\Phi + 14344g_{11p}g'^3x_H^2x_\Phi \\
& + 14344g_1g'^2g_{1p1}x_H^2x_\Phi + 14344g_{11p}g'g_{1p1}^2x_H^2x_\Phi + 14344g_1g_{1p1}^3x_H^2x_\Phi + 4016g'^4x_H^3x_\Phi \\
& + 8032g'^2g_{1p1}^2x_H^3x_\Phi + 4016g_{1p1}^4x_H^3x_\Phi + 1638g_1^2g'^2x_\Phi^2 + 6030g_{11p}^2g'^2x_\Phi^2 + 8784g_1g_{11p}g'g_{1p1}x_\Phi^2 \\
& + 6030g_1^2g_{1p1}^2x_\Phi^2 + 1638g_{11p}^2g_{1p1}^2x_\Phi^2 + 162g'^2g_2^2x_\Phi^2 + 162g_{1p1}^2g_2^2x_\Phi^2 - 192g'^2g_3^2x_\Phi^2 - 192g_{1p1}^2g_3^2x_\Phi^2 \\
& + 15160g_{11p}g'^3x_Hx_\Phi^2 + 15160g_1g'^2g_{1p1}x_Hx_\Phi^2 + 15160g_{11p}g'g_{1p1}^2x_Hx_\Phi^2 + 15160g_1g_{1p1}^3x_Hx_\Phi^2 \\
& + 6030g'^4x_H^2x_\Phi^2 + 12060g'^2g_{1p1}^2x_H^2x_\Phi^2 + 6030g_{1p1}^4x_H^2x_\Phi^2 + 4660g_{11p}g'^3x_\Phi^3 + 4660g_1g'^2g_{1p1}x_\Phi^3 \\
& + 4660g_{11p}g'g_{1p1}^2x_\Phi^3 + 4660g_1g_{1p1}^3x_\Phi^3 + 4660g'^4x_Hx_\Phi^3 + 9320g'^2g_{1p1}^2x_Hx_\Phi^3 + 4660g_{1p1}^4x_Hx_\Phi^3 \\
& + 1360g'^4x_\Phi^4 + 2720g'^2g_{1p1}^2x_\Phi^4 + 1360g_{1p1}^4x_\Phi^4 + 765g_1^2y_t^2 + 765g_{11p}^2y_t^2 + 1215g_2^2y_t^2 + 4320g_3^2y_t^2 \\
& + 1530g_{11p}g'x_Hy_t^2 + 1530g_1g_{1p1}x_Hy_t^2 + 765g'^2x_H^2y_t^2 + 765g_{1p1}^2x_H^2y_t^2 + 900g_{11p}g'x_\Phi y_t^2 \\
& + 900g_1g_{1p1}x_\Phi y_t^2 + 900g'^2x_Hx_\Phi y_t^2 + 900g_{1p1}^2x_Hx_\Phi y_t^2 + 360g'^2x_\Phi^2y_t^2 + 360g_{1p1}^2x_\Phi^2y_t^2 \\
& + 135g_1^2\text{Tr}[Y_\nu Y_\nu^\dagger] + 135g_{11p}^2\text{Tr}[Y_\nu Y_\nu^\dagger] + 405g_2^2\text{Tr}[Y_\nu Y_\nu^\dagger] + 270g_{11p}g'x_H\text{Tr}[Y_\nu Y_\nu^\dagger] \\
& + 270g_1g_{1p1}x_H\text{Tr}[Y_\nu Y_\nu^\dagger] + 135g'^2x_H^2\text{Tr}[Y_\nu Y_\nu^\dagger] + 135g_{1p1}^2x_H^2\text{Tr}[Y_\nu Y_\nu^\dagger] + 540g_{11p}g'x_\Phi\text{Tr}[Y_\nu Y_\nu^\dagger] \\
& + 540g_1g_{1p1}x_\Phi\text{Tr}[Y_\nu Y_\nu^\dagger] + 540g'^2x_Hx_\Phi\text{Tr}[Y_\nu Y_\nu^\dagger] + 540g_{1p1}^2x_Hx_\Phi\text{Tr}[Y_\nu Y_\nu^\dagger] + 1080g'^2x_\Phi^2\text{Tr}[Y_\nu Y_\nu^\dagger] \\
& + 1080g_{1p1}^2x_\Phi^2\text{Tr}[Y_\nu Y_\nu^\dagger] - 1458y_t^4 - 486\text{Tr}[Y_\nu Y_\nu^\dagger Y_\nu Y_\nu^\dagger] - 162\text{Tr}[y_{NS}y_{NS}^\dagger Y_\nu^T Y_\nu^*])y_t \\
& - 9\left(- (223g_1^2 + 223g_{11p}^2 + 405g_2^2 + 768g_3^2 - 576\lambda_1 - 202g_{11p}g'x_H \right. \\
& - 202g_1g_{1p1}x_H + 223g'^2x_H^2 + 223g_{1p1}^2x_H^2 + 100g_{11p}g'x_\Phi + 100g_1g_{1p1}x_\Phi + 100g'^2x_Hx_\Phi \\
& \left. + 100g_{1p1}^2x_Hx_\Phi + 64g'^2x_\Phi^2 + 64g_{1p1}^2x_\Phi^2 - 324y_t^2 - 108\text{Tr}[Y_\nu Y_\nu^\dagger])y_t^3 + 12(-6y_t^5)\right)
\end{aligned} \tag{2.12}$$

- 
- [1] **CMS** Collaboration, S. Chatrchyan *et al.*, “Observation of a new boson at a mass of 125 GeV with the CMS experiment at the LHC,” *Phys. Lett.* **B716** (2012) 30–61, [arXiv:1207.7235 \[hep-ex\]](#).
- [2] **ATLAS** Collaboration, G. Aad *et al.*, “Observation of a new particle in the search for the Standard Model Higgs boson with the ATLAS detector at the LHC,” *Phys. Lett.* **B716** (2012) 1–29, [arXiv:1207.7214 \[hep-ex\]](#).

- [3] P. Minkowski, “ $\mu \rightarrow e \gamma$  at a Rate of One Out of 1-Billion Muon Decays?,” *Phys.Lett.* **B67** (1977) 421.
- [4] M. Gell-Mann, P. Ramond, and R. Slansky *Proc.Supergravity Workshop* (1979) 315–318.  
[www.scopus.com](http://www.scopus.com).
- [5] T. Yanagida *Workshop on Unified Theory and Baryon Number in the Universe* (1979) 95–98.  
[www.scopus.com](http://www.scopus.com).
- [6] R. N. Mohapatra and G. Senjanovic, “Neutrino Mass and Spontaneous Parity Violation,”  
*Phys.Rev.Lett.* **44** (1980) 912.
- [7] S. M. Boucenna, S. Morisi, and J. W. F. Valle, “The low-scale approach to neutrino masses,” *Adv. High Energy Phys.* **2014** (2014) 831598, [arXiv:1404.3751](https://arxiv.org/abs/1404.3751) [hep-ph].
- [8] F. F. Deppisch, P. S. Bhupal Dev, and A. Pilaftsis, “Neutrinos and Collider Physics,” *New J. Phys.* **17** no. 7, (2015) 075019, [arXiv:1502.06541](https://arxiv.org/abs/1502.06541) [hep-ph].
- [9] Y. Cai, T. Han, T. Li, and R. Ruiz, “Lepton Number Violation: Seesaw Models and Their Collider Tests,” *Front.in Phys.* **6** (2018) 40, [arXiv:1711.02180](https://arxiv.org/abs/1711.02180) [hep-ph].
- [10] A. Das, “Searching for the minimal Seesaw models at the LHC and beyond,” *Adv. High Energy Phys.* **2018** (2018) 9785318, [arXiv:1803.10940](https://arxiv.org/abs/1803.10940) [hep-ph].
- [11] R. Mohapatra and J. Valle, “Neutrino Mass and Baryon Number Nonconservation in Superstring Models,” *Phys.Rev.* **D34** (1986) 1642.
- [12] A. Datta, A. Elsayed, S. Khalil, and A. Moursy, “Higgs vacuum stability in the  $B - L$  extended standard model,” *Phys. Rev.* **D88** no. 5, (2013) 053011, [arXiv:1308.0816](https://arxiv.org/abs/1308.0816) [hep-ph].
- [13] S. Iso, N. Okada, and Y. Orikasa, “The minimal B-L model naturally realized at TeV scale,” *Phys. Rev.* **D80** (2009) 115007, [arXiv:0909.0128](https://arxiv.org/abs/0909.0128) [hep-ph].
- [14] S. Iso, N. Okada, and Y. Orikasa, “Classically conformal  $B - L$  extended Standard Model,” *Phys. Lett.* **B676** (2009) 81–87, [arXiv:0902.4050](https://arxiv.org/abs/0902.4050) [hep-ph].
- [15] S. Iso and Y. Orikasa, “TeV Scale B-L model with a flat Higgs potential at the Planck scale: In view of the hierarchy problem,” *PTEP* **2013** (2013) 023B08, [arXiv:1210.2848](https://arxiv.org/abs/1210.2848) [hep-ph].
- [16] J. Chakraborty, P. Konar, and T. Mondal, “Constraining a class of BL extended models from vacuum stability and perturbativity,” *Phys. Rev.* **D89** no. 5, (2014) 056014, [arXiv:1308.1291](https://arxiv.org/abs/1308.1291) [hep-ph].

- [17] C. Coriano, L. Delle Rose, and C. Marzo, “Vacuum Stability in U(1)-Prime Extensions of the Standard Model with TeV Scale Right Handed Neutrinos,” *Phys. Lett.* **B738** (2014) 13–19, [arXiv:1407.8539 \[hep-ph\]](#).
- [18] C. Coriano, L. Delle Rose, and C. Marzo, “Constraints on abelian extensions of the Standard Model from two-loop vacuum stability and  $U(1)_{B-L}$ ,” *JHEP* **02** (2016) 135, [arXiv:1510.02379 \[hep-ph\]](#).
- [19] A. Das, N. Okada, and N. Papapietro, “Electroweak vacuum stability in classically conformal B-L extension of the Standard Model,” *Eur. Phys. J.* **C77** no. 2, (2017) 122, [arXiv:1509.01466 \[hep-ph\]](#).
- [20] E. Accomando, C. Coriano, L. Delle Rose, J. Fiaschi, C. Marzo, and S. Moretti, “Z, Higgses and heavy neutrinos in U(1) models: from the LHC to the GUT scale,” *JHEP* **07** (2016) 086, [arXiv:1605.02910 \[hep-ph\]](#).
- [21] S. Oda, N. Okada, and D.-s. Takahashi, “Classically conformal U(1) extended standard model and Higgs vacuum stability,” *Phys. Rev.* **D92** no. 1, (2015) 015026, [arXiv:1504.06291 \[hep-ph\]](#).
- [22] A. Das, S. Oda, N. Okada, and D.-s. Takahashi, “Classically conformal U(1) extended standard model, electroweak vacuum stability, and LHC Run-2 bounds,” *Phys. Rev.* **D93** no. 11, (2016) 115038, [arXiv:1605.01157 \[hep-ph\]](#).
- [23] S. Alekhin, A. Djouadi, and S. Moch, “The top quark and Higgs boson masses and the stability of the electroweak vacuum,” *Phys.Lett.* **B716** (2012) 214–219, [arXiv:1207.0980 \[hep-ph\]](#).
- [24] D. Buttazzo, G. Degrassi, P. P. Giardino, G. F. Giudice, F. Sala, A. Salvio, and A. Strumia, “Investigating the near-criticality of the Higgs boson,” *JHEP* **12** (2013) 089, [arXiv:1307.3536 \[hep-ph\]](#).
- [25] **Planck** Collaboration, P. A. R. Ade *et al.*, “Planck 2015 results. XIII. Cosmological parameters,” *Astron. Astrophys.* **594** (2016) A13, [arXiv:1502.01589 \[astro-ph.CO\]](#).
- [26] T. Basak and T. Mondal, “Constraining Minimal  $U(1)_{B-L}$  model from Dark Matter Observations,” *Phys. Rev.* **D89** (2014) 063527, [arXiv:1308.0023 \[hep-ph\]](#).
- [27] S. Oda, N. Okada, and D.-s. Takahashi, “Right-handed neutrino dark matter in the classically conformal U(1) extended standard model,” *Phys. Rev.* **D96** no. 9, (2017) 095032, [arXiv:1704.05023 \[hep-ph\]](#).

- [28] W. Rodejohann and C. E. Yaguna, “Scalar dark matter in the BL model,” *JCAP* **1512** no. 12, (2015) 032, [arXiv:1509.04036 \[hep-ph\]](#).
- [29] J. Cao, L. Feng, X. Guo, L. Shang, F. Wang, and P. Wu, “Scalar dark matter interpretation of the DAMPE data with U(1) gauge interactions,” *Phys. Rev.* **D97** no. 9, (2018) 095011, [arXiv:1711.11452 \[hep-ph\]](#).
- [30] S. Singirala, R. Mohanta, and S. Patra, “Singlet scalar Dark matter in  $U(1)_{B-L}$  models without right-handed neutrinos,” *Eur. Phys. J. Plus* **133** no. 11, (2018) 477, [arXiv:1704.01107 \[hep-ph\]](#).
- [31] D. A. Camargo, M. D. Campos, T. B. de Melo, and F. S. Queiroz, “A Two Higgs Doublet Model for Dark Matter and Neutrino Masses,” [arXiv:1901.05476 \[hep-ph\]](#).
- [32] P. Langacker, “Grand Unified Theories and Proton Decay,” *Phys.Rept.* **72** (1981) 185.
- [33] J. L. Hewett and T. G. Rizzo, “Low-Energy Phenomenology of Superstring Inspired E(6) Models,” *Phys. Rept.* **183** (1989) 193.
- [34] L. Basso, A. Belyaev, S. Moretti, and C. H. Shepherd-Themistocleous, “Phenomenology of the minimal B-L extension of the Standard model:  $Z'$  and neutrinos,” *Phys. Rev.* **D80** (2009) 055030, [arXiv:0812.4313 \[hep-ph\]](#).
- [35] M. Lindner, M. Platscher, and F. S. Queiroz, “A Call for New Physics : The Muon Anomalous Magnetic Moment and Lepton Flavor Violation,” *Phys. Rept.* **731** (2018) 1–82, [arXiv:1610.06587 \[hep-ph\]](#).
- [36] A. Ekstedt, R. Enberg, G. Ingelman, J. Lfgren, and T. Mandal, “Constraining minimal anomaly free U(1) extensions of the Standard Model,” *JHEP* **11** (2016) 071, [arXiv:1605.04855 \[hep-ph\]](#).
- [37] E. Accomando, L. Delle Rose, S. Moretti, E. Olaiya, and C. H. Shepherd-Themistocleous, “Extra Higgs boson and Z as portals to signatures of heavy neutrinos at the LHC,” *JHEP* **02** (2018) 109, [arXiv:1708.03650 \[hep-ph\]](#).
- [38] **ATLAS** Collaboration, M. Aaboud *et al.*, “Search for high-mass new phenomena in the dilepton final state using proton-proton collisions at  $\sqrt{s} = 13$  TeV with the ATLAS detector,” *Phys. Lett.* **B761** (2016) 372–392, [arXiv:1607.03669 \[hep-ex\]](#).
- [39] **CMS** Collaboration, V. Khachatryan *et al.*, “Search for narrow resonances in dilepton mass spectra in proton-proton collisions at  $\sqrt{s} = 13$  TeV and combination with 8 TeV data,” *Phys. Lett.* **B768** (2017) 57–80, [arXiv:1609.05391 \[hep-ex\]](#).

- [40] **ATLAS** Collaboration, G. Aad *et al.*, “Search for high-mass dilepton resonances using  $139 \text{ fb}^{-1}$  of  $pp$  collision data collected at  $\sqrt{s} = 13 \text{ TeV}$  with the ATLAS detector,” [arXiv:1903.06248](#) [hep-ex].
- [41] K. Kannike, “Vacuum Stability Conditions From Copositivity Criteria,” *Eur. Phys. J.* **C72** (2012) 2093, [arXiv:1205.3781](#) [hep-ph].
- [42] J. Chakraborty, P. Konar, and T. Mondal, “Copositive Criteria and Boundedness of the Scalar Potential,” *Phys. Rev.* **D89** no. 9, (2014) 095008, [arXiv:1311.5666](#) [hep-ph].
- [43] H. Huffel and G. Pocsik, “Unitarity Bounds on Higgs Boson Masses in the Weinberg-Salam Model With Two Higgs Doublets,” *Z. Phys.* **C8** (1981) 13.
- [44] M. Duerr, F. Kahlhoefer, K. Schmidt-Hoberg, T. Schwetz, and S. Vogl, “How to save the WIMP: global analysis of a dark matter model with two s-channel mediators,” *JHEP* **09** (2016) 042, [arXiv:1606.07609](#) [hep-ph].
- [45] W. T. V. W. H. Press, S. A. Teukolsky and B. P. Flannery, *Numerical Recipes in Fortran 90, Second Edition*. Cambridge Univ, 1996.
- [46] I. Esteban, M. C. Gonzalez-Garcia, M. Maltoni, I. Martinez-Soler, and T. Schwetz, “Updated fit to three neutrino mixing: exploring the accelerator-reactor complementarity,” *JHEP* **01** (2017) 087, [arXiv:1611.01514](#) [hep-ph].
- [47] **Planck** Collaboration, N. Aghanim *et al.*, “Planck 2018 results. VI. Cosmological parameters,” [arXiv:1807.06209](#) [astro-ph.CO].
- [48] I. Esteban, M. C. Gonzalez-Garcia, A. Hernandez-Cabezudo, M. Maltoni, and T. Schwetz, “Global analysis of three-flavour neutrino oscillations: synergies and tensions in the determination of  $\theta_{23}$ ,  $\delta_{CP}$ , and the mass ordering,”.
- [49] F. Capozzi, E. Lisi, A. Marrone, D. Montanino, and A. Palazzo, “Neutrino masses and mixings: Status of known and unknown  $3\nu$  parameters,” *Nucl. Phys.* **B908** (2016) 218–234, [arXiv:1601.07777](#) [hep-ph].
- [50] S. Antusch and O. Fischer, “Probing the nonunitarity of the leptonic mixing matrix at the CEPC,” *Int. J. Mod. Phys.* **A31** no. 33, (2016) 1644006, [arXiv:1604.00208](#) [hep-ph].
- [51] **MEG** Collaboration, A. M. Baldini *et al.*, “Search for the Lepton Flavour Violating Decay  $\mu^+ \rightarrow e^+ \gamma$  with the Full Dataset of the MEG Experiment,” [arXiv:1605.05081](#) [hep-ex].

- [52] R. Coy and M. Frigerio, “Effective approach to lepton observables: the seesaw case,” [arXiv:1812.03165 \[hep-ph\]](#).
- [53] **SINDRUM II** Collaboration, W. H. Bertl *et al.*, “A Search for muon to electron conversion in muonic gold,” *Eur. Phys. J.* **C47** (2006) 337–346.
- [54] A. Sirlin and R. Zucchini, “Dependence of the Quartic Coupling  $H(m)$  on  $M(H)$  and the Possible Onset of New Physics in the Higgs Sector of the Standard Model,” *Nucl.Phys.* **B266** (1986) 389.
- [55] K. Melnikov and T. v. Ritbergen, “The Three loop relation between the  $\overline{MS}$ -bar and the pole quark masses,” *Phys.Lett.* **B482** (2000) 99–108, [arXiv:hep-ph/9912391 \[hep-ph\]](#).
- [56] M. Holthausen, K. S. Lim, and M. Lindner, “Planck scale Boundary Conditions and the Higgs Mass,” *JHEP* **1202** (2012) 037, [arXiv:1112.2415 \[hep-ph\]](#).
- [57] F. Staub, “SARAH 4 : A tool for (not only SUSY) model builders,” *Comput. Phys. Commun.* **185** (2014) 1773–1790, [arXiv:1309.7223 \[hep-ph\]](#).
- [58] G. Blanger, F. Boudjema, A. Pukhov, and A. Semenov, “micrOMEGAs4.1: two dark matter candidates,” *Comput. Phys. Commun.* **192** (2015) 322–329, [arXiv:1407.6129 \[hep-ph\]](#).
- [59] **PandaX-II** Collaboration, X. Cui *et al.*, “Dark Matter Results From 54-Ton-Day Exposure of PandaX-II Experiment,” *Phys. Rev. Lett.* **119** no. 18, (2017) 181302, [arXiv:1708.06917 \[astro-ph.CO\]](#).
- [60] **XENON** Collaboration, E. Aprile *et al.*, “First Dark Matter Search Results from the XENON1T Experiment,” *Phys. Rev. Lett.* **119** no. 18, (2017) 181301, [arXiv:1705.06655 \[astro-ph.CO\]](#).
- [61] G. Belanger, F. Boudjema, A. Pukhov, and A. Semenov, “*micrOMEGAs3*: A program for calculating dark matter observables,” *Comput. Phys. Commun.* **185** (2014) 960–985, [arXiv:1305.0237 \[hep-ph\]](#).
- [62] P. Langacker, “The Physics of Heavy  $Z'$  Gauge Bosons,” *Rev. Mod. Phys.* **81** (2009) 1199–1228, [arXiv:0801.1345 \[hep-ph\]](#).